

***DOE SBIR Topic# 33a: Integrated Use of Surface and Subsurface NMR for Measuring and Mapping Saturated Hydraulic Conductivity in Three Dimensions. Vista Clara Inc.***

## **Project Narrative**

### **Integrated Use of Surface and Subsurface NMR for Measuring and Mapping Saturated Hydraulic Conductivity in Three Dimensions**

**DoE SBIR Topic # 33a**

**Grant Award # DE-SC0004623**

**Vista Clara Inc.**

**12201 Cyrus Way, Suite 104**

**Mukilteo, WA 98275**

**(425) 493-8122**

**David Oliver Walsh, Ph.D.**

**Principal Investigator**

## **Proprietary Data Legend**

### **Proprietary Data Legend:**

The data contained in pages 8, 10, 11, 67, 68 and 69 of this application have been submitted in confidence and contain trade secrets or proprietary information, and such data shall be used or disclosed only for evaluation purposes, provided that if this applicant receives an award as a result of or in connection with the submission of this application, DOE shall have the right to use or disclose the data herein to the extent provided in the award. This restriction does not limit the government's right to use or disclose data obtained without restriction from any source, including the applicant.

## **A. Significance, Background Information, and Technical Approach**

### ***A.1 Problem addressed:***

This proposal addresses the challenge of measuring and mapping hydraulic conductivity in three dimensions in the saturated zone of the shallow subsurface (first ~100 m below land surface).

### ***A.2 Significance:***

Throughout the U.S., the Department of Energy (DoE) is faced with the challenge of remediating, managing and monitoring sites at which there are high levels of subsurface contamination that pose threats to human populations and natural ecosystems.

Information about hydraulic conductivity, the parameter that characterizes the ease with which groundwater flows in the subsurface, is critical for efforts to predict the fate and transport of subsurface contaminants and to manage the remediation of contaminated sites. The traditional methods for measuring hydraulic conductivity (K) involve conducting hydraulic tests of varying levels of complexity in wells. These tests provide K information that either pertains only to the immediate vicinity of the well (slug test or borehole flowmeter test) or is an average (pumping test) over such a large volume of the subsurface that it is of limited value for contaminant investigations (Butler 2005, 2009). There is a critical need to develop techniques that provide K information at the scale of relevance for contaminant investigations at locations other than in the immediate vicinity of a well.

This proposal addresses the challenge of measuring and mapping K in the saturated shallow subsurface in a way that 1) minimizes the impact on the environment and/or human health and safety, 2) is economical, and 3) is reliable. Decisions regarding the long-term management of contaminated sites inevitably involve an assessment of risk. Quantifying uncertainty must therefore be an essential part of any method of subsurface characterization. Our research will advance the use of minimally invasive, economical, and reliable geophysical measurements to measure and map K, as well as provide a measure of uncertainty in the K estimates.

### ***A.3 Background:***

Proton NMR is a method of measurement that has been used in the Earth Sciences for the past ~50 years to study and quantify the pore-scale physical and chemical properties of water-saturated materials. The NMR experiment that is the focus of our research (conducted with a borehole, DP, or surface instrument) consists of measuring the time it takes for the bulk nuclear magnetization of the pore water, within the sampled volume, to return (relax) to equilibrium after being perturbed by a radio-frequency pulse. The initial magnetization  $M(0)$  is proportional to the total water content (i.e. the water-filled

**DOE SBIR Topic# 33a: Integrated Use of Surface and Subsurface NMR for Measuring and Mapping Saturated Hydraulic Conductivity in Three Dimensions. Vista Clara Inc.**

porosity), while the form of the relaxation contains information about the geometry of the pore space.

The relaxation rate of a single pore ( $T_2^{-1}$ ) can be described as a sum of the relaxation rate of the bulk fluid  $T_{2B}^{-1}$  and the surface relaxation rate,  $T_{2S}^{-1}$  (Brownstein and Tarr, 1979),

$$\frac{1}{T_2} = \frac{1}{T_{2B}} + \frac{1}{T_{2S}}. \quad (1)$$

The surface relaxation rate is given by (Senturia and Robinson, 1970; Brownstein and Tarr, 1979; Cohen and Mendelsen, 1981),

$$\frac{1}{T_{2S}} = \rho_2 \frac{S}{V} \quad (2)$$

where  $S/V$  is the surface-area-to-volume ratio of the pore and  $\rho_2$  is the surface relaxivity. This expression is the basis for the assumed link between NMR measurements and  $K$ . There is an additional relaxation mechanism that can arise due to local inhomogeneities in the magnetic field. For a borehole or laboratory NMR instrument, the effect of this can be minimized during data acquisition, so is neglected here.

The NMR response of a geological material will contain contributions from all water-filled pores, so results in a distribution of  $T_2$  values, with “fast” values taken as corresponding to the smaller pores (high  $S/V$ ) and the “slow” values taken as corresponding to the large pores. The NMR relaxation behavior is typically described using the arithmetic mean of  $\log T_2$  ( $T_{2ML}$ ), calculated from the distribution of relaxation times. Equation (1) then becomes:

$$\frac{1}{T_{2ML}} = \frac{1}{T_{2B}} + \frac{1}{T_{2S}} \quad (3)$$

$T_{2s}$ ,  $\rho_2$ , and  $S/V$  are now taken to be average values for the entire pore space of the sample.

While the borehole and DP NMR measurements in the proposed work will measure  $T_2$ , the NMR relaxation time measured using surface NMR is referred to as  $T_2^*$ . This time constant is similar to  $T_2$ , but is further influenced by magnetic susceptibility contrasts in a sample that give rise to a magnetic fields inhomogeneities. The equation for  $T_2^*$  is given by

$$\frac{1}{T_2^*} = \frac{1}{T_2} + \gamma \Delta H \quad (4)$$

where  $\gamma$  is the gyromagnetic ratio of hydrogen protons in water and  $\Delta H$  is the average magnetic field variation across the sampled region.

**DOE SBIR Topic# 33a: Integrated Use of Surface and Subsurface NMR for Measuring and Mapping Saturated Hydraulic Conductivity in Three Dimensions. Vista Clara Inc.**

The objective of our research is to obtain estimates of K from NMR measurements. Much of the research on this topic has been framed in terms of estimating permeability  $k$ , which is related to K as follows:

$$K = \frac{k \rho_w g}{\eta} \quad (5)$$

where  $\rho_w$  is the density of water,  $g$  is gravitational acceleration,  $\eta$  is the dynamic viscosity. There have been ongoing efforts in the oil industry to develop k estimators based on borehole logging measurements of  $T_2$ . One approach has been to interpret the  $T_2$  distributions so as to determine the bound-fluid volume (BFV), which is the volume of water tightly held in the pore space, and the free-fluid volume (FFV), the rest of the water. This involves defining a  $T_2$  cut-off (typically 33 ms) below which the water is assumed to be bound. This approach has led to transforms such as the Timur-Coates equation (Allen et. al, 2000):

$$k_{TC} = a \phi^m (FFV / BFV)^n \quad (6)$$

where  $\phi$  is the porosity; porosity can be obtained from other logs or from the NMR measurement of  $M(0)$ . An alternate approach, the Schlumberger-Doll Research (SDR) equation (Allen et. al 2000, Kenyon & Gubelin 1995), uses the average value  $T_{2ML}$ :

$$k_{SDR} = b \phi^m (T_{2ML})^n \quad (7)$$

where  $T_{2LM}$  is the logarithmic mean of the continuous  $T_2$  relaxation distribution. In equations (6) and (7) the exponents are typically  $m = 4$  and  $n = 2$ , but can vary with local conditions (Allen et. al, 2000). The lithology-dependent constant  $b$  in equation (7) is highly variable in itself, typically 4 for sandstones and 0.1 for carbonates (Kenyon & Gubelin 1995).

There has also been considerable research into the use of surface NMR measurements for k estimation. The resulting mathematical models have tended to follow the form of equation (7), with the exponential factors  $m$  and  $n$  ranging wildly between 0 and 4, depending on the experimental data and methods used to develop the empirical relationships. Lubczynski and Roy (2003) cite a generic empirical formula derived from surface NMR estimates of porosity and  $T_2^*$ :

$$k = C \phi_{MRS}^m T_d^n \quad (8)$$

where  $C$ ,  $m$  and  $n$  are site specific parameters to be calibrated in the field against K values obtained from pumping tests. Legchenko et al. (2002) compared transmissivity measurements with MRS-derived transmissivity estimates and reported the best correlation was obtained with the exponents  $m = 1$  and  $n = 2$ . A contemporaneous analysis of NMR measurements of unconsolidated glacial sediments (Yaramanci et al. 2002) reported that the exponents  $m = 0$  and  $n = 4$  provided best fit between NMR-predicted and measured k.

***DOE SBIR Topic# 33a: Integrated Use of Surface and Subsurface NMR for Measuring and Mapping Saturated Hydraulic Conductivity in Three Dimensions. Vista Clara Inc.***

The relationship between NMR relaxation times and permeability or hydraulic conductivity is likely to be a site-specific, and probably lithology-specific, phenomenon. Key site-specific geological factors that influence the NMR relaxation times can include magnetic susceptibility, iron content and redox state, and the pore size and throat size distributions. It is unrealistic to expect that we can ever develop a universally applicable function for transforming NMR measurements into reliable estimates of K. It is, however, realistic to expect the relationships between measured NMR parameters and K to follow similar patterns within similar hydrostratigraphic units.

Hence, the focus of our proposed research is to develop economical field methods for determining these site-specific NMR-to-K transforms within hydrostratigraphic units, and economical methods for applying these transform to map K across a site.

***A.4 Technical Approach:***

The proposed R&D program seeks to develop an economical and reliable field method for measuring and mapping K via surface NMR. The proposed field methodology includes:

1. Use borehole or DP measurements at a limited number of locations to relate NMR measurements to K.
  - Perform direct subsurface measurement of K using borehole or DP methods.
  - Perform subsurface NMR measurements in the same borehole or in a DP installation immediately adjacent to where the DP K measurements were obtained using newly available small-diameter NMR instruments.
  - Use the subsurface measurements of K and NMR parameters to develop a site-specific transform between NMR parameters and K for recognized hydrostratigraphic units.
2. Translate the site-specific NMR-K transform to the surface NMR measurement regime.
  1. Perform surface NMR measurements ( $T_2$  and  $T_{2^*}$ ) at the same location(s) as the subsurface NMR and K measurements.
  2. Translate the site-specific NMR-K transforms to the surface NMR measurement regime.
3. Use surface NMR as the primary means for measuring and mapping K over wide areas in the vicinity of the site-specific subsurface calibration(s). Use site-specific lithologic information and cataloged empirical data to estimate the uncertainty in the surface NMR K estimates.

**Leveraging recent advances in NMR and direct-push tools:**

Over the past few years, technological advancements by Vista Clara Inc. have made available the NMR geophysical tools that will enable the proposed methodology:

**DOE SBIR Topic# 33a: Integrated Use of Surface and Subsurface NMR for Measuring and Mapping Saturated Hydraulic Conductivity in Three Dimensions. Vista Clara Inc.**

- a commercial surface-based NMR system, “GMR”, that can be deployed in the vicinity of electrical lines and other cultural noise sources, and that can conduct efficient 1D and 2D NMR groundwater investigations,
- a borehole NMR system that can be used in the shallow, small-diameter wells common at sites of groundwater contamination, and, most recently,
- an NMR probe that can be integrated with direct-push technology (specifically with a Geoprobe system) to perform subsurface NMR measurements.

In addition, over the last two years, technical advancements by the Kansas Geological Survey (KGS) at the University of Kansas, working jointly with Geoprobe Systems, have resulted in the development of an instrument, the High-Resolution K (HRK) tool, that can perform direct subsurface measurement of K in unconsolidated sediments [Butler et al., 2007; Liu et al., 2008, 2009], thereby enabling reliable K estimates to be obtained away from existing wells.

**Graphical description of the proposed methodology:**

The proposed field application is illustrated in Figures 1 – 3. In the first step (Figure 1), NMR and K measurements are performed in a limited number of boreholes or DP locations. These two measurements are performed in the same borehole, using K and borehole NMR instruments with similar spatial resolution. On this basis, we develop a site-specific mathematical transform to convert the NMR signal parameters into estimates of K.

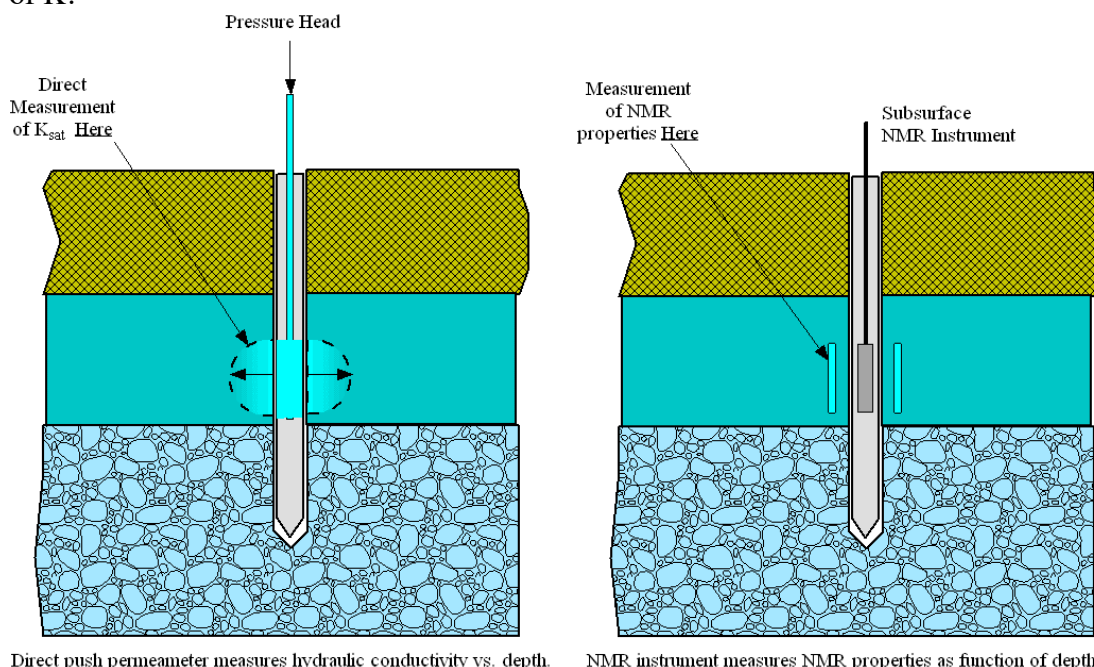


**Figure 1: The first step of the field procedure is to obtain subsurface direct measurements of hydraulic conductivity and NMR signal properties over the same localized intervals.**

The second step of the field methodology is to perform surface NMR measurements at the same location(s) as the borehole or DP measurements. This data now enables a direct

**DOE SBIR Topic# 33a: Integrated Use of Surface and Subsurface NMR for Measuring and Mapping Saturated Hydraulic Conductivity in Three Dimensions. Vista Clara Inc.**

comparison of NMR properties measured in the localized, high-field regime of the borehole NMR instrument and the large volume, low-field regime of the surface NMR measurement. This critical second step results in the construction of a second transform, which translates the NMR-to-K relationship from the borehole regime to the surface NMR regime.

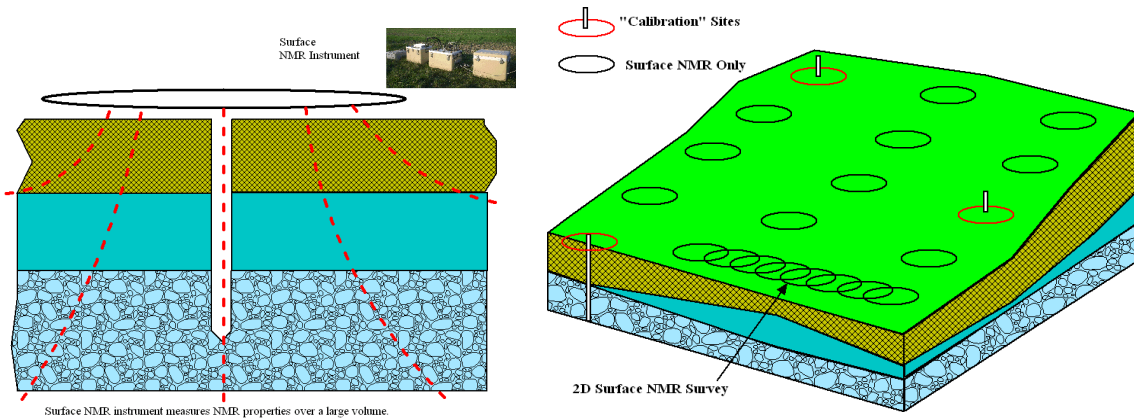


**Figure 2:** Left: The second step of the field procedure is to obtain surface NMR measurements at the same location as the subsurface NMR and flow measurements. Right: Wide area application of the proposed field methodology. A small number of subsurface NMR and K measurements are used to develop surface-NMR to K transforms. Surface NMR is applied on a wide scale for economical mapping of K across the site or basin.

The third step of the field methodology is to use surface NMR measurements, with the derived surface NMR-to-K transform, to estimate and map K on a wide scale in three dimensions. The reliance on surface NMR as the primary geophysical technique is the key to economical, widespread mapping of K.

#### **NMR measurement of flow within the formation:**

*The following paragraph contains proprietary information that Vista Clara Inc. requests not be released to persons outside the Government, except for purposes of review and evaluation.*

As part of this R&D effort, we also propose to develop and evaluate a new form of in-situ NMR measurement: the NMR measurement of moving water as it is pumped into or out of the adjacent formation. The idea is to design a borehole or DP NMR sensor that induces water flow, via a pressure head, within the sensitive region of the NMR sensor (Figure 3). Specific flow measurement NMR sequences, such as those already used in medical MRI to measure flow in blood vessels and blood diffusion in tissues, could be developed to differentiate the bound and mobile water fractions directly. This type of simultaneous NMR/flow measurement could also

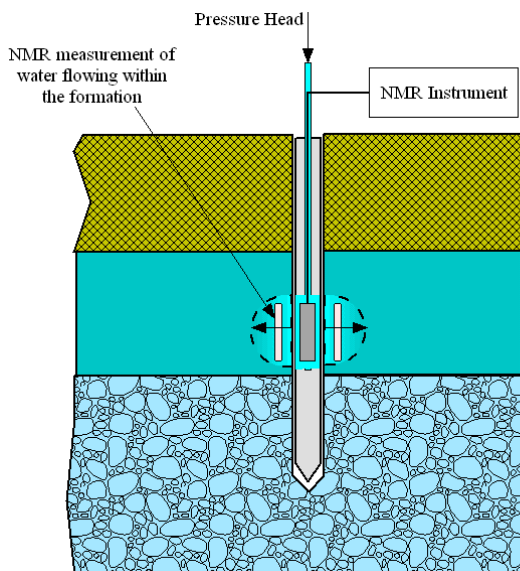


**Figure 3:Proposed NMR flow tool.**

yield flow velocity distribution as a function of depth, and these could conceivably shed additional light on pore/throat size ratios, and distributions.

#### ***Relevance to transport and fate of contaminants***

The ability to measure a groundwater velocity distribution can improve the prediction of the migration rate and density of subsurface contaminants. The simple graphics in Figures 4 and 5 illustrate the effect that different flow velocity distributions can have on the dispersion of a contaminant plume over space and time.

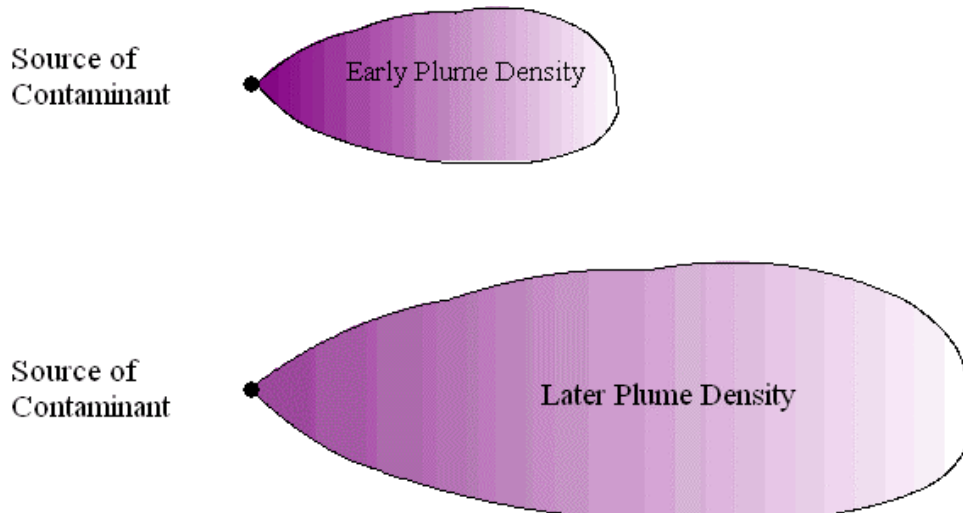


**Figure 4: Contaminant plume density and its change over time for a velocity distribution that is concentrated at low velocities, with some static (non moving) water.**

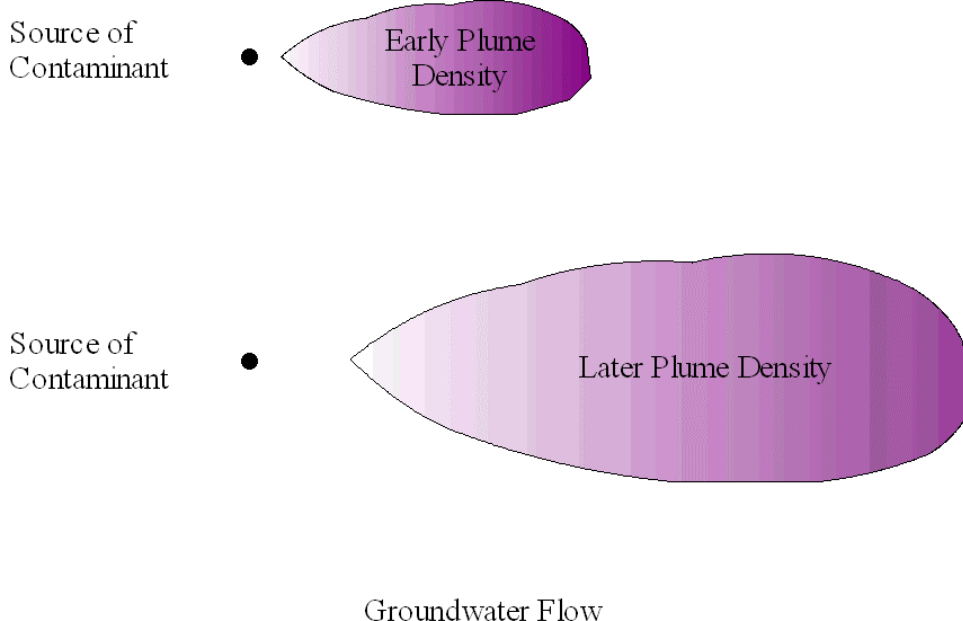


**Figure 5: Contaminant plume density and its change over time for a velocity distribution that is concentrated at higher velocities, with all of the water moving at some non zero velocity.**

## **B. Anticipated Public Benefits**

There is a recognized need for the development of new methods of site characterization that can provide accurate, yet cost-effective ways of determining subsurface properties. The successful completion of this research will provide a new methodology that integrates, and builds on, recently developed technology. The new field methodology would be valuable for a wide range of commercial applications related to groundwater hydrology, including local or regional groundwater exploration and production, groundwater management at the basin or regional scale, and investigations of groundwater contamination.

Specific groups in the commercial sector that would benefit from this technology are the private companies, utilities and landowners who must pay for groundwater development, site remediation, or compliance with environmental laws. These groups will benefit from the increased spatial resolution, reduced ambiguity and lower costs afforded by the proposed method. Specific groups in the Federal government that would benefit from this technology include the Department of Energy, the Department of Defense who are responsible for a variety of groundwater contamination sites, and other agencies with responsibility for groundwater management and remediation including the EPA, the US Department of the Interior, and the USGS.

### *End products of Phase II development:*

The end products of the Phase 2 development will be proven methods for using surface NMR and logging NMR tools to map hydraulic conductivity in three dimensions, and one or more novel methods for using logging NMR to measure flow velocity distributions at the pore scale.

### *Commercial Potential:*

Vista Clara will use the proposed methodology within our commercial groundwater services division. In the coming years we anticipate revenues from our commercial field services to constitute the largest and most rapidly growing segment of our business. Vista Clara is a leading manufacturer of surface NMR equipment, and Vista Clara is presently the only company producing small diameter, low cost NMR logging tools. Thus, Vista Clara expects to benefit also from increased sales of our NMR geophysical tools as the proposed methodology is adopted by commercial groundwater and environmental services companies.

Frost and Sullivan estimates the total market size for “US Soil and Groundwater Remediation Technology” to be worth \$8 billion in 2004, with a compounded growth rate of 7.2 percent, with the market value expected to increase to \$13 billion by 2010 (Frost and Sullivan). Other companies and organizations with access to the required NMR technologies may also apply the proposed method for commercial gain.

*The following paragraph contains proprietary information that Vista Clara Inc. requests not be released to persons outside the Government, except for purposes of review and evaluation.* The development of logging NMR for measuring flow velocity distributions

***DOE SBIR Topic# 33a: Integrated Use of Surface and Subsurface NMR for Measuring and Mapping Saturated Hydraulic Conductivity in Three Dimensions. Vista Clara Inc.***

at the pore scale, and using this information to predict contaminant migration, is likely a patentable invention. Vista Clara will file patents in the logging NMR flow measurement area as needed to protect our intellectual property rights.

**Benefits to the Federal Government:**

Specific groups in the Federal government that would benefit from this technology include the Department of Energy, the Department of Defense who are responsible for a variety of groundwater contamination sites, and other agencies with responsibility for groundwater management and remediation including the EPA, the US Department of the Interior, and the USGS.

**Benefits to the Commercial Environmental and Hydrology Sectors:**

More than half of all professionals in the Hydrology and Environmental Services in the US are employed in the private sector. These private sector companies and professionals deal with the same problems relating to groundwater development and contamination, but typically provide their services to municipalities, private landowners and commercial interests. The development of economical and reliable methods to map hydraulic conductivity in three dimensions will improve the efficiency and value that these professionals bring to their clients. This provides an important and direct benefit to the general public and commercial interests alike.

## **C. Degree to Which Phase 1 has Established Technical Feasibility**

### ***C.1 Phase 1 Technical Objectives and Top Line Feasibility Assessment***

The following Phase 1 Technical Objectives are copied verbatim from the Phase 1 Proposal. Our top-line summary of Phase 1 results and feasibility assessment is added in blue font for emphasis:

“The feasibility of performing the various field measurements (surface NMR, borehole/DP NMR and in-situ K measurements) has been previously established. The innovations proposed here involve: 1) developing site-specific relationships between the borehole/DP NMR and K measurements, and 2) translating these site-specific relationships from the borehole/DP NMR regime to the surface NMR regime. Hence, the following Phase I technical objectives will determine the technical feasibility of our proposed approach for subsurface characterization:

1. Demonstrate the feasibility of developing site-specific NMR-to-K transforms using borehole/DP NMR and K measurements.

**Phase 1 Results: Site-specific NMR-to-K transform approach is technically feasible.**

**DOE SBIR Topic# 33a: Integrated Use of Surface and Subsurface NMR for Measuring and Mapping Saturated Hydraulic Conductivity in Three Dimensions. Vista Clara Inc.**

We demonstrated the ability to make repeatable logging NMR measurements using a small diameter (< 2") borehole NMR tool and a direct push NMR logging tool. NMR-to-K transforms produced an uncertainty/error of ½ order of magnitude when evaluated over all depth samples at a depth resolution of 0.5m, and lower error/uncertainty when applied to estimate the average K of the investigated aquifer.

The Phase 1 results also strongly indicated that the construction of the well, the development of the well, and the method of NMR measurement (i.e. logging a drilled well vs. DP NMR logging) affect the measured NMR response in consistent and repeatable ways. When applied at two newly installed wells using the same construction technique, approximately ¼ mile apart, the NMR-K calibration derived from the first well predicted the mean K in the aquifer at the second well with an error factor of only 1.5.

The key questions to be answered in Phase 1 include:

- Can we develop a reliable mathematical transform between the NMR measurement and K, which is repeatable and accurate, at a site and within a defined hydrostratigraphic unit?

**Phase 1 Feasibility Assessment: Yes.**

NMR-to-K transforms produced an uncertainty/error of ½ order of magnitude when evaluated at a depth resolution of 0.5m, across 4 measurement locations spread over a ½ mile, and lower error when applied to estimate the average K of the investigated aquifer. This compared favorably to the use of the “standard” oilfield SDR NMR-K estimation parameters for sandstones, which produced an uncertainty/error range of 2 orders of magnitude.

- Can we predict the uncertainty in K using such a mathematical transform?

**Phase 1 Feasibility Assessment: Yes.**

Uncertainty/error was quantified for all comparisons between NMR-derived K and directly measured K.

2. Demonstrate the feasibility of translating the NMR-to-K transform from the borehole/DP NMR measurement regime to the surface NMR measurement regime.

**Phase 1 result: Surface NMR to logging NMR transform is technically feasible.**

We have shown that the NMR properties derived from SNMR measurements are not the same as those determined from logging NMR measurements. Specifically, the relaxation time T2\* measured by SNMR differs from the relaxation time T2 measured by logging. We have shown a relationship between T2 and T2\* can be calibrated on a site-specific basis to transform the SNMR relaxation times to pseudo-NMR logging relaxation times. Transformed surface NMR T2\* measurements at the KGS test sites tracked logging NMR T2 even more closely than did direct surface NMR measurement of T2.

***DOE SBIR Topic# 33a: Integrated Use of Surface and Subsurface NMR for Measuring and Mapping Saturated Hydraulic Conductivity in Three Dimensions. Vista Clara Inc.***

We have also shown that estimates of water content and spatial location of NMR signals using SNMR can be negatively affected when electrical conductivity effects are not incorporated into the inversion. To some degree, estimates of SNMR water content can be related to logging NMR water content estimates based on a scaling relationship, however, more robust conductivity modeling would be a preferred approach.

The key questions to be answered in Phase 1 are:

- Is it feasible to determine a site-specific relationship between surface NMR measurement(s) and the borehole/DP NMR measurement?

**Phase 1 Feasibility Assessment: Yes.**

We have shown that a relationship between T2 and T2\* can be calibrated on a site-specific basis to transform the SNMR relaxation times to pseudo-NMR logging relaxation times. We have shown that after transforming the surface NMR data to pseudo T2 data, the SNMR data can be used in place of the logging data with the same calibrated relationship to provide reasonable estimates of K. Transformed surface NMR T2\* measurements at the KGS test sites tracked logging NMR T2 even more closely than did direct surface NMR measurement of T2.

- Is there a good basis for predicting the uncertainty in the NMR-to-K transform when translated from the borehole/DP measurement regime to the surface NMR regime?

**Phase 1 Feasibility Assessment: Yes.**

We have shown that after transforming the surface NMR data to pseudo T2 data, the SNMR data can be used in place of the logging data with the same calibrated relationship to provide reasonable estimates of K. These estimates tend to resolve average K rather than small-scale K features. In terms of uncertainty, the greatest uncertainty is associated with transforming the SNMR data to pseudo logging NMR data. Other approaches may more appropriately distribute this uncertainty: see below.

We have also seen that estimates of K directly from T2\* data provide a lower bound on K, while estimates of K from spin echo T2 provide an upper bound on K.

- Is it feasible to develop advanced surface NMR spin-echo sequences to enable direct measurement of T2 relaxation rates using surface NMR?

**Phase 1 Feasibility Assessment: Yes.**

A surface NMR spin echo sequence was programmed and used extensively to measure and map T2 distributions for the Phase 1 research. Surface NMR-derived T2 appeared to track the upper range of the logging NMR T2 distribution at the KGS test sites.

3. Demonstrate the feasibility of gaining additional information on K and groundwater flow through in-situ NMR measurement of flow.

**Phase 1 Result: Demonstrated.**

NMR-detection of flow was demonstrated using a small diameter NMR logging tool in a tank of water. A simple field test was performed, but the rate of flow was insufficient for detection under the experimental conditions. Existing patents were identified that could limit the scope of measurements and interpretation that Vista Clara can commercialize.

- What are the feasible approaches and NMR pulse sequences for measuring groundwater flow characteristics using a borehole/DP NMR instrument?

**Phase 1 Feasibility Assessment:** We showed that the standard CPMG pulse sequence may be used to identify the fraction of moving water, under reasonable flow conditions. Other potential methods for in-situ NMR flow measurement include pre-saturation inflow, and time-of-flight methods.

- What hydrogeological information can be derived from such measurements?"

**Phase 1 Feasibility Assessment:** The fraction of moving water, its mean velocity, and its velocity distribution may all be potentially measured using borehole or DP NMR. These characteristics of the flow regime within an aquifer can improve the accuracy for modeling contaminant migration and fate.

## **C.2 Detailed Summary of Phase 1 Research and Results**

### **C.2.1 Demonstrate the feasibility of developing site-specific NMR-to-K transforms using borehole/DP NMR and K measurements**

Of interest is the development of a methodology for using a combination of logging and surface NMR to obtain estimates of hydraulic conductivity K at a site. A critical component in this methodology is the availability of NMR and K measurements that can be used to obtain a site-specific understanding of the relationship between measured NMR parameters and K at a site.

Our approach involves first acquiring co-located NMR logging data and K data, where the NMR logging data are acquired in a borehole or with a direct push (DP) method and the K data are acquired in a well or with a DP method; the latter K measurements will be referred to as the "true" K and taken as "ground truth". This data set is used as a form of calibration, to determine the empirical relationship between the NMR measured parameters and true K that provides the best estimate of K within a single lithologic unit. A comparison of the NMR-derived K values to the true K values, in this calibration data set, provides a measure of the uncertainty. The determined relationship is then used to estimate K from other logging or surface NMR data.

### **Collection of Borehole/DP NMR and K Data**

*This portion of the Phase 1 research was performed by Vista Clara Inc., and the Kansas Geological Survey. Stanford University also participated in some of the Phase 1 NMR logging data collection.*

A significant portion of the Phase 1 research effort involved the collection of new NMR logging data in and around the GEMS field research facility in Lawrence Kansas. Vista Clara and KGS acquired borehole NMR and Geoprobe NMR data in and around the GEMS field site in Lawrence Kansas, over a 4-day period in April 2010, and over a 2-week period in October 2010. This document summarizes the data that were collected and reduced to basic NMR signal responses that were subsequently analyzed by Stanford and KGS researchers. A complete summary of all of the borehole NMR and DP NMR data collected in the Phase 1 effort is described in a 37-page report, included as Appendix A of this proposal.

An overhead view of the measurement locations is shown in Figure 6. The surface NMR loops are shown in yellow, and were located in the “new areas” A, C and D. The original GEMS research site is located in the lower right corner labeled “GEMS”. A close up map of the original GEMS research site, which was the focus of the DP-NMR data collection in Phase 1, is shown in Figure 7.

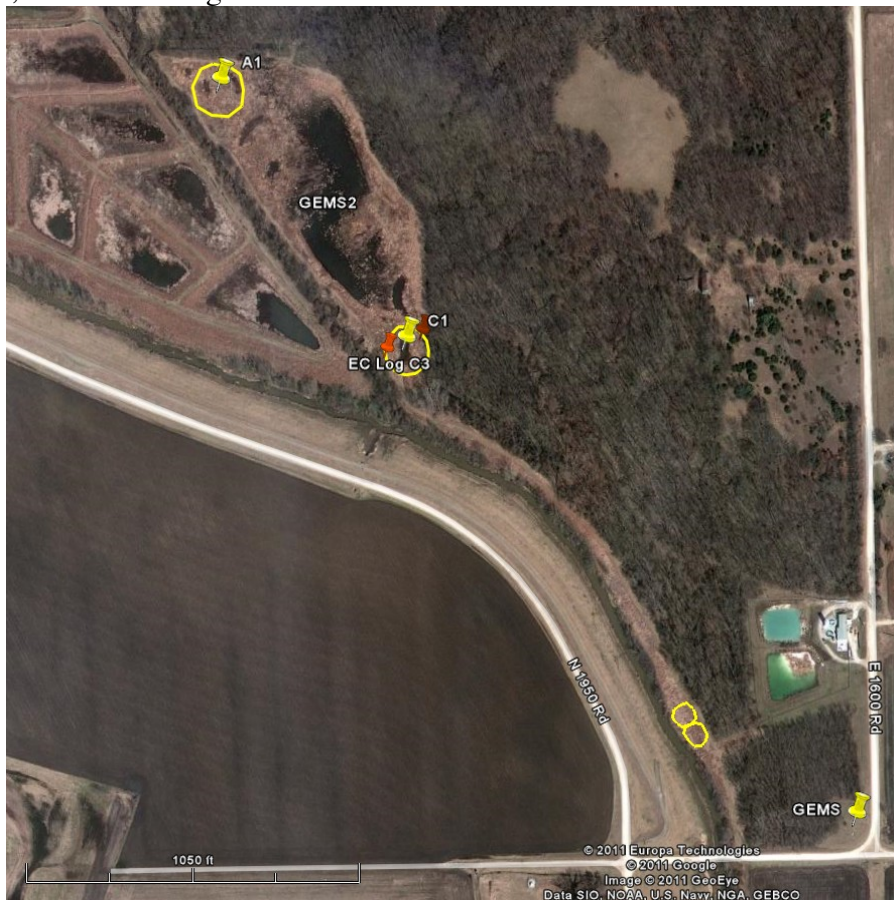


**Figure 6: Overview of surface NMR and borehole NMR measurement locations used in Phase 1.**

**DOE SBIR Topic# 33a: Integrated Use of Surface and Subsurface NMR for Measuring and Mapping Saturated Hydraulic Conductivity in Three Dimensions. Vista Clara Inc.**

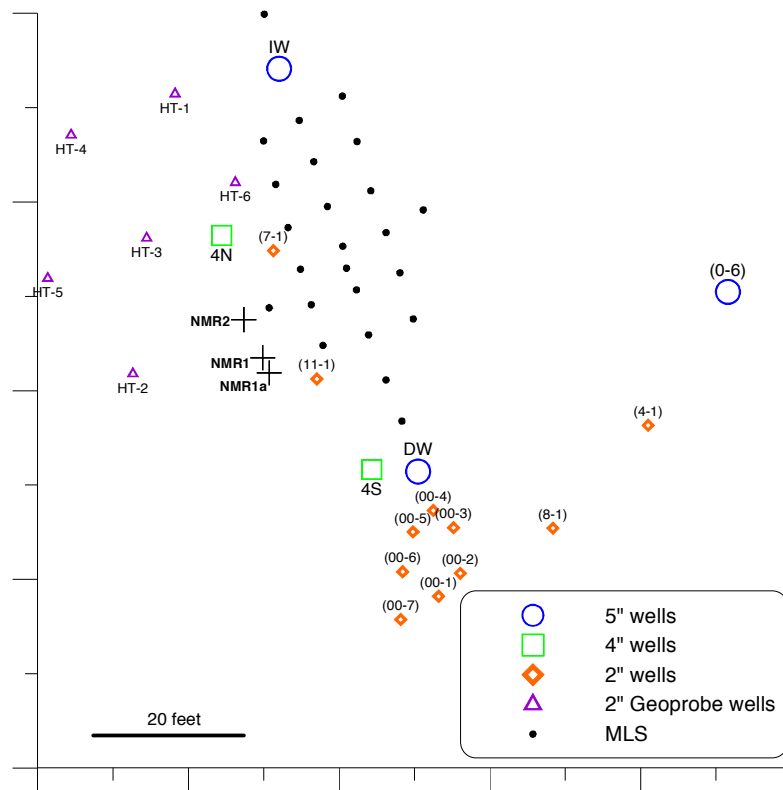


**Figure 7: Map view of the original GEMS research site, which contains a high density of pre-existing wells and DP-K measurements.**

All borehole NMR and DP NMR measurements were performed using Vista Clara's Javelin NMR logging instrument. Figure 8 is a photo of the Javelin instrument logging a 2" diameter well at GEMS in October 2010.



**Figure 8: Javelin NMR instrument logging well C1 at GEMS, October 2010.**

### **Initial borehole NMR measurements (April 2010)**

In April 2010, prior to the start of this SBIR effort, Vista Clara and KGS performed NMR logging on two existing 4" diameter wells at GEMS (wells 4N and 4S). These two wells were previously installed using an 11 inch diameter hollow-stem auger, and were subjected to substantial well development (intensive pumping) and a variety of traditional hydraulic conductivity tests. The NMR log from well 4S, shown in Figure 9, clearly illustrates the very short NMR T2 relaxation in the silt and clay unit above 11m, and the much longer T2 relaxation in the sand and gravel unit below 11m.

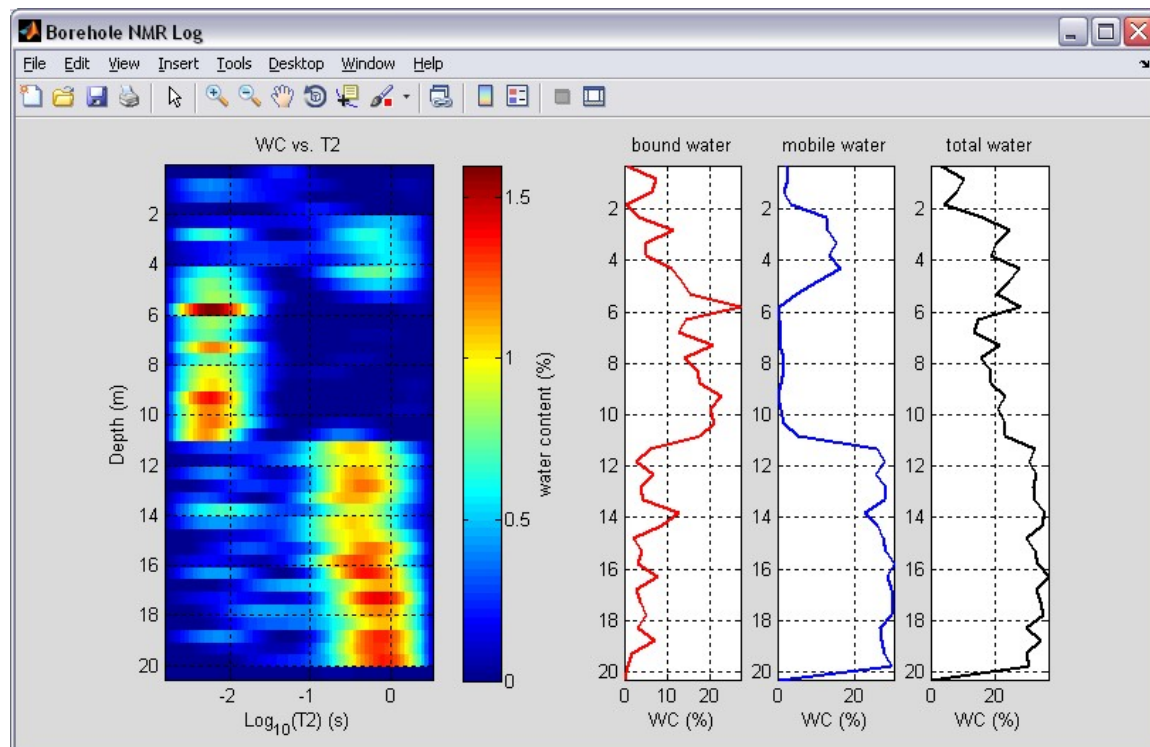


**Figure 9: NMR log of 4" diameter well 4S at GEMS, acquired in April 2010.**

### **New borehole NMR measurements (October 2010)**

Additional borehole NMR measurements were performed in three 2" diameter wells in and around GEMS: HT6, A1 and C1. These three wells were all installed using a Geoprobe machine. The Geoprobe well installation procedure involves using the 3.25" Geoprobe rods to create the borehole, installing 2" ID screened PVC through the center of the drill rods, and then withdrawing the drill rods and allowing the formation to collapse against the screened PVC pipe. Two of these 2" wells, A1 and C1, were installed in October 2010 specifically to obtain borehole NMR logs at the two new GEMS sites (Area A and Area C), and also to measure the effect of well development on the NMR response. Figure 10 is a photo taken as KGS personnel are completing the installation of well A1. The borehole NMR log of well C1, in its pre-development state, is shown in Figure 11.

**DOE SBIR Topic# 33a: Integrated Use of Surface and Subsurface NMR for Measuring and Mapping Saturated Hydraulic Conductivity in Three Dimensions. Vista Clara Inc.**



Figure 10: KGS personnel completing the installation of well A1, October 2010.

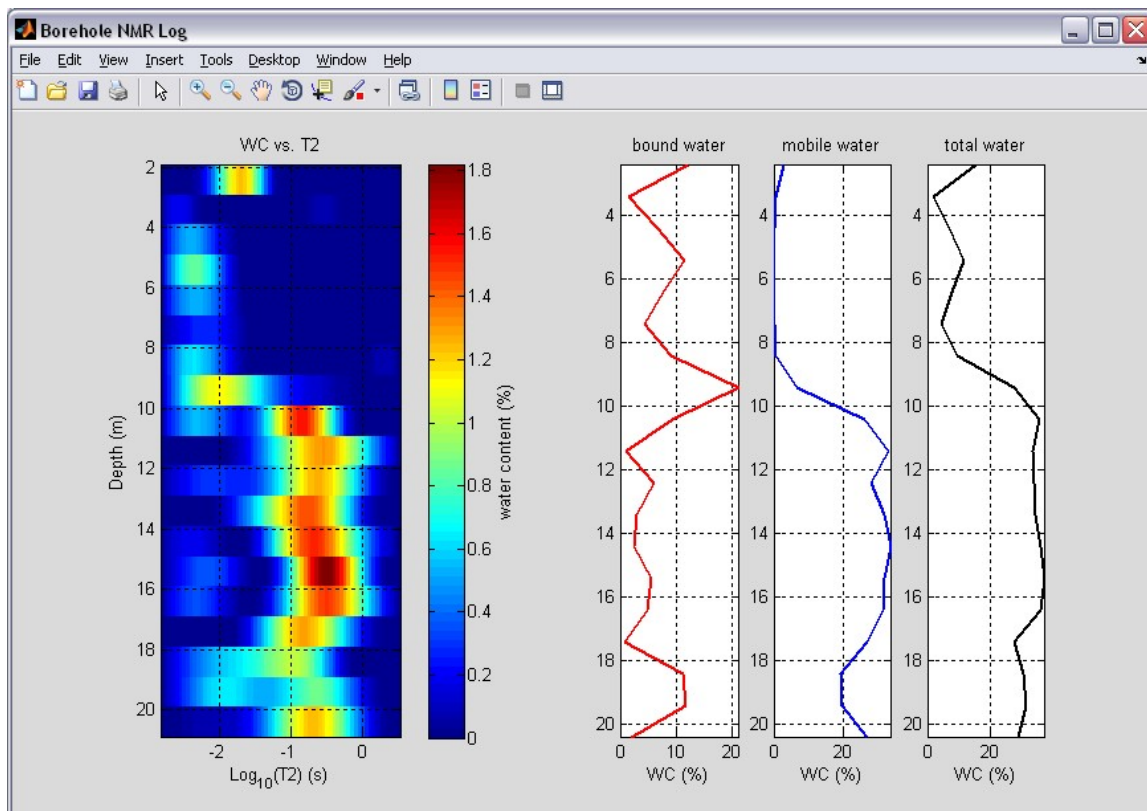


Figure 11: Borehole NMR log of well C1, prior to development, October 2010. Note the apparent decrease in T2 relaxation rate and increase in bound water content between 18m and 20m.

***DOE SBIR Topic# 33a: Integrated Use of Surface and Subsurface NMR for Measuring and Mapping Saturated Hydraulic Conductivity in Three Dimensions. Vista Clara Inc.***

The Geoprobe well installation method is expected to have a significantly different affect on the formation in the first few inches around the well, than the augering method. Specifically, when the auger was used for wells 4N and 4S, a significant amount of material was removed from the formation, and the formation was allowed to collapse back onto the installed 4" pvc pipe, resulting in an expected net increase in the porosity and/or pore sizes available to groundwater in the immediate vicinity of the well. In contrast, when the Geoprobe was used to install the three 2" diameter wells, material around the wells was compacted, resulting in an expected net decrease in the porosity and/or pore sizes in the immediate vicinity in those wells.

Additionally, the well development process – intensive localized pumping of water – is designed and performed to remove fine materials from the formation in the immediate vicinity of the well (Figure 12), and hence to increase the hydraulic conductivity of the formation in the immediate vicinity of the well casing. By installing two new wells in Phase 1, and performing NMR logging in those wells before, during and after development, we collected data to directly measure the effect of well development on the NMR logging results.



**Figure 12: Silty water being pumped out of well C1, as part the “well development” process.**

***Direct push NMR measurements (October 2010)***

Direct push NMR measurements were performed using a KGS-owned and operated Geoprobe machine, and the Javelin NMR logging instrument with an NMR logging probe specifically designed to operate with the Geoprobe machine. A photo Rosemary Knight and Dave Walsh with the Javelin direct push NMR probe is shown in Figure 13.

With the direct push NMR logging tool, the measurement is as follows:

1. A Geoprobe machine with 3.25" drill rods is used to create the borehole.
2. The NMR logging tool is pushed down the center of the drill rods to the bottom, using extendable plastic rods.
3. The drill rods are withdrawn upward approximately 4 feet as the NMR tool is held in place forcing the expendable drill point out of the bottom of the drill rods and exposing the NMR sensor to the formation. (See Figure 14 left.) The NMR probe has a special collar that locks the top part of the sensor in the lowest part of the Geoprobe drive shoe.
4. NMR logging is performed from the bottom up, using the Geoprobe machine to slowly withdraw both the drill rods and the NMR tool. (See Figure 14 right.)

We initially performed several partial direct push NMR measurements at GEMS, expecting to observe long relaxation times near the bottom of the sand/gravel aquifer. To our surprise, and initial concern, the partial DP NMR logs exhibited significantly shorter T2 decay rates, and significantly lower derived K estimates, than NMR borehole logs in nearby wells 4N and 4S that had been drilled and developed. The differences appeared to be largest in the section of the sand/gravel aquifer below 17m. We ultimately acquired 3 partial DP NMR logs and one complete DP NMR log at GEMS (complete DP NMR log shown in Figure 15). A number of intermediate tests were also performed to test the possibility that the Geoprobe drill rods were somehow influencing the results. These tests and analysis are described in the next subsection.

**DOE SBIR Topic# 33a: Integrated Use of Surface and Subsurface NMR for Measuring and Mapping Saturated Hydraulic Conductivity in Three Dimensions. Vista Clara Inc.**



**Figure 13:** Rosemary Knight (left, Stanford University) and Dave Walsh (right, Vista Clara) with the Javelin direct push NMR logging tool. Ed Reboulet (KGS) is in the background.



**Figure 14:** Left: KGS personnel deploying the direct push NMR logging tool through the bottom of the Geoprobe drill rods at GEMS. Right, NMR logging is performed from the bottom up, using the Geoprobe machine to slowly withdraw the drill rods and the exposed NMR tool.

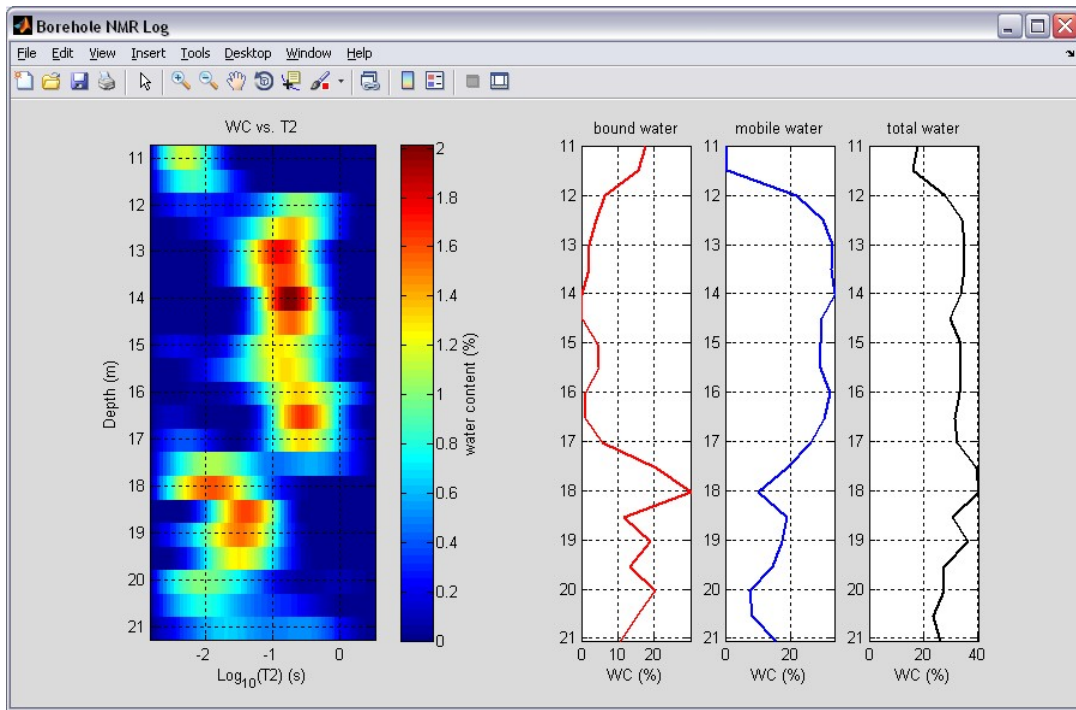


**Figure 15:** Direct push NMR log at GEMS. The source of initial concern was the unexpectedly low T2 relaxation below 17m.

### ***Existing direct K measurements at GEMS***

Two sets of previously collected K data from GEMS were used in Phase 1:

**Multilevel slug test K data from GEMS wells 4N and 4S** – The multilevel slug tests at these wells are described in Butler (2005). Both 4N and 4S were installed with hollow-stem augers (0.286-m OD flights) and constructed from PVC (0.102 m ID). A natural filter pack was used in the screened intervals and both wells were grouted across the overlying silt and clay interval. The multilevel slug test is an extension of the traditional slug test that is specifically tailored for characterizing vertical variations in hydraulic conductivity along the screened interval of a well. This approach involved the performance of slug tests in a 0.61-m portion of the screen isolated with a two-packer tool. A number of tests were performed in each isolated interval in order to assess the viability of test assumptions (Butler et al., 1996; Butler, 1998). Test data were analyzed using the methods discussed in Butler (1998) and Butler et al. (2003). A K profile was obtained through the sand and gravel aquifer at GEMS by repeating this process as the tool is moved in 0.61-m steps through the screened interval. The tool was specifically developed for slug tests in highly permeable aquifers, so the pneumatic method was used for test initiation to minimize the noise introduced by non-instantaneous initiation (Butler et al., 2003).

**Direct-push permeameter K data from DP profiles CP1029a and CP1029b** - The direct-push permeameter (DPP), the forerunner of the HRK tool used in phase 1, and the tests

**DOE SBIR Topic# 33a: Integrated Use of Surface and Subsurface NMR for Measuring and Mapping Saturated Hydraulic Conductivity in Three Dimensions. Vista Clara Inc.**

performed with it at GEMS are described in Butler et al. (2007). Twelve levels were tested with the DPP in profile CP1029a and nine levels in profile CP1029b. At each level, two tests were performed using similar injection rates (3.6 L/min). At the end of the second test, the DPP was advanced without altering the injection rate. A K estimate was calculated using the spherical form of Darcy's Law for each of the two tests performed at a given level as described in Butler et al. (2007). The difference between the two K estimates at each level was relatively small (<11% of average for all but one level [19% at that level]). These K estimates compared favorably to results of slug tests performed in nearby direct-push installations (Sellwood et al., 2005).

**New DP-K measurements obtained in Phase 1 near wells A1 and C1**

Shortly after NMR measurements were completed in wells A1 and C1 at GEMS2, two DP K profiles were obtained in the immediate vicinity (< 1.5 m) of each well using the High-Resolution K (HRK) tool recently developed at Kansas Geological Survey (Liu et al., 2009). The HRK tool combines two previous DP approaches, the direct-push permeameter (DPP; Butler et al., 2007) and the direct-push injection logger (DPIL; Dietrich et al., 2008), into a single probe. This combination produces collocated DPIL and DPP profiling data, allowing the high-resolution DPIL data to be directly converted into K estimates through a calibration procedure. The calibration procedure proposed by Liu et al. [2009] uses a numerical model to account for the DPIL measurements at their acquired resolution, thereby circumventing the need to compare measurements at different support scales. The HRK tool can produce K profiles at a vertical resolution (0.015 m) and speed that has not previously been possible. The focus of this work was on the K estimates obtained from the DPP profiling data, which can be more readily compared to the NMR measurements.

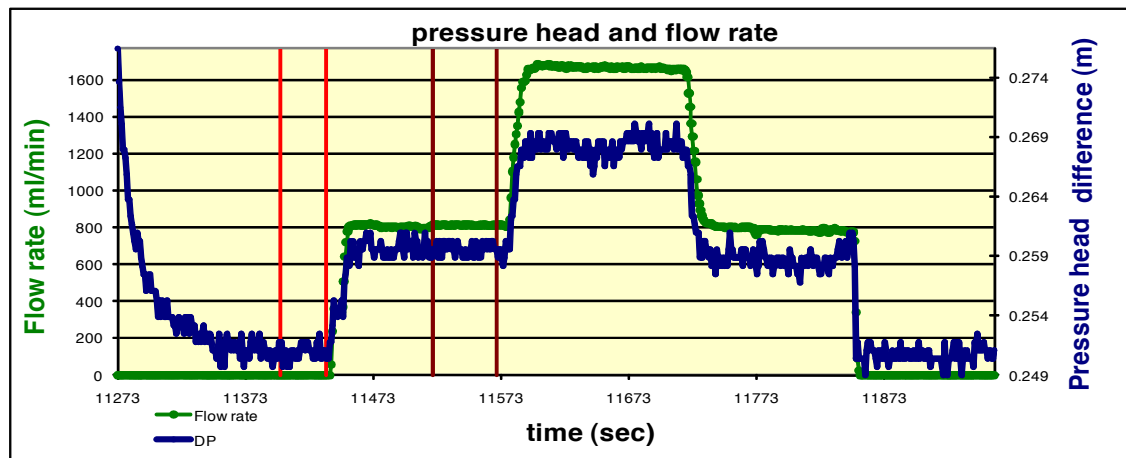
Consistent with the NMR measurements in wells A1 and C1, the HRK profiles were performed in the confined sand and gravel aquifer at GEMS2. The extremely low permeability of the upper silt and clay confining layer presented a difficult challenge for the HRK tool. During two initial profiling runs, very high injection pressures (> 100 psi) were produced when the HRK tool was advanced through the silt and clay layer. These high pressures caused disconnection of the DPIL flow line inside the probe. To overcome this challenge, a 2.5" solid drive point was used to pre-probe the upper silt and clay layer. The HRK tool was then pushed through the pre-drilled hole and K profiling started at the top of the confined sand and gravel aquifer. During the advancement of the tool in DPIL mode, flow rates for the top pressure transducer, bottom pressure transducer and tip screen were fixed at 800, 200 and 800 mL/min, respectively. When the tool reached the same depths as the NMR measurements in the nearby well, advancement was stopped and a series of DPP injection tests were conducted. The effective vertical sampling depth interval for each DPP test is about 0.4 m (Liu et al., 2008), which is comparable to that of the NMR measurement. A total of ten depth intervals were tested with the DPP in each HRK profile.

Figure 16 shows an example DPP test sequence conducted at a depth of 17.45 m in the profile near well A1. Figure 16(a) shows the injection rate through the tip screen (green

**DOE SBIR Topic# 33a: Integrated Use of Surface and Subsurface NMR for Measuring and Mapping Saturated Hydraulic Conductivity in Three Dimensions. Vista Clara Inc.**

curve) and the injection-induced pressure head difference between the top and bottom transducers (blue curve). Three step injection rates were applied in the sequence; flow was turned on at 800 mL/min, then increased to 1650 mL/min and finally cut back to 800 mL/min to check for repeatability. Figure 16(b) shows the individual pressures measured at both transducers during DPP flow injection. The pressure measured at the top transducer has a lower signal-to-noise ratio as the injection-induced pressure change is smaller (the top transducer is further away from the tip screen). The estimated K from the DPP flow tests at this depth is 66 m/d.

**(a) Injection rate and injection-induced pressure head difference between the top and bottom transducers**



**(b) Transducer pressures during DPP flow injection**

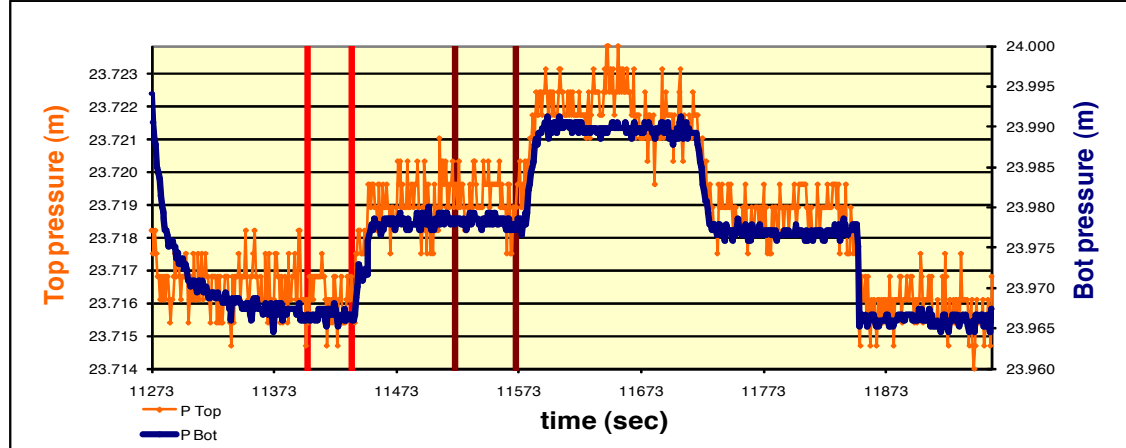


**Figure 16:** An example DPP test conducted at a depth of 17.45 m near well A1 at GEMS2. The estimated K at this depth is 66 m/d.

**DOE SBIR Topic# 33a: Integrated Use of Surface and Subsurface NMR for Measuring and Mapping Saturated Hydraulic Conductivity in Three Dimensions. Vista Clara Inc.**

**Summary of new and existing DP NMR, Borehole NMR and K data**

Tables 1 and 2 summarize the pre-existing and new logging NMR and direct K data that were collected and used in the Phase 1 research.

Well Name (Type)	NMR method	Location	Drill Method	NMR Tool	NMR Pre- development	NMR Post- development
4N (4" PVC)	Borehole NMR	GEMS	11" auger	3.5" Javelin borehole NMR	No	Yes
4S (4" PVC)	Borehole NMR	GEMS	11" auger	3.5" Javelin borehole NMR	No	Yes
HT6 (2" PVC)	Borehole NMR (new)	GEMS (near 4N)	3.125" Geoprobe	1.7" Javelin borehole NMR	No	Yes
NMR2 (DP)	DP NMR (new)	GEMS (btw. 4N/4S)	3.125" Geoprobe	2.5" Javelin DP NMR	Yes	No
A1 (2" PVC)	Borehole NMR (new)	New Area A	3.125" Geoprobe	1.7" Javelin borehole NMR	Yes	Yes
C1 (2" PVC)	Borehole NMR (new)	New Area C	3.125" Geoprobe	1.7" Javelin borehole NMR	Yes	Yes

**Table 1: Summary of borehole/DP NMR logging data collected before and during Phase 1, and used to develop/evaluate logging NMR-K transforms.**

Direct K ID	Measurement type	Location	Drill method	K tool	Pre- or Post- development
4N	MLST	GEMS	11" auger		Post
4S	MLST	GEMS	11" auger		Post
HT6		GEMS (near 4N)	3.125" Geoprobe		
CP1029a	DP-K	GEMS (near 4S)	2.375" Geoprobe	DP permeameter	Pre
CP1029b	DP-K	GEMS (near 4N)	2.375" Geoprobe	DP permeameter	Pre
DP808	DP-ST	GEMS (btw. 1029a/b)			
A1-DPK	DP-K (new)	New Area A	2.375" Geoprobe	HRK	Pre
C1-DPK	DP-K (new)	New Area C	2.375" Geoprobe	HRK	Pre

**Table 2: Summary of direct K measurements collected before and during Phase 1, and used to develop/evaluate logging NMR-K transforms.**

**Observed differences in DP NMR and borehole NMR data**

We initially performed several partial direct push NMR measurements at GEMS, expecting to observe long relaxation times near the bottom of the sand/gravel aquifer. To

**DOE SBIR Topic# 33a: Integrated Use of Surface and Subsurface NMR for Measuring and Mapping Saturated Hydraulic Conductivity in Three Dimensions. Vista Clara Inc.**

our surprise, and initial concern, the partial DP NMR logs exhibited significantly shorter T2 decay rates, and significantly lower derived K estimates, than NMR borehole logs in nearby wells 4N and 4S that had been drilled and developed. The differences appeared to be largest in the section of the sand/gravel aquifer below 17m.

We were concerned that some form of magnetic effect from Geoprobe drill rods could be the cause of the observed shorter T2 relaxation. We performed a number of analytical tests in the field at GEMS and later in the laboratory to test the theory that the Geoprobe drill rods were responsible for the shorter than expected T2 relaxation rates:

- Direct measurement and mapping of the static B0 magnetic field from the NMR sensor, with the Geoprobe rods positioned near the head of the sensor. (See Figure 17 left). This test showed that the presence of the Geoprobe rods caused negligible distortion of the static magnetic field in the NMR sensitive region.
- NMR measurement of bulk water in a plastic barrel, with the NMR probe attached to the Geoprobe drill rods. (See Figure 17 right). This test resulted in a normal NMR T2 relaxation of approximately 1000ms, which is typical for bulk water measurements with this tool.
- Laboratory measurements of bulk water, to which we had added significant amounts of metal filings sanded off of a Geoprobe rod. We added enough rusted and non-oxidized rod filings to significantly discolor the water, but the T2 of the bulk water only decreased slightly (from 2.3s to 1.2s) as a result.



**Figure 17: Left: direct measurement of static magnetic field of sensor with Geoprobe rods attached, showed no significant distortion of field. Right: NMR measurement of bulk water in close vicinity of Geoprobe showed normal water content and long T2 relaxation.**

Thus, several tests were designed and performed to prove that the DP NMR measurements were biased by a magnetic and/or redox effect caused by the use of the steel Geoprobe drill rods. All of these tests have proven negative. One complete direct push NMR log of the sand/gravel unit was obtained in the vicinity of two previous direct push K measurements at GEMS, and this DP NMR log is shown in Figure 18. Two other

**DOE SBIR Topic# 33a: Integrated Use of Surface and Subsurface NMR for Measuring and Mapping Saturated Hydraulic Conductivity in Three Dimensions. Vista Clara Inc.**

partial DP NMR logs performed within a few feet of this measurement were very consistent with this one complete DP NMR log, and a fourth partial DP NMR log obtained 15 meters to the east of this location also showed short T2 relaxation in the section of the sand/gravel unit below 17m, and consistent NMR-derived K values (see Figure 18). This indicates that the DP NMR measurement is a repeatable over a 1m lateral distance, and is perhaps sampling the spatial heterogeneity over a 15m lateral distance at GEMS.

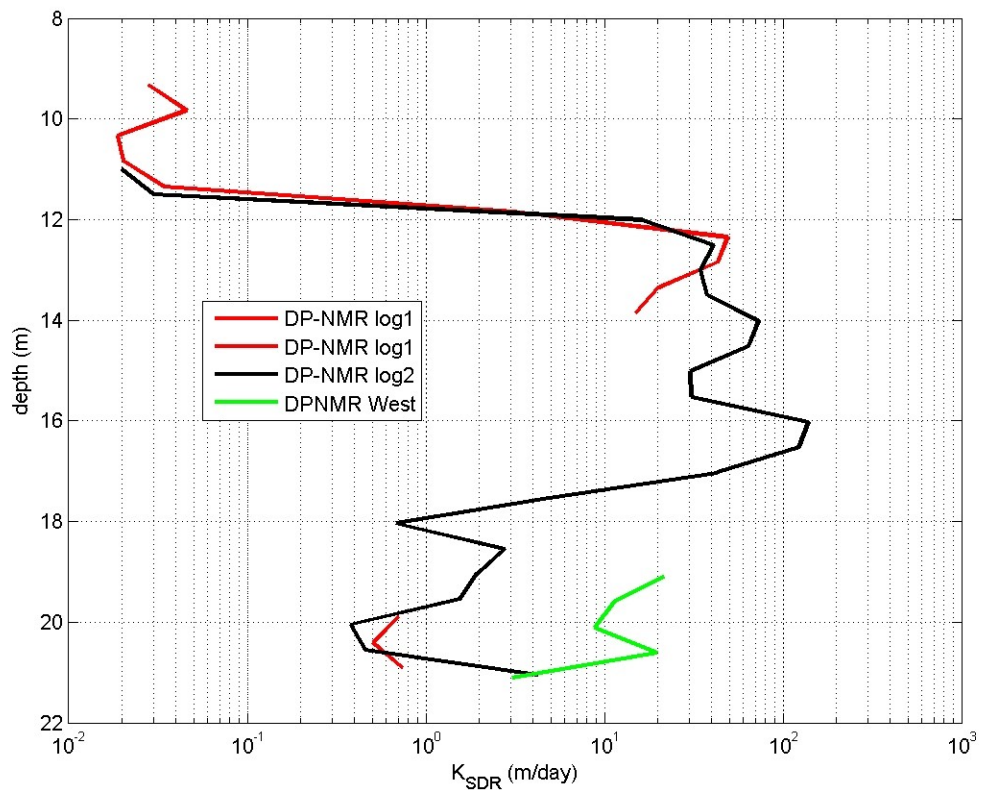


**Figure 18: Derived K values for DP NMR logs at GEMS, October 2010. The partial log (DP-NMR log 1) and the completed NMR log (DP-NMR log 2) were separated by approximately one meter, and the partial log (DPNMR West) was obtained approximately 15 m away (actually to the East of the other DP NMR logs).**

#### ***Change in NMR response due to well development***

Two new 2" pvc wells were installed in the new areas A and C near the GEMS facility. These were installed using the Geoprobe machine, with the screened sections of PVC installed through the entire sand/gravel unit except the bottom 5 feet, which were not screened. On each of these two new wells, we performed complete NMR logs of the sand/gravel section before any development was performed, and also after one or two stages of development. This allowed us to directly measure the effect of development on the NMR logging response, and the NMR-derived estimates of hydraulic conductivity.

**DOE SBIR Topic# 33a: Integrated Use of Surface and Subsurface NMR for Measuring and Mapping Saturated Hydraulic Conductivity in Three Dimensions. Vista Clara Inc.**

Figure 19 shows the NMR log of well C1 before any development. Figure 20 shows the NMR log of well C1 after two stages of development. Short T2 NMR signal components are clearly reduced in the NMR data after development. Figures 21 and 22 show the mean Log T2 and NMR-derived hydraulic conductivity, respectively, before and after development. Mean log T2 is uniformly higher in the post-development data, on average by a factor of approximately 2 to 3. The NMR-estimated K is also uniformly higher after development. In the zone between 18m and 19m, the NMR-derived K is increased by a factor of 6 to 8, due to well development.

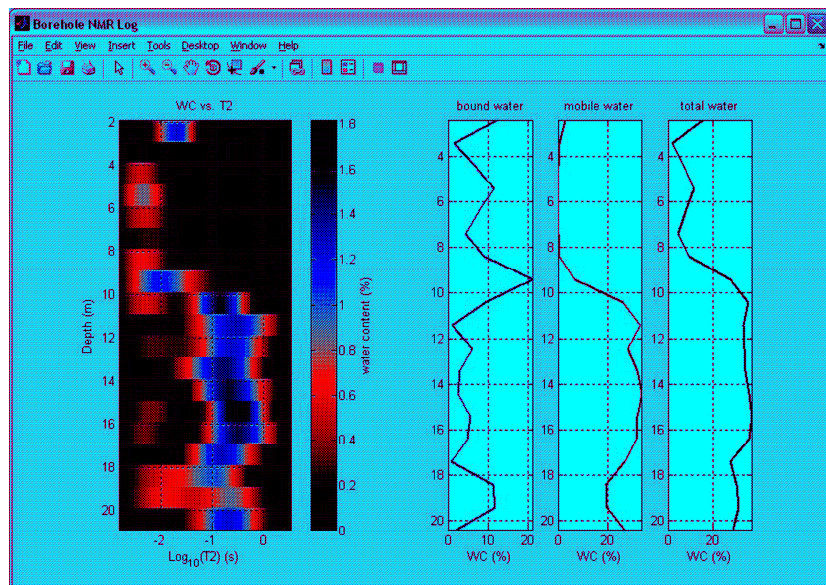


**Figure 19:** NMR log of well C1 before development. Note the significant detection of bound water throughout the sand unit below 10m.

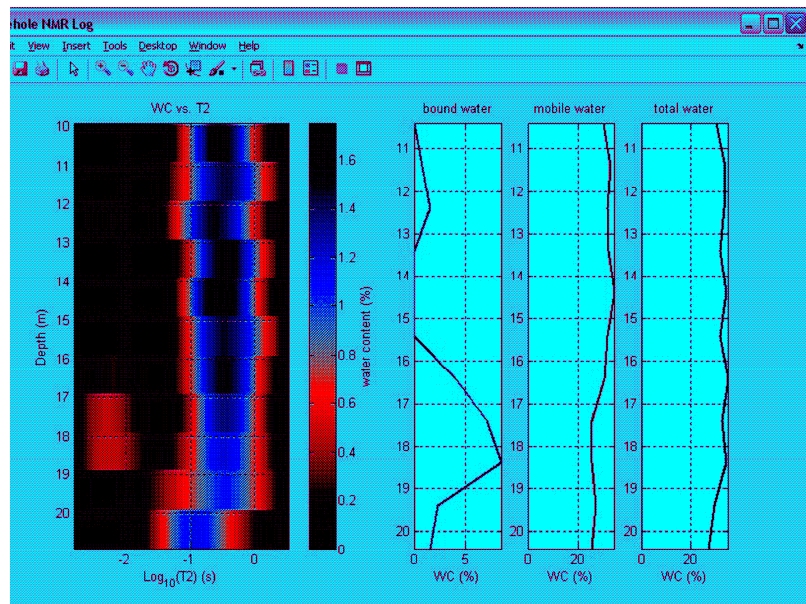


**Figure 20:** NMR log of well C1 after 2 stages of development. The NMR-estimated bound water content is now reduced or absent compared to the pre-development NMR log.

**DOE SBIR Topic# 33a: Integrated Use of Surface and Subsurface NMR for Measuring and Mapping Saturated Hydraulic Conductivity in Three Dimensions. Vista Clara Inc.**

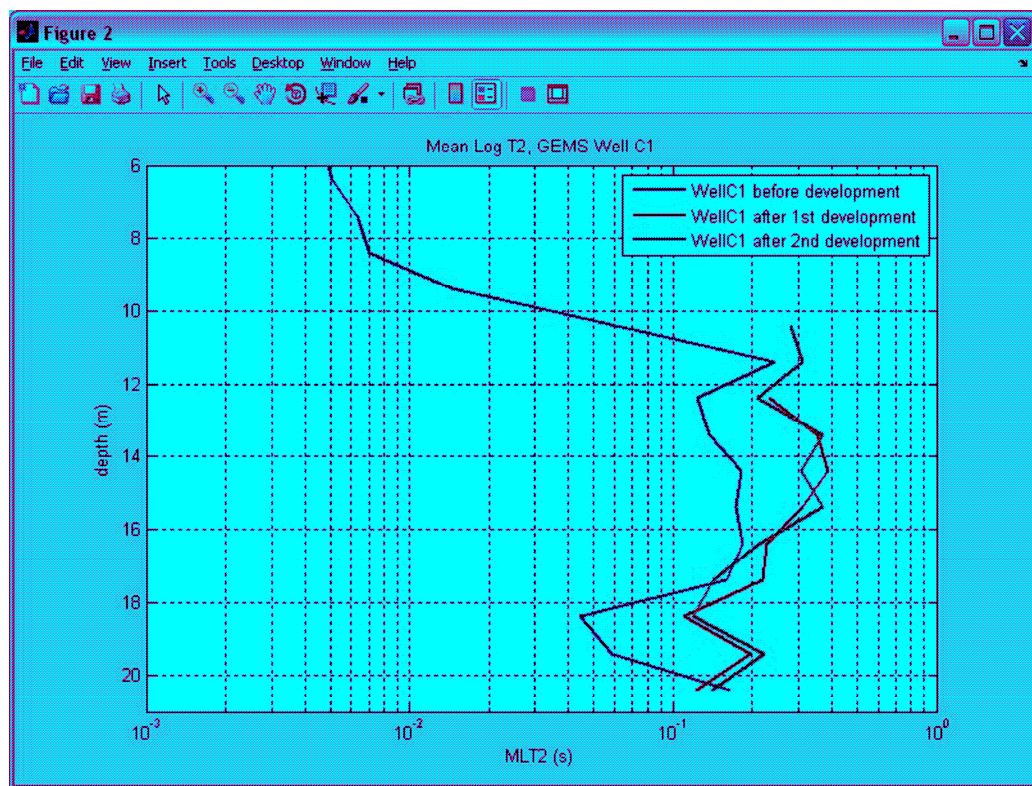


**Figure 21:** T2 mean log of NMR data from well C1, before and after development.

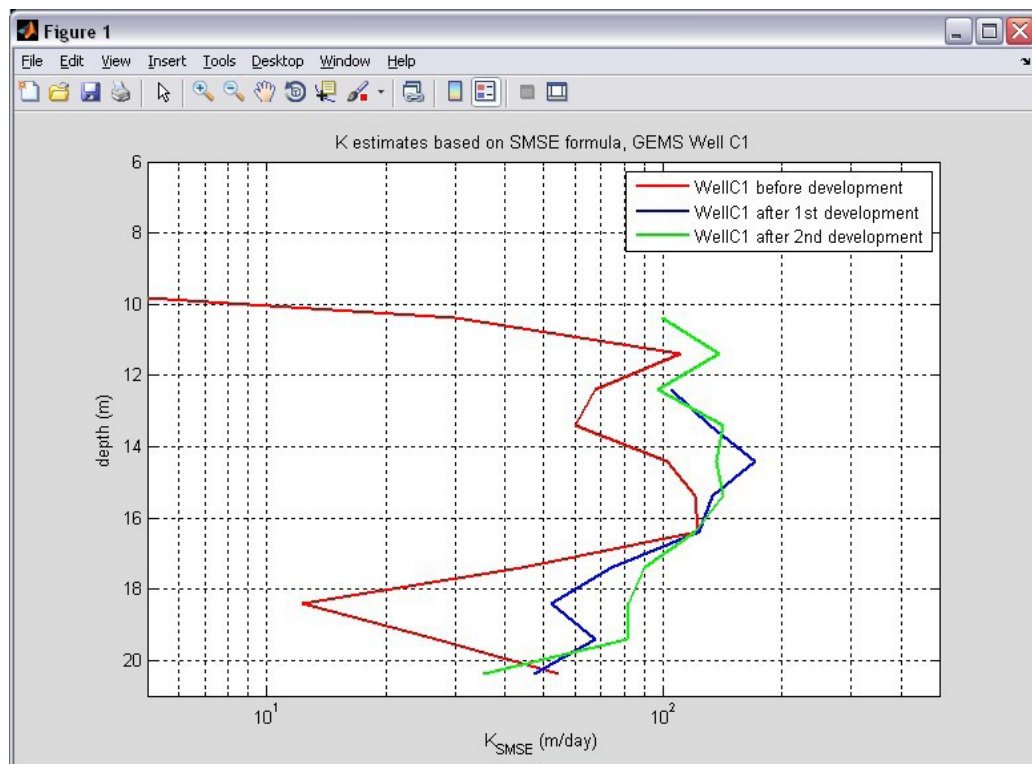


**Figure 22:** NMR-derived K estimates from well C1, before and after development.

***DOE SBIR Topic# 33a: Integrated Use of Surface and Subsurface NMR for Measuring and Mapping Saturated Hydraulic Conductivity in Three Dimensions. Vista Clara Inc.***

At the conclusion of the Phase 1 research, we had not developed a consensus among the members of our research team to explain the observed differences between the DP NMR and borehole NMR measurements at GEMS. We performed several tests to examine whether the Geoprobe drill rods could be causing the NMR signals to exhibit faster T2 decay. We showed that there is no significant distortion of the static magnetic field in the NMR sensitive zone. We showed that the addition of iron filings from the Geoprobe drill rods to bulk water (both heavily oxidized and fresh steel filings) did not significantly reduce the T2 relaxation time of bulk tap water in Mukilteo Washington. There are lingering questions as to whether the Geoprobe rods could be causing a temporary change in the NMR surface relaxivity of sand in the lower section of the aquifer, through some change in the redox conditions, presumably triggered by the Geoprobe rods.

Some members of our research team are now inclined to believe that the differences observed between DP NMR and borehole NMR measurements are measurement of real differences in the physical pore environments within the NMR sensitive region, due to the different well construction methods and development effects (or lack thereof).

There is one conclusive way to settle the possibility that the Geoprobe rods are contaminating the T2 measurement: perform DP NMR logging at GEMS using entirely non-magnetic and non-reactive (e.g. stainless steel) drill rods. We have included this testing in our Phase 2 research plan.

**Calibration Using NMR Logging Data and K Data to Determine NMR-to-K Transform**

*This portion of the Phase 1 research was performed by Stanford University.*

Available from the GEMS and GEMS2 sites are Phase 1 NMR logging measurements obtained using the Vista Clara Javelin NMR logging instrument. NMR logging measurements included use of the 1.7 in and 3.5 in diameter borehole NMR logging tools, and a 2.5 in diameter DP NMR logging tool that was deployed using the KGS Geoprobe machine. Also available for this study were previously-obtained K estimates from multilevel slug tests (MLST) and from DP measurements. We limited our analysis in Phase 1 to data acquired in the gravel and sand unit at the sites. The depth interval for the sampling was typically on the order of 0.5 m. The data selected for analysis were:

- 1) borehole NMR (acquired using the 3.5 in diameter tool) and MLST-K measurements made in Wells 4N and 4S at the GEMS site;
- 2) borehole NMR (acquired using the 1.7 in diameter tool) and DP-K measurements made at sites A (well A1) and C (well C1) in the GEMS2 area.
- 3) DP-NMR and DP-K measurements made at one location at the GEMS site.

K can be estimated from the NMR measurements using the following Schlumberger-Doll Research (SDR) equation:

$$K_{SDR} = b \phi^m (T_{2ML})^n \quad (9)$$

***DOE SBIR Topic# 33a: Integrated Use of Surface and Subsurface NMR for Measuring and Mapping Saturated Hydraulic Conductivity in Three Dimensions. Vista Clara Inc.***

where b, m, and n are empirically determined constants,  $T_{2ML}$  is the mean log of the NMR logging  $T_2$  relaxation time distribution (provided by Vista Clara) and  $\phi$  is the porosity determined from the NMR data (provided by Vista Clara). The constant b is referred to as the lithologic constant. In using the above equation we elected, as is common practice, to set the exponent n on the  $T_{2ML}$  term equal to 2.

The objectives of this component of the study were to 1) determine the values of the empirical constants in the SDR equation that would optimize the agreement between K predicted from the NMR data and K from the MLST or DP measurements acquired at the same location; 2) assess the error/uncertainty in K predictions when the empirical constants were used to predict K at a nearby site. The optimization was done using a least squares inversion. We used five different inversion methods, including unconstrained, semi-constrained, and constrained inversions. In the semi-constrained inversion, the exponent m on the porosity term was constrained to be positive, ranging from 0.5 and 4, increasing in value with an interval of 0.5; there was no constraint on the lithologic constant. In three forms of a constrained inversion, the exponent m on porosity was constrained to be 1, 2 and 4; there was no constraint on the lithologic constant.

The inversion could be conducted in two ways. The first would be to set our objective function to be minimized as the difference between NMR-derived K, denoted as NMR-K, and true K, denoted as TRUE-K; i.e. we minimize  $[(NMR-K)-(TRUE-K)]$ . To do this, we would use a nonlinear least squares method, with equation 1 as given above used to calculate NMR-K. Alternatively we can rewrite equation 9 in linear form:

$$\log(K_{SDR}) = \log b + 2\log(T_{2ML}) + m \log \phi \quad (10)$$

and use a linear least squares method to solve for b and m. In this case we would minimize  $[\log(NMR-K)-\log(TRUE-K)]$ . Due to the distribution observed in the K measurements at the sampling locations, we elected to use this second approach.

### **Logging NMR to K Calibration Results**

*This portion of the Phase 1 research was performed by Stanford University.*

Let us start by presenting a Table that clearly illustrates the need for improved relationships to predict K from NMR data. In Table 3 we present the measured true K values from the various sample locations at GEMS and GEMS2, and the K that would be predicted from the acquired NMR data using the standard values for the empirical constants ( $b=4$ ,  $m=4$ ) in the SDR equation. We note that these values have been adopted after many years of research for oil and gas applications, where the geologic materials tend to be consolidated sandstones, not sands and gravels. Clearly the predictions are not accurate, indicating a need to develop relationships that are valid for the types of high permeability materials encountered in near-surface environments.

**DOE SBIR Topic# 33a: Integrated Use of Surface and Subsurface NMR for Measuring and Mapping Saturated Hydraulic Conductivity in Three Dimensions. Vista Clara Inc.**

Dataset	Mean K values (m/day)	
	TRUE-K	NMR-K (using standard oilfield SDR coefficients)
Well 4S	81.5	2.1
Well 4N	79.4	0.36
Well C1	109	
Pre-development		0.92
Post-development #1		2.5
Post-development #2		2.3
Well A1	42	
Pre-development		0.29
Post-development		0.66
NMR2	182	0.42

**Table 3: Comparison of the mean TRUE-K values and means of the NMR-K derived using the standard SDR coefficients ( $b=4$  and  $m=4$ ) derived for sandstones in oil/gas exploration. Results are shown for all available datasets.**

We began our analysis of the data by determining, for each data set, the empirical constants that provided optimal fit between K predicted from the acquired NMR data and true- K from the same, or nearby, location. A detailed discussion of the data analysis and results is given in Appendix 1. Table 4 contains the results. In the unconstrained inversion, there is a wide range of values, including negative values for m. Given the relatively small variation in observed porosity within the sand/gravel unit at the GEMS sites, we opted to constrain the inversion by setting m equal to values in the range typically observed. When m is constrained such that  $m > 0$ , the lithologic constant (b) varied considerably, even though we were in the same sand and gravel unit at the different locations.

Dataset	Method 1: Unconstrained Inversion	Method 2: Semi- Constrained Inversion $0.5 < m < 4$	Method 3: Constrained Inversion $m=1$	Method 4: Constrained Inversion $m=2$	Method 5: Constrained Inversion $m=4$
Well 4S	$b=1.3e7; m=8$	$b=1.3e5 ; m=4$	$b=4.4e3$	$b=1.4e4$	$b=1.3e5$
Well 4N	$b=3.4e3; m=-0.8$	$b=2.0e4; m=0.5$	$b=4.0e4$	$b=1.6e5$	$b=2.4e6$
Well C1					
Pre	$b=2; m=-7.5$	$b=1.2e4; m=0.5$	$b=2e4$	$b=5.9e4$	$b=5.2e5$
Post #1	$b=65; m=-2.7$	$b=2.6e3; m=0.5$	$b=4.7e3$	$b=1.5e4$	$b=1.4e5$
Post #2	$b=4.3e5; m=5$	$b=2.9e3; m=0.5$	$b=5e3$	$b=1.5e4$	$b=1.5e5$
Well A1					
Pre	$b=7.8e6; m=7$	$b=5.4e3; m=0.5$	$b=9.4e3$	$b=2.9e4$	$b=2.7e5$
Post	$b=1.2e4; m=1.5$	$b=6.7e3 ; m=1$	$b=6.7e3$	$b=2.2e4$	$b=2.3e5$
NMR2	$b= 4e2; m=-3.1$	$b=2.7e4; m=0.5$	$b=4.9e4$	$b=1.6e5$	$b=1.6e6$

**Table 4: The values for the empirical constants found for each data set using the different inversion methods. “Pre” and “Post” are used to indicate that the NMR data were acquired before (Pre) and after (Post) development of the well. The addition of #1 and #2 indicates that there were two stages of development.**

**DOE SBIR Topic# 33a: Integrated Use of Surface and Subsurface NMR for Measuring and Mapping Saturated Hydraulic Conductivity in Three Dimensions. Vista Clara Inc.**

In defining these empirical constant, we used all of the data acquired at depth intervals of ~0.5 m in the sampled locations; the figures in the Appendix show a comparison of the NMR-predicted-K and true K at all depths, for all data sets. An example is shown here in Figure 23 for the data from Well 4S. As described, given the form of the optimization, the residuals are presented in terms of log K for each data set. We also include a presentation of the error, defined as  $[(\text{NMR-K}) - (\text{TRUE-K})]/(\text{TRUE K})$ , in order to better see the expected agreement between NMR-derived and true K values.

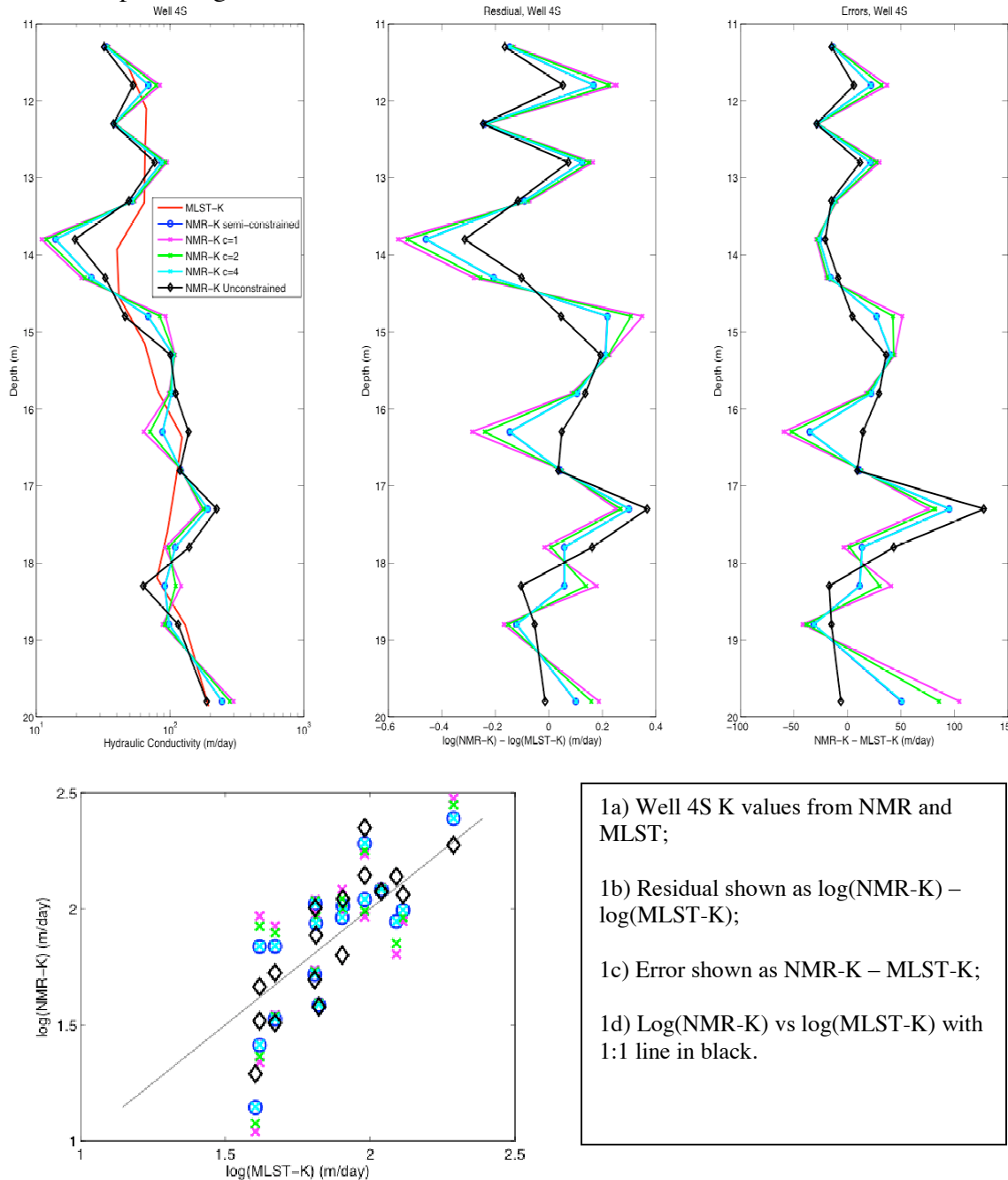


**Figure 23: Comparison of NMR-derived and MLST-derived K estimates from GEMS well 4S, at all measured depth levels.**

**DOE SBIR Topic# 33a: Integrated Use of Surface and Subsurface NMR for Measuring and Mapping Saturated Hydraulic Conductivity in Three Dimensions. Vista Clara Inc.**

We also compared the arithmetic mean of true K, using all of the K measurements across the entire sand and gravel unit, to the arithmetic mean of the predicted K values. The results are given in Table 5.

Dataset	Arithmetic Mean K values (m/day)					
	True-K	Predicted NMR-K				
		Method 1	Method 2	Method 3	Method 4	Method 5
Well 4S	81.5	91.0	90.5	94.0	92.6	91.0
Well 4N	79.4	127	156	169	201	295
Well C1	109					
Pre		167	149	150	154	164
Post #1		110	109	114	115	120
Post #2		117	116	116	116	116
Well A1	42					
Pre		24.5	30.6	29.7	28.2	26.0
Post		44.0	43.0	43.0	45.1	51.0
NMR2	182	206	213	215	220	232

**Table 5: Comparison of the arithmetic mean of the TRUE-K values and arithmetic mean of each set of NMR-K values, derived using the empirical constants from each inversion method. Results are shown for all available datasets. “Pre” and “Post” are used to indicate that the NMR data were acquired before (Pre) and after (Post) development of the well. The addition of #1 and #2 indicates that there were two stages of development.**

As can be seen, with this site-specific calibration, we get good agreement between the predicted and true K values. We note that the development of the well clearly impacts the measured NMR parameters. Our understanding, at this stage of our research, is that the NMR data acquired post-development are the appropriate data to compare with the DP K data.

The methodology that we propose involves acquiring NMR and K data at one location, referred to as the calibration location, that are used to establish the best empirical relationship to use to complete an NMR-to-K transform from NMR data acquired at other locations. We were therefore interested in comparing, for a number of data sets, the arithmetic mean of TRUE-K at a location to the arithmetic mean of NMR-K at the same location, where NMR-K is estimated using the NMR-K relationship established at some other calibration location. In order to simplify the presentation of these results, we elected to use the empirical constants determined using inversion method 5, setting m=4.

In our analysis we have used NMR and K data from:

- 1) Well 4S, with the NMR data transformed to K using the NMR-K relationship determined at Well 4N, approximately 11 m away;
- 2) Well 4N, with the NMR data transformed to K using the NMR-K relationship determined at Well 4N, approximately 11 m away;

***DOE SBIR Topic# 33a: Integrated Use of Surface and Subsurface NMR for Measuring and Mapping Saturated Hydraulic Conductivity in Three Dimensions. Vista Clara Inc.***

- 3) Well C1, with the NMR data (post-development #2) transformed to K using the NMR-K relationship determined at Well A1 (using the post-development data), approximately 300 m away;
- 4) Well A1, with the NMR data (post-development) transformed to K using the NMR- K relationship determined at Well C1 (using the post-development #2 data), approximately 300 m away.

The results are compiled in Table 6. We compare the K values and also the log K values, given that our calibration method was set up to optimize the agreement between the log K, measured and predicted, values. The results from Wells C1 and A1 are very encouraging, while the results from Wells 4S and 4N suggest that we need to conduct a more complete analysis of both the NMR and K data to understand the source of the error in the predicted values.

Dataset	Calibration Location	Mean K (m/d)		Mean Log (K (m/d))	
		TRUE-K	NMR-K	TRUE-K	NMR-K
Well 4S	Well 4N	81.5	1700	1.87	3.14
Well 4N	Well 4S	79.4	15.6	1.65	0.374
Well C1	Well A1	109	181	1.97	2.16
Well A1	Well C1	42	32.7	1.31	1.12

**Table 6: Comparison of true K values to K predicted from NMR data, using a calibration from another location.**

**C.2.2 Demonstrate the feasibility of translating the NMR-to-K transform from the borehole/DP NMR measurement regime to the surface NMR measurement regime**

**Collection of Surface NMR Data**

*This portion of the Phase 1 research was performed by Vista Clara and the Kansas Geological Survey in Lawrence Kansas. Stanford University also participated in some of the GMR data collection.*

GMR surface NMR measurements were collected at three areas in the vicinity of GEMS in October 2010. A photo of the GMR instrumentation at GEMS new area C is shown in Figure 24. At each of the three sites, we collected the 5 sets of high quality surface NMR data:

- FID sequence with 10ms pulse, for best resolution of short T2\* signals.
- FID sequence with 20ms pulse, for good resolution of short T2\* and depth of investigation > 20m
- FID sequence with 40ms pulse, for highest spatial resolution in the sand.gravel unit and ability to investigate the underlying limestone formation.
- Spin echo sequence with 3 echo delays, to directly measure T2 relaxation.
- 90-90 sequence to measure T1 relaxation.

Figures 25 – 28 show representative surface NMR data collected at GEMS in Phase 1. We used relatively small diameter loops (22m – 44m diameter) to produce high resolution data covering the targeted sand/gravel aquifer over its depth range of 9m – 22m. The acquired data generally exhibit good to excellent signal to noise ratios (e.g. Figure 25) and high spatial resolution in the upper 25m as depicted in Figure 26. For the free induction decay (FID) sequences, which measure water content and T2\* relaxation, we used three different pulse lengths of 10ms, 20ms and 40ms, at each location to produce a wide range of data. The short-pulse (10ms) FID data are best able to detect and resolve very short T2\* NMR signals in silt and clay. The long-pulse (40ms) FID data provide the highest spatial resolution of long T2\* NMR signals in the sand and gravel and also in the underlying limestone formation.

Figure 27 shows the multi-exponential inversion of the water content and T2\* distribution vs. depth at new area C, using a 44m circular loop and a 20ms transmit pulse. This image graphically reveals the key aquifer properties vs. depth, including: detection of very short T2\* signals in the silt/clay in the top 10m; the sharp transition to longer T2\* signals in the sand unit from 10m – 16m, an apparent change in character between 16m and 22m to include probable isolated clay/silt lenses, and the limestone aquifer below 25m. Spin-echo surface NMR measurements (Figure 28) provided a direct surface NMR measurement of T2 at each site, though only the T2 signals longer than 50ms are detected due to relaxation during the pulse sequence. T1 measurements were also performed at each site, but due to the limited scope of effort were not evaluated in Phase 1.

**DOE SBIR Topic# 33a: Integrated Use of Surface and Subsurface NMR for Measuring and Mapping Saturated Hydraulic Conductivity in Three Dimensions. Vista Clara Inc.**



Figure 24: Jim Butler (KGS) setting up the GMR equipment at GEMS new area C.

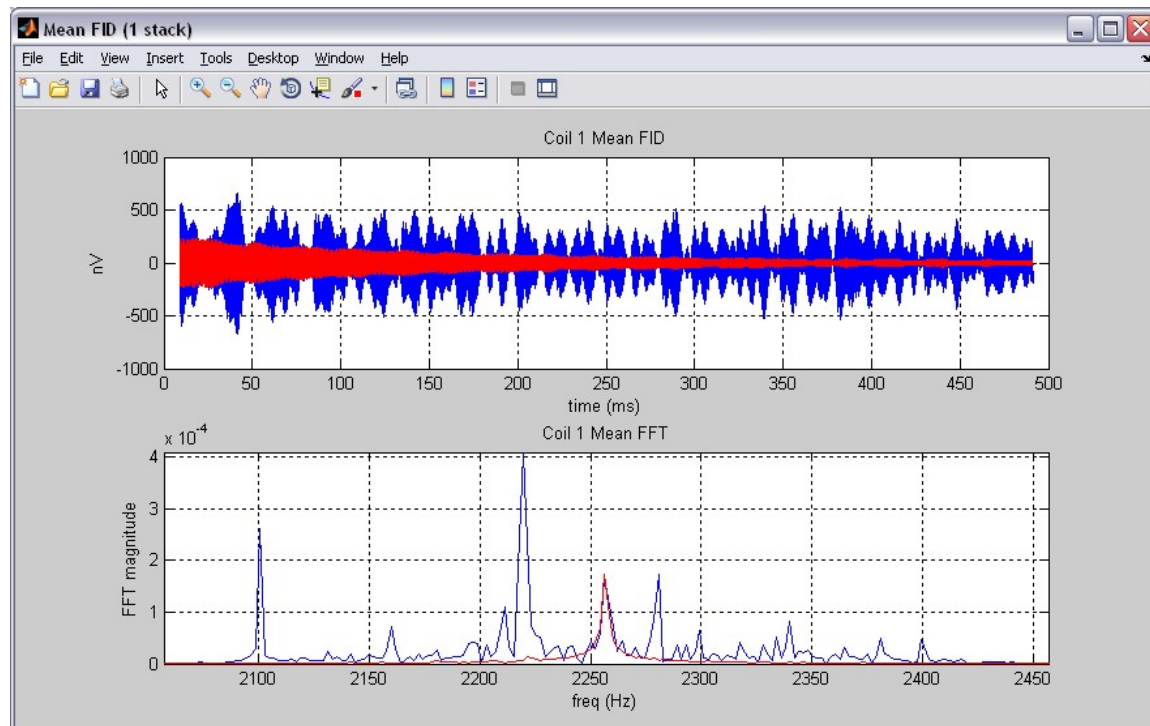
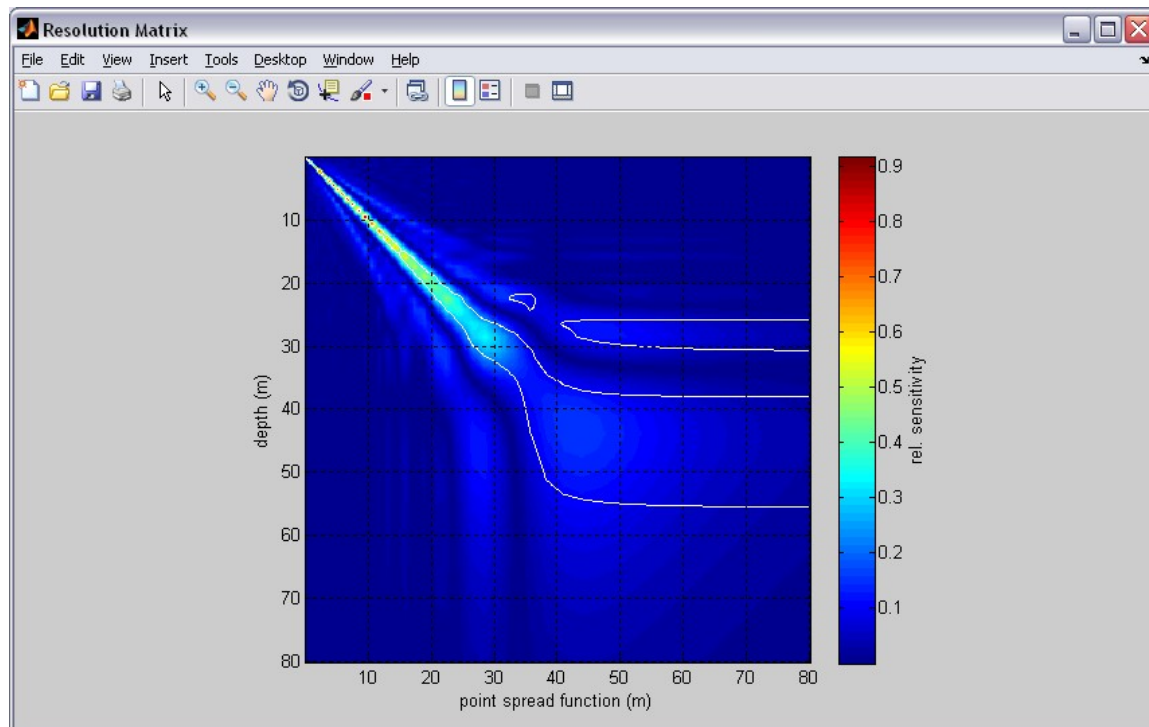
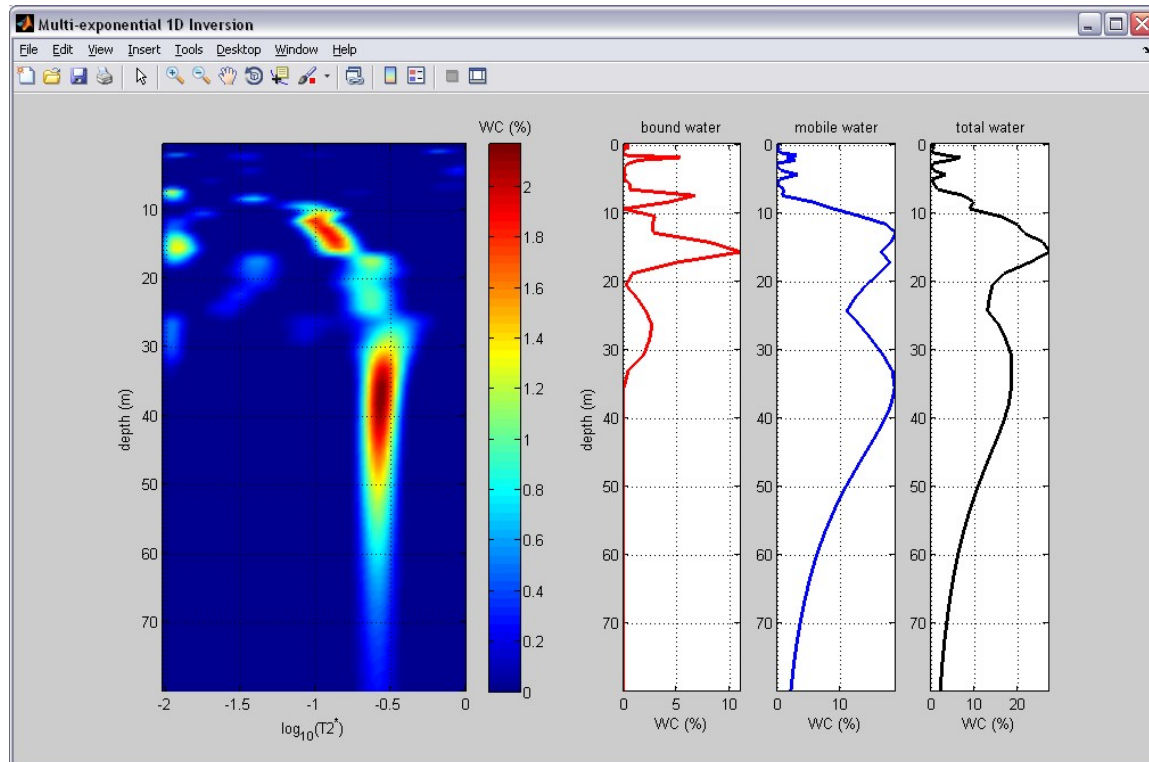


Figure 25: Surface NMR free induction (FID) signal from 44m circular loop at new area C. (Red trace shows the FID signal and its frequency spectrum after noise cancellation.)

**DOE SBIR Topic# 33a: Integrated Use of Surface and Subsurface NMR for Measuring and Mapping Saturated Hydraulic Conductivity in Three Dimensions. Vista Clara Inc.**



**Figure 26:** Resolution matrix for 20ms FID sequence indicates good sensitivity and depth resolution to a depth of about 30m.



**Figure 27:** Multi-exponential inversion from new area C shows distinct transition between silt/clay and sand at 10m, increased silt or clay around 17m, and long  $T2^*$  signals from the underlying limestone formation below about 25m.

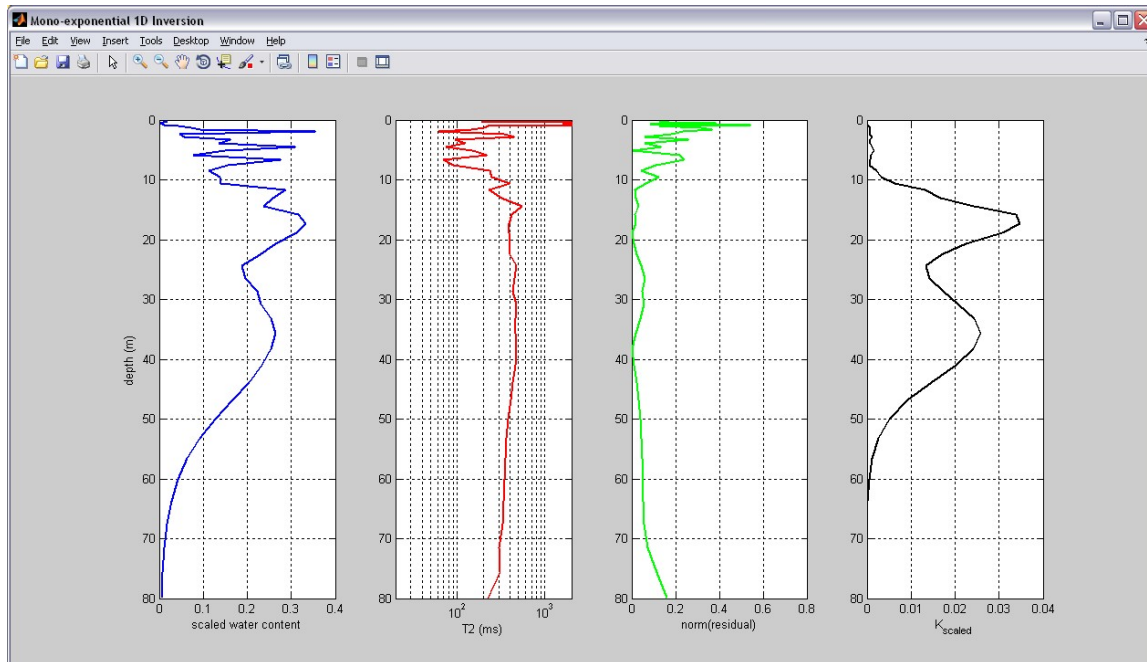


**Figure 28:** Spin echo data from new area C provide mono-exponential fit of  $T_2$ , and spin echo derived water content.

### Transform linking surface NMR to borehole NMR Data

*This portion of the Phase 1 research was performed by Stanford University.*

We have proposed that estimating  $K$  from SNMR data will involve two transform steps. The first transform is required to account for differences in the NMR physics between the logging (borehole and DP) NMR and surface NMR measurements. The details of our development of this transform, and a number of figures presenting the analyzed data, are given in Appendix 1.

In order to develop this first transform, we compared NMR logging and surface datasets acquired at sites A, C, and D in the GEMS2 Area. The surface data included SNMR Free Induction Decay (FID) datasets (both 20 ms and 10 ms shown), which provide estimates of water content and the relaxation time  $T_2^*$ , shown as  $T_{2ML}^*$ ; SNMR spin echo (SE) datasets, which provide estimates of water content and the relaxation time  $T_2$ , determined from a mono-exponential fit to the decay curve.

There are two key observations that guided the development of the transform. First, we found that FID measurements of  $T_{2ML}^*$  consistently under-predict the logging measurements of  $T_{2ML}$ . This reflects the fact that the physics controlling  $T_2^*$  is different from that controlling  $T_2$ .  $T_2^*$ , unlike  $T_2$ , is affected by dephasing in an inhomogeneous magnetic field. The magnitude of this dephasing effect is represented by the term  $T_{2IH}$  and tends to have a more significant effect on measured relaxation rates in coarser materials. In the coarse sand and gravel unit under investigation here, the  $T_{2IH}$  term is likely the main factor leading to differences between  $T_2^*$  and  $T_2$ .

Second, we find that SNMR estimates of water content are consistently much lower than the logging NMR estimates. This discrepancy likely results from the fact that the SNMR inversion approach used here does not take into account the effect of a conductive earth on the attenuation of NMR transmit and receive signals. Neglecting the influence of a conductive earth will have two effects: First it will lead to underestimation of water content, and second, it will make NMR signals appear deeper than they actually are.

Given the observed differences between the SNMR data and the logging data, we quantify a water content scaling relationship and the magnitude of the  $T_{2IH}$  term. We make a simple assumption that differences in water content between the two types of data can be described by a simple linear scaling parameter  $z$ . We estimate the value of  $z$  for each site as the ratio of the maximum water content estimated from logging NMR divided by the maximum estimated water content from surface NMR. We estimate the magnitude of the  $T_{2IH}$ , based on the equation

$$1/T_2^* = 1/T_2 + 1/T_{2IH} \quad (11)$$

taking the maximum values of  $T_2$  and  $T_2^*$  determined over the sand and gravel interval. For all sites, we find that  $z$  is around 2 (1.7-2.9) and  $T_{2IH}$  is around 0.150 (0.13-2.1).

The transformed estimates of water content provide slightly better agreement with the logging data. However, because a scaling coefficient cannot account for errors in depth resolution, we find that water content is still greatly underestimated at shallower depths. Compared to the original  $T_{2ML}^*$  values, the transformed estimates of  $T_{2ML}$  show greater consistency with the logging  $T_{2ML}^*$  values.

### **Predicting K from surface NMR Data**

*This portion of the Phase 1 research was performed by Stanford University.*

Having transformed the SNMR data to be more closely representative of NMR logging data, the second, and final, transform is to apply the coefficients determined from analysis of the logging NMR data. Our hypothesis is that the NMR-  $K$  relationships developed for borehole NMR can also be used for the SNMR data after we first establish a basic transform between the NMR parameters measured by logging and surface NMR.

We worked with the SNMR datasets transformed, as described above (using  $n=2$  and  $T_{2IH}=0.15$ ), and estimated  $K$  using the previously determined coefficients. For each site, we used just one set of SDR calibration coefficients determined from the closest coincident logging NMR and true  $K$  measurements. We chose to examine only one set of coefficients given that the uncertainty associated with the SNMR/logging transform is much greater than the uncertainty associated with the  $K$  transform coefficients. Given that the majority of sites showed the best fit with a value of  $m=0.5$ , we fixed this value and for each site used the calibrated values of  $b$  determined from the predevelopment

***DOE SBIR Topic# 33a: Integrated Use of Surface and Subsurface NMR for Measuring and Mapping Saturated Hydraulic Conductivity in Three Dimensions. Vista Clara Inc.***

data. (We note that in Phase 2 one of the issues that requires resolution is whether we should be using the pre-development or post-development data for the calibration).

We found that K estimates based on the  $T_2^*$  surface data prior to any transform show trends consistent with the true K data but significantly underestimate the true K value, by approximately 1 order of magnitude. Following the surface/logging transform, we found that the K predicted from the SNMR data shows in general good agreement with true K, particularly in the deeper zones. K is underestimated at some sites in the shallow zones; this is likely due to depth resolution errors.

In the table 7 we list the arithmetic mean of true K and K predicted from the SNMR data using the various estimators. The K values from the SNMR data are averaged over the region representing the sand and gravel layer, identified by an initial rise in  $T_2^*$ . We find that the average values of K derived from NMR after the surface/logging transform are in very close agreement with the average values of K determined from direct measurements.

Well Site	SNMR Site	True K	SNMR K $T_2^*$ before transform	SNMR K $T_2^*$ SE before transform	NMR K $T_2^*$ after transform
A1	A	42	7	263	41
C1	C	109	35	307	135
1029a	D	182	17	267	141
4N	D	81	--	--	--
4S	D	79	--	--	--

**Table 7: Comparison of true K and surface-NMR derived K estimates, averaged over the entire sand/gravel aquifer unit. The  $T_2^*$ -derived K consistently under-estimates K, and the surface NMR  $T_2^*$ -derived K consistently overestimates K. The  $T_2^*$ -derived K after surface/logging transform is highly consistent with true K at all three measurement locations.**

We find that estimates of K from SNMR determined after the surface/logging transform and using NMR/K transform coefficients provide good estimates of permeability in the sand and gravel unit at the KGS test site. This serves to demonstrate the feasibility of our integrated logging and surface NMR approach.

### **C.2.3 Demonstrate the feasibility of gaining additional information on K and groundwater flow through in-situ NMR measurement of flow**

#### **Demonstration of borehole NMR flow data**

*This portion of the Phase 1 research was performed by Vista Clara Inc. and the Kansas Geological Survey.*

Simple experiments were performed in the laboratory and in the field to demonstrate that the Javelin NMR logging tool with the standard CPMG sequence could detect moderate

**DOE SBIR Topic# 33a: Integrated Use of Surface and Subsurface NMR for Measuring and Mapping Saturated Hydraulic Conductivity in Three Dimensions. Vista Clara Inc.**

flow rates in bulk water. These experiments were conducted by positioning various Javelin borehole NMR tools in a plastic drum containing fresh water, and performing CPMG measurements (the standard Javelin NMR logging measurement) with the water circulating slowly in the barrel at different velocities.

A comparison of two such experiments is shown in Figures 29 and 30. In Figure 29 the water was circulating slowly, after being stirred slowly by hand, and the mean log T<sub>2</sub> is measured as 0.23 s. In Figure 30 the same water was measured after the water had been allowed to settle for 30 minutes. The measured mean log T<sub>2</sub> is more than twice as long at 0.59s. Even after 30 minutes there was still some very slow circulation and convection occurring. In a perfectly motionless sample the mean log T<sub>2</sub> is expected to be 1.0s or longer.

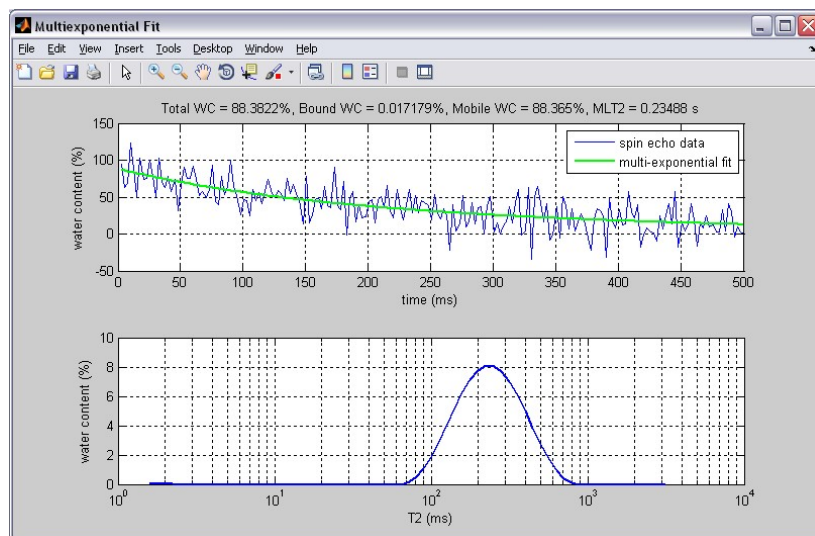


**Figure 29:** T<sub>2</sub> distribution for bulk water circulating slowly in a plastic barrel, measured using Javelin with 2.5" direct push NMR tool.

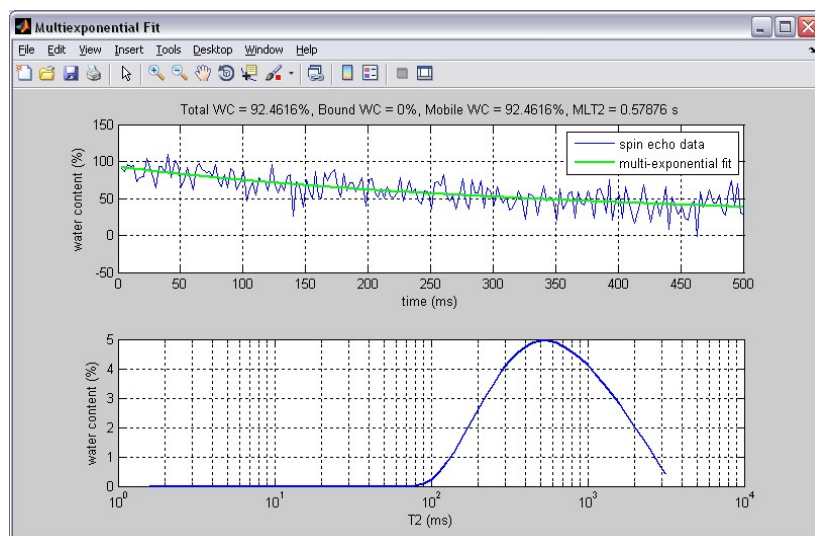


**Figure 30:** T<sub>2</sub> response 30 minutes later, when the water was almost motionless in the barrel (some slow convection was still occurring). Note the shift towards longer T<sub>2</sub>.

We performed one NMR flow experiment in a well at GEMS. This test is shown in Figure 31. The 3.5" Javelin NMR tool was lowered to a depth of 16.5m in GEMS well 4N. A small electric pump was used to draw water from another well at the eastern edge of the site and into the top of well 4N, at a rate of approximately 14 gallons per minute. We performed standard CPMG measurements, first with the pump off, then with the pump on. However, the resulting T2 distributions were not significantly different, both had a measured mean log T2 of 0.24s.

We subsequently estimated the velocity of flow expected within the 2mm thick, 15-inch diameter NMR sensitive region, assuming the inflow from the pump at 15 gallons/minute (1 liter/s) was exiting uniformly within the 10m thick sand/gravel unit, and also assuming uniform flow velocity within the ~30% mobile water fraction in that unit. The volume of a 15" diameter, 2mm thick, 10m long cylinder was calculated as  $0.0241\text{m}^3$ , or approximately 24 liters. The lateral flow velocity within the NMR sensitive region was thus estimated as:

$$V = \frac{(1.0l / s)}{24l} \cdot \frac{2mm}{.3} = 0.278\text{mm/s}. \quad (12)$$

Thus we estimate that under these assumptions the water was being completely in the NMR sensitive was being replaced approximately once every 7s. Thus we would not expect such a low flow rate to be detectable using the standard CPMG sequence.

These results demonstrate that the proposed flow measurement concept is feasible. They also indicate that for future in-situ NMR flow measurements we should plan to increase the localize flow velocity in the NMR sensitive region in order to ensure that we can measure flow and its velocity distribution through the NMR response. In particular the following modifications to the experiment should enable NMR detection of flow within the sand/gravel unit at GEMS:

1. Increase the inflow rate, using a water tank and/or larger pump.
2. Use inflatable packers to force most of the water to flow through a narrow depth interval where the NMR tool is located.
3. Use an NMR tool with a smaller diameter, and thinner sensitive region, such as the 1.7" borehole tool, and/or by operating each tool at a higher frequency. Detecting flow at a small radius is easier because the average flow is assumed proportional to  $1/(radius)$ .
4. Possibly, synchronize the NMR measurement with an electronically-triggered slug test.

**DOE SBIR Topic# 33a: Integrated Use of Surface and Subsurface NMR for Measuring and Mapping Saturated Hydraulic Conductivity in Three Dimensions. Vista Clara Inc.**



**Figure 31: Attempted flow NMR measurement of flow, well 4N, at GEMS.**

### **Borehole NMR-Flow Patent Status**

*This portion of the Phase 1 research was performed by Vista Clara Inc.*

In Phase 1, we performed a quick literature and patent search to identify the existence of possible intellectual property barriers to performing in-situ NMR flow measurements in commercial practice. We found several relevant patents held by oil field services companies that could limit our ability to commercialize the proposed NMR flow measurement method.

US Patent No. 6,710,596, filed in 2002 and assigned to Schlumberger Technology Corporation in 2004, appears to hold the broadest set of claims in this area. This patent includes two independent claims, which describe the deployment of an NMR logging tool in a wellbore, inducing flow within the formation, and using the NMR tool to measure the velocity of flow within the formation to determine the formation pressure. These two independent claims also disclose a requirement that the wellbore include “a pressurized mudcake” which is apparently utilized to induce and control the flow, and that the objective of the procedure is to “determine a formation pressure”. These latter requirements are not relevant to our proposed methodology, and there is no mention in the patent of measuring a “velocity distribution” or using such a distribution to predict contaminant transport.

So, while there appears to be significant prior art and patented methodology in this area, there also appears to be some space for Vista Clara to develop distinct and focused intellectual property protection, and eventually commercialize a methodology for using borehole NMR flow measurements in applications to near surface aquifer characterization and remediation.

### ***C.3 Summary Assessment of Technical Feasibility***

In summary, the key tenets of our proposed methodology are technically feasible:

- We demonstrated a site-specific logging NMR to K transform that is repeatable and provides reasonable estimates of K from logging NMR measurements along a  $\frac{1}{2}$  mile stretch of aquifer in Lawrence KS. When evaluated for high-resolution (0.5m depth resolution) K measurements across a set of 8 borehole NMR and DP NMR measurements with various well construction methods and various stages of development, the K estimation error/uncertainty was less than 1 order of magnitude. When evaluated for estimating the average K of an aquifer, using a set of two wells constructed using the same method and spaced  $\frac{1}{4}$  mile apart, the K estimation uncertainty factor was +/- 1.5.
- We demonstrated that surface NMR measurements of the same aquifer, over the same investigated areas, can provide reasonable estimates of the average K of the aquifer. The use of an intermediate transform, between the logging NMR T2 regime and the surface NMR T2\* regime, reduces the error/uncertainty in the

***DOE SBIR Topic# 33a: Integrated Use of Surface and Subsurface NMR for Measuring and Mapping Saturated Hydraulic Conductivity in Three Dimensions. Vista Clara Inc.***

surface NMR-derived K estimates. The depth resolution of surface NMR derived K measurements and errors in SNMR-derived total water content were thought to be the largest sources of residual error in the Phase 1 study. The incorporation of electrical conductivity effects in the surface NMR inversion (part of the Phase 2 work plan) should mitigate this source of error/uncertainty in the future.

- We demonstrated that borehole NMR measurements of induced flow in a high-K formation can provide information on the flow velocity distribution within the formation. Other more sophisticated NMR measurements could be applied in Phase 2 and beyond. There are existing “live” patents in this technology area, but there also appears to be space to develop and commercialize new NMR flow measurement techniques for applications in hydrology and groundwater remediation.

Our Phase 1 research and results also raised new and interesting questions, and possible new opportunities:

- How does the drilling method affect the NMR-derived K estimates (and also the direct K methods that we are calling “true K”)?
- Well development activities clearly have a significant influence on the borehole NMR measurements. How can we account for these effects? Is it better to measure the NMR in a pre- or post-developed well, or both?
- Why does the direct push NMR consistently measure lower T<sub>2</sub>, than the borehole NMR measurements, in the lowest section of the GEMS sand/gravel aquifer?
- Can the borehole NMR tool be used, commercially, to inspect the construction and condition of the well bore and/or grout seal outside the PVC casing? What are the potential impacts of this application in groundwater remediation efforts?

## **D. The Phase II Project**

### **D.1 Phase II Technical Objectives**

Overall Phase 2 will extend upon the work from phase one to include a broader range of lithologies. The aim is to develop and demonstrate a robust and site-transferable approach for integrating logging NMR and SNMR to map K across a wide range of environments.

- 1. Develop and demonstrate methodology for predicting K and uncertainty from logging NMR in a broad class of near-surface lithologies. Methodology will follow from phase 1 approach but with additional focus on (1) quantifying measurement variance; (2) rigorously investigating validity of logging NMR/K transforms; (3) and doing so across a broader range of lithology types.**

- 1.1. Quantify the repeatability of different K and logging NMR measurements and variance of measurements over very short distances. Key questions to answer include:**

- To what extent, if any, does iron content in the Geoprobe drill rods affect the DP-NMR measurements?
- Which types logging NMR and direct K measurements provide the highest repeatability over a very short lateral distance?
- How do the following individual factors quantitatively impact the error and uncertainty in the NMR-derived K estimates at GEMS?
  - Well construction method, including variance in the quality and repeatability of work performed by drilling contractor(s).
  - Well development.
  - Radial depth of investigation of the logging NMR probe.

- 1.2. Develop and demonstrate improvements upon existing NMR/K transforms for various near-surface lithology types, including high and low K, based on controlled investigations of pore-scale NMR/K physics. Key questions to answer include:**

- How does differing lithology impact the transform coefficients in three different regional and hydrogeological settings?
  - Does a lithology with higher magnetic susceptibility significantly alter the logging NMR-K transform coefficients?
  - What is the performance and limitations of the proposed methodology in moderate to low-K aquifers?
- What is the expected error and uncertainty of NMR-derived K estimates applied to a broader range of near surface unconsolidated and semi-consolidated lithologies?

- 2. Develop and demonstrate methodology for using limited logging NMR and K measurements, with higher density surface NMR measurements, to map hydraulic conductivity in three dimensions.**
  - 2.1. Incorporate state-of-the-art field coil modeling software to improve surface NMR inversion accuracy in electrically conductive geology.
  - 2.2. Determine the extent to which the approach from phase 1 (dual transforms) is valid/transferable within other lithologies:
    - lower permeability aquifers
    - aquifer materials with high magnetic susceptibility
    - different geological areas of the US.
  - 2.3. Demonstrate high resolution mapping of hydraulic conductivity in two and three dimensions at one field site, using the proposed integrated NMR/K methodology.
- 3. Develop and demonstrate a methodology for using NMR-derived (and perhaps DP-K-derived) flow velocity distributions to predict a contaminant plume distribution over space and time.**
  - 3.1. Design and assemble a new Javelin NMR logging tool to measure flow velocity distributions at different radial depths within a formation.
  - 3.2. Develop a commercially viable methodology for using the Javelin NMR logging probe to directly measuring flow and the velocity distribution within a formation.
  - 3.3. Demonstrate NMR-based measurement of velocity distribution, and estimation of moving and static fluid in pore spaces, in the laboratory and in boreholes.

## **D.2 Phase II Work Plan**

The proposed Phase 2 STTR research will be performed by three separate organizations, each contributing significant and focused efforts to achieve the overall project goals:

- **Vista Clara Inc.**, the designated “Small Business Concern”, will provide the NMR geophysical equipment, field measurement expertise and interpretation software that is central to the proposed methodology. The Phase 2 work plan includes significant new data collection efforts at three field sites in the US, and Vista Clara will lead the NMR data collection and processing efforts at all three sites. Vista Clara will also be responsible for scheduling and coordinating all field work in the State of Washington. Vista Clara’s President, **Dr. David O. Walsh**, will serve as Principal Investigator for the project and oversee the technical direction and management of the Phase 2 STTR project and budget.

- **Stanford University**, the designated “Research Institution”, will be responsible for development of mathematical methods for translating surface and logging NMR measurements into estimates of hydraulic conductivity, and for assessing the performance of these transformations across a broad range of lithological settings. Stanford University will also design and execute supporting laboratory NMR and petrophysical measurements, through their extensive laboratory NMR and geochemistry facilities. **Dr. Rosemary Knight** of Stanford University will direct the Stanford University portion of the Phase 2 research, manage the Stanford subcontract and budget, and directly manage all participating Stanford University personnel and facilities.
- **Kansas Geological Survey**, under a major subcontract, will provide a wide range of direct push machinery and instrumentation, traditional hydrological testing methods, drilling, well construction and well development services, and general expertise in the application of hydrogeophysical methods to aquifers in Kansas. KGS will also be responsible for the scheduling and coordination of all field work in Kansas. **Dr. James (Jim) Butler** of the Kansas Geological Survey will direct the KGS portion of the Phase 2 research, manage the KGS subcontract and budget, and directly manage all participating KGS personnel and facilities.

### **D.2.1 Develop and demonstrate a methodology for predicting K and uncertainty from logging NMR in a broad class of near-surface lithologies.**

This section of the Phase 2 work plan is aimed at improving and refining the mathematical/statistical link between logging NMR data (including DP-NMR) and hydraulic conductivity K. We seek to answer some of the important questions raised by the Phase 1 results, and develop a methodology that is robust and appropriate for applying subsurface NMR to estimate K in unconsolidated and semi-consolidated near surface aquifers.

The methodology will follow from the phase 1 approach but with additional focus on:

1. Quantifying measurement variance, including inherent bias due to methodology.
2. Rigorously investigating validity of LNMR/K transforms.
3. Increasing the range of lithologies to low-K and high magnetic susceptibility.

#### **D.2.1.1 Assess and quantify the repeatability of different K and logging NMR measurements and variance of measurements over very short distances.**

*This portion of the Phase 2 research will be performed by Vista Clara and the Kansas Geological Survey, in and around the GEMS facility in Lawrence Kansas. Most of the data collection for this task will be performed in year 1.*

**Determine effect (or absence of effect) of Geoprobe rods on DP NMR measurements**

The direct push NMR measurements in Phase 1 showed decreased T2 relaxation in lower zones of the GEMS sand/gravel unit. This result was unexpected at the time of the measurements. We performed a variety of experiments in the field at GEMS and later in the laboratory to try to prove that the shortening of the NMR signal was due in some way to the magnetic effect of the steel Geoprobe drill rods. The results of all tests that we have performed to date have been negative. That is, none of the tests indicate that the steel drill rods are the cause of the shorter observed NMR signals in the direct push NMR logs.

In Phase 2 we will perform DP-NMR measurements in the same area of GEMS using specially manufactured non-magnetic Geoprobe rods to conclusively determine whether the steel Geoprobe rods are a source of influence on the measured NMR relaxation rates. Vista Clara will purchase a small number of new sections of 3.125" diameter Geoprobe drill rods, manufactured from two different types of metal. The rods will be manufactured to order by Geoprobe, in Salina KS.

The first rod material will be manufactured using a steel stock that has been treated with nitride gas to harden the outer surface. Geoprobe has made these nitride-treated rods in the past, and the Kansas Geological Survey has used these rods in the past for sampling dissolved oxygen in the same aquifer at GEMS. In their previous use, KGS determined that the use of the nitride-treated steel rods significantly reduced contamination of the dissolved oxygen measurement (presumably through redox reaction with iron particles introduced by the standard drill rods) in the lower section of the aquifer.

The second rod material will be stainless steel. Some grades of stainless steel are almost completely non-magnetic, and stainless steel is relatively inexpensive and easy to machine. Stainless steel is softer than the high carbon steel used in standard Geoprobe rods, and hence the rods are more likely to deform and the threads more likely to jam under heavy hammering. We are not expecting these rods to be useful for more than a few tests at GEMS. However we only need to use them once (or perhaps a few times) to determine whether the standard steel rods are a source of error/uncertainty. Geoprobe has previously manufactured stainless steel rods for special applications such as this, and stainless steel probes have been used at GEMS.

As part of the first year data collection at GEMS, Vista Clara and KGS will perform DP-NMR measurements in a small area of GEMS using the three different drill rods in the following order: stainless steel, nitride treated steel, and standard steel. The nitride-treated and stainless drill rods, approximately 8 five-foot sections of each, and a set of stainless steel drive points, will be manufactured by Geoprobe and delivered to KGS. We will log the entire sand/gravel unit including the lower section where redox changes have been suspected and investigated in the past.

If the data from the three types of drill rods in the same vicinity show significant repeatable differences, then we will conclude that the differences are due to the magnetic influence or redox changes due to the drill rod material. If there are no significant

***DOE SBIR Topic# 33a: Integrated Use of Surface and Subsurface NMR for Measuring and Mapping Saturated Hydraulic Conductivity in Three Dimensions. Vista Clara Inc.***

observed differences, then we will conclude that hydrological and pore space differences, rather than the standard steel Geoprobe rods, are responsible for the observed shorter T2 NMR signals.

**Assess the repeatability and variance of logging NMR and direct K measurements at GEMS**

The phase 1 results indicated significant differences between DP-NMR (Geoprobe NMR) measurements and borehole NMR measurements spaced only a few meters apart. The phase 1 results also showed that borehole NMR measurements are sensitive to well development activities – specifically, intensive pumping to develop the well invariably caused the measured NMR T2 relaxation to get longer. Assessment of previous DP-K and borehole-derived-K measurements at GEMS indicate that DP-K profiles using the same tool within a few meters are consistent, but differ significantly from K profiles derived from other DP-K tools (i.e. DP slug test) and also differ significantly from nearby borehole K measurements (i.e. multilevel slug tests).

In the first year of Phase 2, Vista Clara and KGS will perform repeated, spatially co-located logging NMR and K measurements at GEMS to assess the repeatability and sources of variance for these different measurements.

***New measurements to assess repeatability and variance:***

A diagram of the proposed co-located measurements is shown in Figure 32. New DP-NMR and DP-K measurements will be performed in a 1m diameter circle surrounding one of the Geoprobe-installed 2" PVC wells:

- Vista Clara and KGS will perform 3 independent DP-NMR logs at GEMS, all within 2m of each other, and all surrounding an existing PVC-cased well (C1).
- KGS will then perform 3 independent DP-K measurements around the same well, using the latest generation HRK-tool.
- KGS will then perform a multi-level slug test in the developed well C1.

This compact measurement geometry will make best use of the existing borehole and phase 1 borehole NMR measurements, and will allow for rigorous quantification of both self-variance and cross-variance between DP-K, DP-NMR, borehole MLST-K, and borehole NMR (both pre- and post-development).

**DOE SBIR Topic# 33a: Integrated Use of Surface and Subsurface NMR for Measuring and Mapping Saturated Hydraulic Conductivity in Three Dimensions. Vista Clara Inc.**

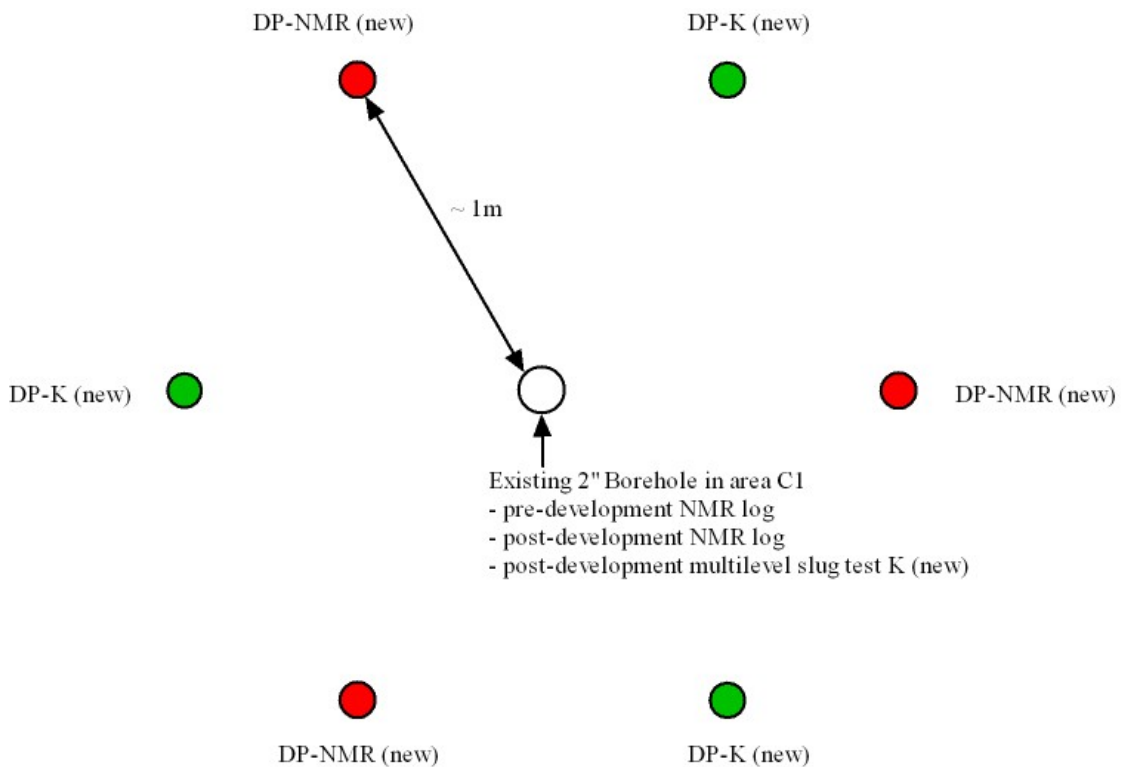


**Figure 32: Overhead view of new DP-K and DP-NMR measurements arranged within 1m of an existing 2" PVC well at GEMS.**

After completion of direct push NMR and K measurements, KGS will install two more 2" diameter PVC wells within a few meters of existing well C1. The first new well will be installed in an identical manner to the existing well C1, using a Geoprobe machine with 3.125" diameter drill rods to install 2" diameter screened PVC over the sand/gravel unit, with a 5 foot non-screened PVC sump at the bottom of the well. The second new well will be installed using a hollow-stem auger. The second well will be cased with 2" screened PVC over the same interval as the Geoprobe-installed wells, and the sand/gravel formation will be allowed to collapse against the screened interval.

NMR logging will be performed using a new 1.75" NMR logging probe (see details in section D.2.3.1). Both new wells will be logged at two or more radial depths of investigation (via two or more frequency-selected NMR detection shells). NMR logging will be performed before any development of the wells, and also after one or two stages of moderate development, to acquire pre- and post-development data that is comparable to what we measured in Well C1 in Phase 1. We will also perform one pre-development NMR log in the two new wells using the same 1.67" NMR logging tool that we used to log well C1 in Phase 1. KGS will perform multi-level slug tests in prescribed sections of all three wells in the post-development condition.

***Assessment of repeatability and variance:***

Vista Clara and KGS will jointly interpret the new and existing data from the 2m diameter study area around Well C1 to quantify the statistical self-variance and cross-variance of the following measurements:

- Variance of 3 DP-NMR measurements within a 2m area.
  - Variance of derived water content at 0.5m depth intervals
  - Variance of mean log T2 at 0.5m depth intervals
  - Variance of DP-NMR-derived K at 0.5m depth intervals.
- Variance of 3 DP-K measurements within a 2m area.
- Variance between DP-NMR and borehole NMR measurements within a 2m area
  - Average DP-NMR vs. borehole NMR pre-development at 0.5m depth intervals
  - Average DP-NMR vs. borehole NMR post-development at 0.5m depth intervals
- Variance between 3 DP-K and borehole MLST within a 2m area.
- Variance between NMR measurements in DP-installed 2" wells and auger-installed 2" wells, at various stages of development.

Vista Clara and KGS will jointly analyze the resulting data to quantify the uncertainty and error in both the NMR-estimated K and direct K measurements, due to various aspects of well construction and development.

**Scheduling:** The majority of new NMR logging measurements and related experiments at GEMS will be performed in the first year of the Phase 2 project, most likely in the Spring of 2012.

**D.2.1.2 Develop and demonstrate improvements upon existing NMR/K transforms for near-surface lithology types, based on controlled investigations of pore-scale NMR/K physics.**

*This portion of the Phase 2 research will be performed by Stanford University.*

With the completion of the feasibility stage of our research, in Phase 1, we are convinced of the validity of our approach – that of developing the NMR-to-K transform at a location where we have logging NMR and K data, and then using that transform in the interpretation of SNMR data. As in Phase 1 we will focus on two distinct aspects of the research: 1) How best to construct the NMR-to-K transform; 2) How best to apply that transform to surface NMR data.

In Phase 1, our approach had been to assume that use of a calibrated the SDR equation was a valid approach to transforming NMR parameters to K. While the site-specific calibration yielded significantly better results than would have been obtained by simply using the standard SDR exponents ( $b=4, m=4$ ), we found such a range of values for the empirical constants that we question whether the use of the SDR equation is the optimal

approach to take when estimating K from NMR data. Both the SDR and TC equations are well established in the petroleum industry and have been used for over 20 years in borehole logging applications. But these equations were developed using samples that resembled typical petroleum reservoir formations: well-consolidated sandstones. While this is an excellent choice for deep reservoirs, it does not fit the needs of shallow groundwater applications where the formations can be semi or unconsolidated. In Phase 2 an important component of our research will involve investigating specific effects likely to impact the relationships between NMR relaxation time constants and K in high permeability unconsolidated materials. The focus of our research will be on the phenomenon referred to as slow diffusion, an aspect of the pore-scale physics that we feel must be considered in the interpretation of NMR data from materials such as sands and gravels.

### ***The Effects of Slow Diffusion on NMR-to-K Transform***

The TC and SDR equations are based on the assumption that NMR relaxation occurs in the fast diffusion regime, defined by the following: the time that it takes for the hydrogen nuclei to travel (diffuse) to the surface of the pore space is negligible when compared to the time it takes for surface relaxation to occur; i.e. diffusion is not the rate-controlling step. In the slow diffusion regime, the hydrogen nuclei still relax due to surface interactions, but the time to travel (diffuse) to a surface becomes significant. Intuitively, as the pores get larger, is it more likely that the NMR response moves into the slow diffusion regime. The diffusion regime is defined as either fast or slow by the Brownstein number (Brownstein and Tarr, 1979), B, given as

$$B = \frac{t_d}{t_s} = \frac{\rho r}{D} \quad (13)$$

where  $r$  is the radius of a spherical pore and  $D$  is the self diffusion coefficient of the fluid (2,500  $\mu\text{m}/\text{s}$  for water). Fast diffusion occurs when  $t_d \ll t_s$ , i.e.  $\rho r/D \ll 1$ . Slow diffusion occurs when  $t_d \gg t_s$ , i.e.  $\rho r/D \gg 10$  (Dunn, 2002; Godefroy et al., 2001; Lonnies, 2003). Relaxation transitions from the fast to the slow diffusion regime for  $1 \ll \rho r/D \ll 10$ .

We show in Figure 33 the importance of considering the effects of slow diffusion when interpreting NMR data. We have used  $\rho$  values ranging from 10 to 160  $\mu\text{m}/\text{s}$ , which was the range of values found in the literature for sandstones (Bowers et al., 1995; Howard et al., 1993; Kenyon et al., 1989). It is clear that for a wide range of  $\rho$  values, the assumption of fast diffusion is likely to be invalid. In addition to the effects of slow diffusion, this figure also highlights the fact that the effect of bulk fluid relaxation must also be considered when the pores become sufficiently large; another effect not accounted for in using the SDR and TC equations.

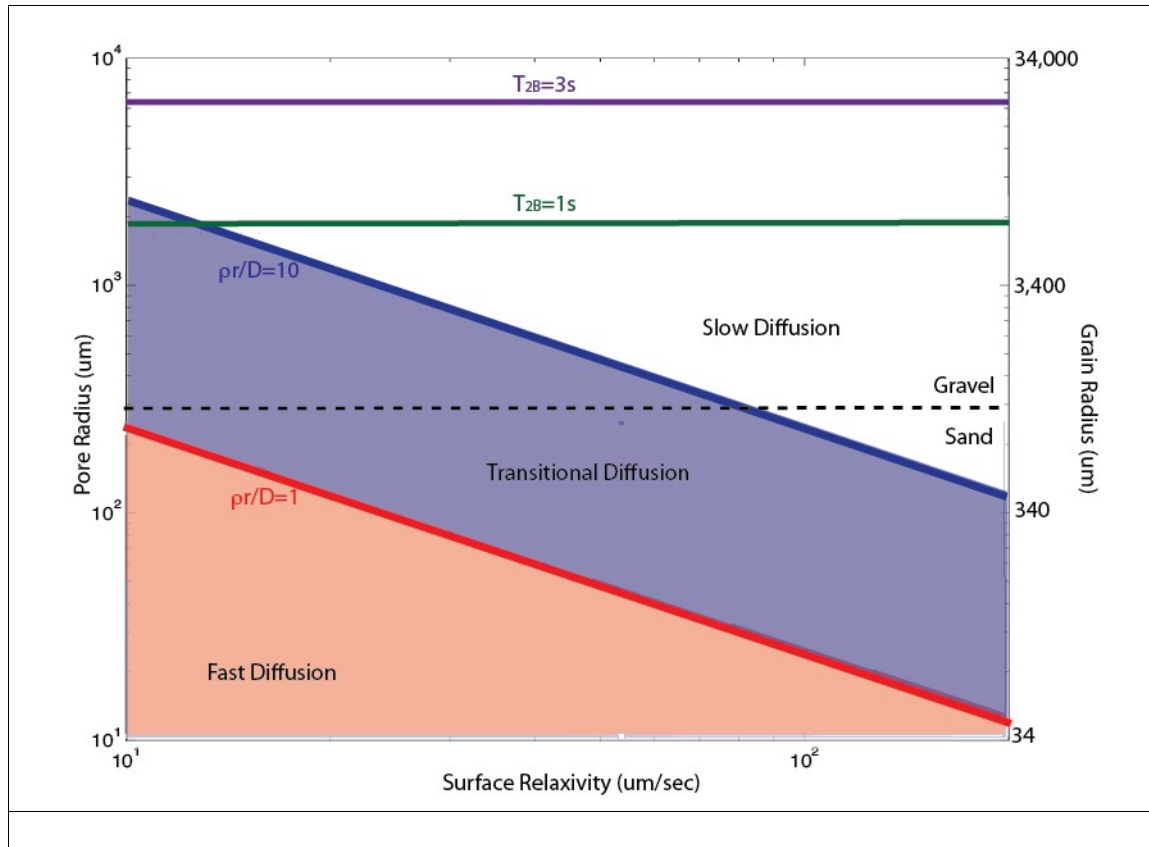


**Figure 33: Log-log plot of pore radius on the left y-axis, grain size on right y-axis and  $r$  on the x-axis. For a given  $r$ , the red line separates fast diffusion from transitional diffusion and the blue line separates transitional diffusion from slow diffusion. The dashed line separates grain sizes corresponding to sands and gravels**

### *Numerical Modeling to Assess the Effects of Slow Diffusions*

We propose to study slow diffusion through numerical modeling of NMR relaxation processes in a numerical grain pack. Our goal is to determine the potential impact of slow diffusion on K estimates from NMR data. We will build our numerical modeling on concepts previously published, as summarized here.

In slow diffusion, the dominant rate at which most relaxation occurs is proportional to the squared distance a relaxing atom must diffuse to reach a grain surface and is given by (Brownstein and Tarr, 1979; Godefroy et al., 2001),

$$T_{2B,\text{Slow}} = \frac{\alpha(\pi/2)^2 D}{r^2} = \frac{2\alpha D}{r^2}. \quad (14)$$

For a spherical pore, this becomes

$$\tau_{\text{NMR}} = \frac{1 - 6D}{r^2} + \frac{2D}{3} \left( \frac{S}{V} \right). \quad (15)$$

Under fast diffusion, the total magnetization across the pore is uniform because relaxation is occurring at the same rate across the pore. However, in the slow diffusion regime, the total magnetization across the pore is non-uniform. This results in a non-uniform magnetization where at any given time the magnetization is high at the center of the pore and low near pore walls (Dunn, 2002; Kenyon, 1997). This results in a multi-exponential decay in a single pore, given by

$$M(t) = \sum_n [I_n e^{-t/T_n}], \quad (16)$$

where  $I_n$  is the intensity of each relaxation mode with corresponding decay time  $T_n$ . The relaxation modes are defined as,

$$T_n = \frac{\alpha [\pi(2n-1)^2]}{r^2} D. \quad (17)$$

In summary, two major changes occur in the surface relaxation rate as relaxation goes from the fast to slow diffusion regime: 1) the relaxation rate is proportional to the squared radius of the pore, and 2) relaxation occurs as a multi-exponential decay within a single pore. We will develop our numerical modeling so as to capture both of these phenomena.

The NMR response of a numerical grain pack will be simulated using a random walk model (Ramakrishnan et al., 1999) that utilizes the First-Passage-Time technique (Toumelin et al., 2003). The code to be used was developed by Kristina Keating (Ph.D. thesis, Stanford University). Homogeneous Finney packs (Finney, 1970) will be created and grains will be assigned a constant surface relaxivity (e.g.  $\rho = 30 \text{ mm/s}$ ). Each pack will consist of grains with different intergranular pore sizes (e.g., grain diameters of 25  $\mu\text{m}$  to 500  $\mu\text{m}$ ). The relationship between the known pore space parameters ( $S/V$ , pore radius, and grain radius) will be related to the modeled relaxation time constant. The ability to control the pore size and  $\rho$  will allow a better understanding of how a system transitions from fast to slow diffusion and the resulting relationship between the relaxation time constants and  $S/V$ . The  $K$  of each grain pack will be estimated using the Navier-Stokes based lattice-Boltzmann method. The code to be used for this portion was developed and described in detail in Keehm (2003). The relationship between the relaxation time constant and the pore space geometry will be analyzed for the effects of slow diffusion. The SDR equation will be modified to account for slow diffusion and used to estimate  $K$  from the NMR data. Results will be compared to the true lattice-Boltzmann  $K$  estimates from each pack.

### ***Analysis of Slow Diffusion in Constructed Lab Samples***

As a companion study to the numerical modeling, K will be estimated from NMR data collected on constructed samples in the lab. Quartz sand (99.995% pure, silicon dioxide, from Alfa Aesar) will be used as an analog for a naturally occurring mineral surface and has been used in previous NMR studies in the Environmental Geophysics Laboratory at Stanford. The surface relaxivity of each pack will be kept homogeneous and each pack will consist of grains with different intergranular pore sizes (e.g., grain diameters of 25 µm to 500 mm). The NMR relaxation time constant for each pack will be analyzed for the transition from fast to slow diffusion as predicted by the numerical modeling and the relaxation time constant will be related to the known pore space parameters (S/V, pore size, grain size). “True” K values will be obtained on each pack using a constant head permeameter. The modified SDR equation determined through the numerical modeling results will be used to estimate K and compared to the permeameter results.

In addition to working with constructed lab samples, the field data acquired in Phase 2 will provide the ideal data set for testing this modified SDR equation.

#### **D.2.1.3 Demonstrate logging NMR to K transforms in a broad range of lithology types (particularly low K, and high magnetic susceptibility)**

*This portion of the Phase 2 research will involve collecting borehole and DP NMR and K measurements at two new locations with different lithologies, and using the acquired data suitable to develop and demonstrate logging NMR-to-K transforms in other environments. Logging NMR data and direct K data will be collected by Vista Clara and KGS at two new sites in Western Kansas and Western Washington. Stanford University will development and demonstrate logging NMR-to-K transforms.*

##### **Data collection at the Larned Research Site in Western Kansas**

A significant amount of work in Phase 2 will be performed at the Larned Research Site (LRS; 38.2° N latitude, 99.0° W longitude) in west-central Kansas (Figure 34).

The LRS was established by the KGS in 2001 to investigate hydrologic and ecohydrologic processes (e.g., Butler et al. 2007) in the vicinity of the Arkansas River (Figure 34a). The site is located adjacent to a USGS stream-gauging station on the Arkansas River near the city of Larned. The hydrostratigraphy at the site, as determined by high-resolution EC profiling and core sampling, is illustrated in Figure 34b. Information about the hydraulic properties of the two aquifers and the intervening aquitard has been obtained from two multi-day pumping tests, slug tests, and analyses of water-level responses to barometric-pressure fluctuations (Butler et al. 2004, Butler et al. 2011, Healey et al. 2001). Ten wells are screened across the water table (D interval in Figure 1xxb), four wells are screened in the lower portion of the Arkansas River alluvial aquifer (C interval), two wells are screened in the aquitard (B1 and B2 intervals), and four wells are screened in the High Plains aquifer (A interval).

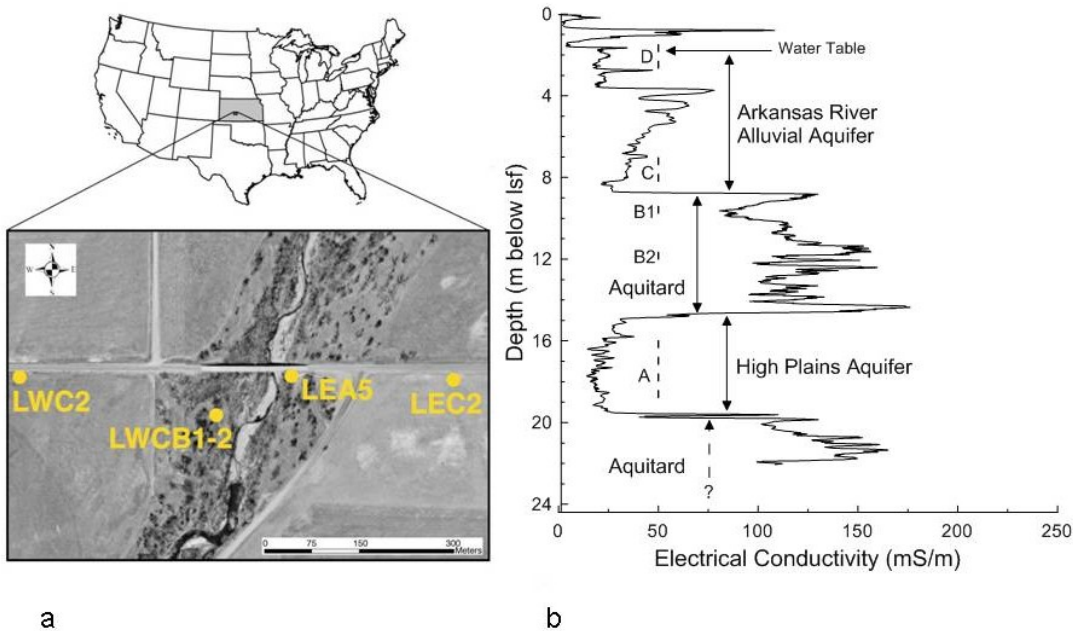


**Figure 34: Location map and aerial photo of the Larned Research Site (LRS).** Aerial photo (year 2000) only shows a subset of the wells at the LRS, wells LEC2, LEA5, and LWC2 are the High Plains aquifer wells in the LEC, LEA, and LWC well nests, respectively; watercourse in photo is the Arkansas River; b) High-resolution direct-push electrical conductivity (EC) log from near the center of the LRS riparian zone. Wells in the High Plains aquifer are screened across the interval marked A, while adjacent wells in the lower portion of the Arkansas River alluvial aquifer and across the water table are screened across the intervals marked B and C, respectively. Two wells (LWCB1-2) are screened in the aquitard across intervals B1 and B2. At this site, high EC values indicate clays and low values indicate sands and gravels.

The major focus of Phase 2 work will be on the aquitard between the Arkansas River alluvial aquifer and the High Plains aquifer (Figure 34b), but we will also perform direct-push K and NMR comparisons in the two aquifers. The LRS is an excellent site for aquitard studies because of the great amount of previous work done on the LRS aquitard (e.g., the aquitard thickness has been measured at over 15 locations across the site with high-resolution EC profiling) that provides a great deal of subsurface control.

**Direct K Measurements:** We will use bulk aquitard K estimates that have been previously obtained from a four-day pumping test at the site (Butler et al., 2004). We will also employ a new method developed at the KGS that uses water level-responses to barometric pressure fluctuations (Butler et al., 2011) to estimate the bulk aquitard K in the vicinity of each well. In addition, we will perform slug tests in the two wells screened in the aquitard and two additional wells that will be emplaced within the aquitard in the first year of this project. We will not perform HRK profiling in the aquitard because the current HRK tool is not designed to assess K below about 0.02 m/d (Butler et al., 2007), while the bulk aquitard K at the LRS is approximately an order of magnitude lower (Butler et al., 2004). We will perform HRK profiling in both the Arkansas River alluvial aquifer and the High Plains aquifer adjacent to existing well nests

**DOE SBIR Topic# 33a: Integrated Use of Surface and Subsurface NMR for Measuring and Mapping Saturated Hydraulic Conductivity in Three Dimensions. Vista Clara Inc.**

(LEC, LEA, and LWC wells nests in Figure 1xx) at which the aquitard K will be calculated from water-level responses to barometric pressure fluctuations.

**Logging NMR Measurements:** Vista Clara and KGS will mobilize the Javelin NMR instrument and the KGS Geoprobe machine to the selected test sites in Western Kansas. We will perform borehole NMR logging in existing 2" diameter and 4" diameter PVC-cased boreholes, and direct push NMR logging with the Geoprobe-compatible 2.5" Javelin NMR tool.

**Scheduling and Data Post-Production:** The majority of NMR logging measurements at the Larned Research Site will be performed in the first year of the Phase 2 project, most likely in the Spring of 2012. All new and pre-existing direct K and logging NMR measurements will be documented and geo-located with sub-meter GPS resolution. The NMR logging data will be reduced to water content/T2 distributions vs. depth. Direct K measurements will be documented as required. All data will be provided to Stanford with sufficient documentation to enable development and analysis of NMR-K transforms.

### **Data Collection in Western Washington**

The Phase 2 research will also include direct K and direct push NMR data at a site in the Puget Sound lowlands of Western Washington. The preferred location for this data collection is Leque Island, near Stanwood Washington, about 45 minutes north of Vista Clara's offices in Mukilteo WA.

The Leque Island property was historically a tidal salt marsh area that was reclaimed and utilized for agriculture (<http://wikimapia.org/11192854/Leque-Island>). Within the past 30 years, the property was acquired by the Washington Department of Fish and Wildlife (WDFW):

[http://wdfw.wa.gov/lands/wildlife\\_areas/skagit/unit.php?searchby=unit&search=Leque%20Island](http://wdfw.wa.gov/lands/wildlife_areas/skagit/unit.php?searchby=unit&search=Leque%20Island).

WDFW proceeded with plans to return a portion of the property into tidelands, to offer improved salmon rearing habitat and also provide opportunities for hunting. However, the Camano Island water district is concerned that the re-introduction of tidal saltwater to the property could harm Camano Island's groundwater supply. A lawsuit has been filed, and extensive geotechnical and hydrological investigations are ongoing at the site to determine the near surface aquifer properties.

Vista Clara has performed preliminary surface NMR measurements at Leque Island, with permission from WDFW. Figure 35 (left) shows an aerial view of the eastern edge of the site, where Vista Clara have previously acquired surface NMR data in 2010 and 2011.

Figure 35 (right) shows the GMR instrumentation at the site. The surface NMR data from this site indicate several well-defined layers in the upper 20m, including two apparent high-permeability aquifers, between 3m- 6 m, and between 10m -16m (Figure 36). Also of interest, the two permeable near surface aquifers exhibit long T2 relation (on the order of 200ms) but very short T2\* relaxation (on the order of 20ms), a sure indication of magnetically susceptible sediments. Geotechnical data from the same vicinity are

**DOE SBIR Topic# 33a: Integrated Use of Surface and Subsurface NMR for Measuring and Mapping Saturated Hydraulic Conductivity in Three Dimensions. Vista Clara Inc.**

consistent with this observation, with descriptions of “black sand” in the same intervals. Hence, the Leque Island site appears to be a very good site for investigating the slow diffusion NMR regime.



**Figure 35:** Leque Island site, near Stanwood WA, is owned by the Washington Department of Fish and Wildlife. Left: aerial view of previous measurement location. Right: Vista Clara personnel and GMR instrumentation at the site in October 2010.

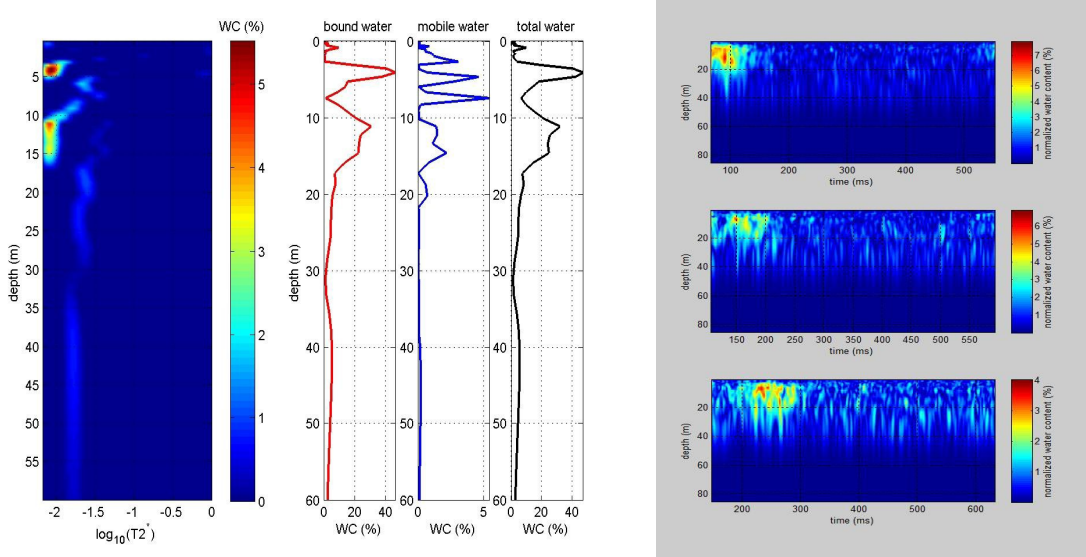


**Figure 36:** Preliminary surface NMR data from Leque Island site indicate the presence of both high-K and low-K units in the top 20m. Left: FID inversion result indicates possible aquifers with short  $T_2^*$  (~15ms) from 3-6m, and 10-16m. Spin echo NMR data indicate long  $T_2$  (~200ms) in these same depth ranges, which indicates relatively high magnetic susceptibility.

Vista Clara has requested a permit from the WDFW to operate at the Leque Island site for the duration of the proposed Phase 2 program, to include both surface NMR and direct push measurements. WDFW has communicated an interest in providing such support, and expressed confidence that the requested permit would be granted by April 2011.

In the unlikely event that we would not gain access to the Leque Island site, Vista Clara has access to alternate sites in the North Puget Sound area, including 40 acres of private farmland in the Snohomish River Valley near Everett WA. Vista Clara presently leases

***DOE SBIR Topic# 33a: Integrated Use of Surface and Subsurface NMR for Measuring and Mapping Saturated Hydraulic Conductivity in Three Dimensions. Vista Clara Inc.***

the use of this farmland for \$1,200 per year for the purpose of acquiring surface NMR data for research, and for providing demonstrations to potential customers. This alternate site exhibits a similar layers of high and low-K in the top 25m, and also short T2\* and long T1 and T2, indicating moderate to high magnetic susceptibility.

***DP-K and DP-NMR Measurements:*** KGS will mobilize their Geoprobe machine for one data collection effort, in the second project year (likely in June or July 2013), to avoid interfering with the fall/winter hunting season. Direct push K measurements will be performed using the latest generation HRK tool. Direct push resistivity measurements will also be collected. During the same 1-2 week period, direct push NMR measurements will be performed using Vista Clara's Javelin instrumentation.

***Core Sampling:*** If it is feasible, some core samples may also be collected using the Geoprobe machine for laboratory NMR analysis at Vista Clara and/or Stanford. Vista Clara also has hand-augering and core sampling equipment that can be used to extract 2" diameter core samples to a depth of 20 feet, depending on subsurface conditions. Any core samples collected from the Western Washington field sites will be preserved and shipped to Stanford for laboratory NMR analysis.

***Scheduling and Coordination:*** Mobilization and use of the Geoprobe in Western Washington will be for a 1 – 2 week period, in the second year of the Phase 2 effort (probably June or July 2013). Vista Clara will be responsible for planning, scheduling, permitting and other coordination with WDFW as required to perform the DP measurements efficiently. KGS will be responsible for the mobilization and operation of the Geoprobe machine, and for collection DP-K measurements. Vista Clara will be responsible for the DP-NMR measurements, and hand-augered core samples. The DP K, NMR and electrical resistivity measurements at Leque Island will be reduced by KGS and Vista Clara to standard formats, and geolocated with sub-meter GPS. The entire data set will be forwarded to Stanford University for development and analysis of NMR-K transforms.

**Calibration of Empirical Equations for Predicting K (Stanford)**

*This portion of the Phase 2 research will be performed by Stanford University.*

As begun in Phase 1, we will continue to evaluate the use of the two empirical equations, SDR and TC, for estimating K. We will again work with NMR and K data acquired at the field sites, and use various inversion methods to find the optimal values for the empirical constants. In Phase 2, we will have available data from different lithologic units, so we will undertake a more rigorous assessment of how and when the values of the empirical constants change.

With data available from different lithologic units, a focus in Phase II will be to determine the value of developing not just site-specific NMR-to-K transforms, but lithostratigraphic- (or hydrostratigraphic-) unit- specific NMR-to-K transforms. We ask the question: Can we identify any relationship between the optimal values for the

**DOE SBIR Topic# 33a: Integrated Use of Surface and Subsurface NMR for Measuring and Mapping Saturated Hydraulic Conductivity in Three Dimensions. Vista Clara Inc.**

empirical constants and lithostratigraphy? If so, we will quantify the potential errors involved when using a developed site-specific transform, without any knowledge of lithology.

In Phase II we will also extend the analysis of the acquired data, and resulting K predictions, to include a detailed assessment of the dependence of the accuracy of the K prediction on the distance from the calibration site. Of particular interest is whether we see a dependence of error on separation distance from the calibration location that suggests that the correlation structure of subsurface hydrologic properties directly impacts the accuracy of our predictions. Does the relationship between error and distance from the calibration site vary for the different lithostratigraphic units. If so, can we begin to develop guidelines that quantify the trade-off between spatial density of calibration sites and accuracy of K predictions. Such guidelines would be extremely useful in the design of a field program for site characterization.

**D.2.2 Develop and demonstrate methodology and best practices for using limited logging NMR and K measurements, with higher density surface NMR measurements, to map hydraulic conductivity in three dimensions.**

This section of the Phase 2 work plan is aimed at improving and refining the mathematical link between surface NMR data, logging NMR data and hydraulic conductivity K. We seek to answer some of the important questions raised by the Phase 1 results, and develop a methodology that is robust and appropriate for applying surface NMR to estimate K in three dimensions in unconsolidated and semi-consolidated near surface aquifers.

The methodology will follow from the phase 1 approach but with additional focus on:

1. Improving the accuracy of the surface NMR inversions in electrically conductive geology.
2. Increasing the range of lithologies to low-K and high magnetic susceptibility.
3. Demonstration of high resolution surface NMR-based mapping of K in two and three dimensions.

**D.2.2.1 Determine extent to which approach from phase 1 (dual transforms) is valid/transferable within other lithologies (particularly those containing magnetic minerals).**

*This portion of the Phase 2 research will be performed by Vista Clara.*

It has been known for more than a decade that an electrically conductive subsurface can cause significant attenuation and distortion of the magnetic fields of surface NMR loops (Shushakov, 1996), and thereby introduce errors into the inversion and interpretation of surface NMR data (Weichmen et al, 2000). The solution to this problem is to use an

***DOE SBIR Topic# 33a: Integrated Use of Surface and Subsurface NMR for Measuring and Mapping Saturated Hydraulic Conductivity in Three Dimensions. Vista Clara Inc.***

accurate 1D, or even 2D profile of the subsurface electrical conductivity distribution to calculate the 3D AC magnetic field lines for the surface coils, which are integral to the inversion and localization of the subsurface NMR signal sources. The numerical algorithms to produce accurate 3D surface coil fields in a layered conductive medium are complex, however, and to date commercial software for this special purpose have not been made available.

In 2009, Vista Clara and the US Geological Survey entered into a Technical Assistance Agreement, under which Vista Clara provided training and some proprietary information to the USGS. In return the USGS agreed to develop advanced software for surface NMR coil field modeling in conductive medium, and to share executable versions of this software and/or similar information to enable Vista Clara to incorporate advanced conductivity effects into our commercial 1D and 2D inversion software. In early 2011 the USGS provided Vista Clara with preliminary executable software for modeling 3D fields of surface NMR coils of arbitrary geometry over and arbitrary 1D layered conductive subsurface. Vista Clara has begun the process of integrating this software into our own inversion software.

As part of the Phase 2 effort, Vista Clara will complete the process of integrating accurate 3D coil field modeling in conductive layered medium into our 1D and 2D inversion software. We will evaluate the USGS-supplied technology, as well as similar executable software developed by the Leibniz Institute of Applied Geophysics (LIAG) in Hannover Germany. The LIAG group are an existing customer of Vista Clara, and have recently indicated their intention to make executable versions of their coil field modeling and inversion package (“MRSMatlab”) available free of charge for all users, including commercial.

In the process of integrating and testing advanced modeling code, Vista Clara will re-process the surface NMR data collected at GEMS in Phase 1, and provide updated surface NMR inversion results to Stanford to assist in their development and evaluation of surface NMR-K transforms.

**D.2.2.2 Determine extent to which approach from phase 1 (dual transforms) is valid/transferable within other lithologies (particularly those containing magnetic minerals).**

**1D Surface NMR data collection**

*This portion of the Phase 2 research will be performed by Vista Clara, with some assistance as needed from KGS and Stanford.*

New surface NMR measurements will be collected at the second study site in Larned Kansas. The timing of these surface measurements will coincide with the Javelin NMR measurements at this new site, in the first year of the Phase 2 project, to make the best use of available human resources and travel budgets. KGS will be responsible for

***DOE SBIR Topic# 33a: Integrated Use of Surface and Subsurface NMR for Measuring and Mapping Saturated Hydraulic Conductivity in Three Dimensions. Vista Clara Inc.***

planning and scheduling the field work, and securing access to appropriate surface NMR measurement locations. Vista Clara will be responsible for planning specific surface NMR measurements, training all field assistants, and ensuring the surface NMR data are of the best possible quality to achieve research objectives. We will perform measurements to characterize water content, T1, T2 and T2\* relaxation.

New surface NMR measurements will also be collected at the new Phase 2 investigation site in Western Washington. These measurements will be made throughout the Phase 2 program, as required. Vista Clara will be responsible for planning specific surface NMR measurements, training all field assistants, collecting the data and ensuring the surface NMR data are of the best possible quality to achieve research objectives. We will perform measurements to characterize water content, T1, T2 and T2\* relaxation.

To achieve faster acquisition of T2 data, Vista Clara will also develop and field test a Carr-Prucell-Meiboom-Gill (CPMG) pulse sequence for surface NMR measurements. This work will involve designing the pulse sequence, programming the CPMG sequence for the GMR system, mapping the forward Kernel function for the 1D inversion, and implementing an accurate 1D inversion algorithm for CPMG-derived water content and T2 distribution.

**2D and 3D Surface NMR data collection**

*This portion of the Phase 2 research will be performed by Vista Clara. This data will be obtained in the second year of the 2-year STTR project.*

2D and 3D surface NMR data will be collected at one selected study sites in the second year of the Phase 2 project. The most economical site, and preferred site, would be the site in Western Washington, due to its proximity (~45 minute drive) to Vista Clara's offices.

2D surface NMR data will be collected using 50% overlapping loops, to construct a linear array of surface NMR measurements. At least one 2D surface NMR transect will be acquired over an area where two or more DP-NMR and DP-K measurements have been obtained. This will provide sufficient data to test the proposed concept of high resolution 2D mapping of hydraulic conductivity, via surface NMR. 3D surface NMR data will be obtained by performing separated 1D (single coil) surface NMR data acquisitions over a wide 3D area, for example, on a 2D grid of 200m spacing across a portion the Leque Island study area.

2D and 3D localization and mapping of hydraulic conductivity will be performed Vista Clara, using the best available NMR-K transform methods available from Stanford University.

**Prediction of K from SNMR Data**

*This portion of the Phase 2 research will be performed by Stanford University.*

As demonstrated in Phase I, the prediction of K from SNMR data requires two steps. The first transforms the SNMR parameter  $T_2^*$  to the NMR parameter  $T_2$ ; the second uses the NMR-to-K transform developed using the logging data to obtain estimates of K, taking into account as needed differences in the scale of the two measurements.

The NMR parameter acquired through the logging measurement,  $T_2$ , is dominated by the pore-scale process referred to as surface relaxation; this relaxation mechanism is strongly influenced by the geometry of the pore space, thus provides a link to K. In contrast, the SNMR parameter  $T_2^*$  can be significantly influenced by dephasing in an inhomogeneous magnetic field, an effect that is more dominant in coarse-grained materials. This is represented by the following equation, where the term represents the enhanced relaxation due to the inhomogeneous magnetic field

$$1/T_2^* = 1/T_2 + 1/T_{2IH} \quad (18)$$

In Phase 1 we estimated the magnitude of  $1/T_{2IH}$  by taking the maximum values of  $T_2$  and  $T_2^*$  determined over the sand and gravel interval; and then subtracted this from the  $1/T_2^*$  values. With available logging NMR data, it is possible to assess the validity of this approach.

In Phase 2 we will take the same approach to estimating  $1/T_2^*$  with the newly acquired field data, to test whether this approach is sufficiently robust so as to be a reliable component of a standard methodology for estimating K from SNMR. In parallel, we plan to take a different approach and investigate, on a fundamental level, the parameters governing the magnitude of  $1/T_{2IH}$ . We plan to build on the numerical modeling (described in Section D.2.1.2) to incorporate relaxation due to dephasing in an inhomogeneous field, and explore the controls on  $1/T_{2IH}$  by varying pore-scale magnetic properties, and also considering the impact of regional-scale gradients on the pore-scale physics. We have particular interest in assessing the potential to use another form of NMR logging measurement, or a different form of logging measurement (e.g. a downhole fluxgate magnetometer) as a means of estimating  $1/T_{2IH}$  at a field site.

In Phase 1, once we had transformed the SNMR data to “pseudo” data, we used the transforms developed with the logging NMR data. In those data sets, the resolution of the  $T_2$  and  $T_2^*$  data were comparable, so we did not consider the differences in scale. In Phase 2 we plan to address the issue of scale by creating a model of subsurface heterogeneity at a site, based on the logging data; use geostatistical methods to populate the subsurface model with estimates of water content and the  $T_2$  distribution, constrained by the logging data; and then forward model the SNMR measurement to obtain a representation of  $T_2$  at the scale of the SNMR measurement. This will allow us to determine the way in which scale differences should be accounted for before applying the NMR-to-K transform.

**D.2.2.3 Demonstrate high resolution mapping of hydraulic conductivity in two and three dimensions at one field site, using the proposed integrated NMR/K methodology.**

*This portion of the Phase 2 research will be performed by Vista Clara. This surface NMR data will be obtained in the second year of the 2-year STTR project.*

**2D and 3D Surface NMR data collection**

2D and 3D surface NMR data will be collected at one selected study sites in the second year of the Phase 2 project. The most economical site, and preferred site, would be the site in Western Washington, due to its proximity (~45 minute drive) to Vista Clara's offices.

2D surface NMR data will be collected using 50% overlapping loops, to construct a linear array of surface NMR measurements. At least one 2D surface NMR transect will be acquired over an area where two or more DP-NMR and DP-K measurements have been obtained. This will provide sufficient data to test the proposed concept of high resolution 2D mapping of hydraulic conductivity, via surface NMR. 3D surface NMR data will be obtained by performing separated 1D (single coil) surface NMR data acquisitions over a wide 3D area, for example, on a 2D grid of 200m spacing across a portion the Leque Island study area.

**2D and 3D Mapping of K**

2D and 3D localization and mapping of hydraulic conductivity will be performed Vista Clara, using the best available NMR-K transform methods available from Stanford University. Vista Clara has existing 2D surface NMR imaging and characterization software that can readily incorporate the new NMR-K transforms to be developed and demonstrated in the Phase 2 work (Walsh, 2008). Vista Clara's existing 3D surface NMR imaging software (Walsh, 2006) will be updated to map hydraulic conductivity in 3 dimensions, using the proposed methodology.

**D.2.3 Develop and demonstrate a methodology for using NMR-derived flow velocity distributions to predict a contaminant plume distribution over space and time.**

This section of the Phase 2 work plan aims to develop and demonstrate new borehole NMR methods of natural or induced flow, to estimate the distribution of flow velocities within an aquifer, and to predict its effect on the spatial/temporal distribution of subsurface contaminants.

**D.2.3.1 Design and assemble a new 1.75" borehole NMR logging tool, and borehole packing accessories, specifically for measurement of flow velocity distributions over a range of expected flow rates.**

*This portion of the Phase 2 work plan will be performed by Vista Clara, with some technical assistance from the Kansas Geological Survey.*

The phase 1 work demonstrated that it is easier to measure flow closer to the NMR sensor, where the induced flow itself is faster and where the static magnetic field gradient is stronger. The existing line of Javelin tools are designed to operate at a relatively low frequency (250 kHz – 300 kHz) so as to position the NMR sensitive region at a relatively larger depth of investigation within the formation.

*The following paragraph contains proprietary information that Vista Clara Inc. requests not be released to persons outside the Government, except for purposes of review and evaluation.*

In Phase 2, we will design and assemble a new Javelin borehole NMR probe to operate over a wider range of frequencies, to perform NMR measurements over a wider range of depths of investigation from the sensor. We will assemble either a 1.75" or 3.5" diameter probe, depending on availability of suitable boreholes in Kansas for the planned NMR flow demonstrations. This task involves:

- modification of the existing downhole electronics to enable remote switching over a wider range of tuning capacitors, to enable the probe to operate over a range of frequencies from 125 kHz to 500 kHz,
- modification of the Javelin software to support acquisition from 125 kHz to 500 kHz.

We will also modify the Javelin data acquisition system and software to enable NMR pulse sequences to be synchronized with an electronically-triggered slug test. The KGS has previously developed and demonstrated an electronic slug test mechanism that makes slug testing highly repeatable. Vista Clara will also consult with KGS to acquire or fabricate appropriate borehole packing devices to isolate and focus inflow in the vicinity of the NMR logging tool.

**D2.3.2 Develop a non-infringing methodology for using a borehole NMR tool to directly measure the flow and velocity distribution within a formation, and develop an approach for integrating these measurements into broader workflow of K estimation and contaminant transport.**

*This portion of the Phase 2 work plan will be performed by Vista Clara, with some technical assistance from the Kansas Geological Survey.*

*The following paragraph contains proprietary information that Vista Clara Inc. requests not be released to persons outside the Government, except for purposes of review and evaluation.*

In phase 2 we will investigate and develop two approaches to using borehole NMR to measure flow distributions within aquifers:

**DOE SBIR Topic# 33a: Integrated Use of Surface and Subsurface NMR for Measuring and Mapping Saturated Hydraulic Conductivity in Three Dimensions. Vista Clara Inc.**

- **NMR measurement of transient flow during a slug test.** This involves synchronizing a CPMG (or other) NMR measurement with a multi-level slug test. The NMR pulse sequence can be triggered to start at the same time as, or at a fixed time before, the release of pressure in a slug test. The NMR measurement of water within a well-defined cylindrical sensitive region will contain information on the transient flow out of the sensitive region as a result of the rapid decrease in pressure in the adjacent well. We will develop and demonstrate the methodology first in our laboratory, using water barrels, PVC pipe and electronically controlled air pressure release valves. We will also develop methods for estimating the relevant formation flow velocity distributions, that can potentially be used to predict contaminant dispersion in space and time.
- **NMR measurement of flow via diffusion.** Diffusion is the process by which the NMR signal from a bulk fluid decays due to random motion of the fluid within a magnetic gradient field, and subsequent loss of coherence of the bulk water. The diffusion effect is readily measured and differentiated from T2 relaxation by performing the same CPMG sequence with different pulse echo spacings. Any difference between the acquisitions is due to diffusion. The application of a pressure gradient, and hence induced flow, will presumably alter the motion of water molecules. Hence the non-random flow of water, due to a pressure gradient, can probably be monitored via NMR diffusion.

We will develop and demonstrate these methodologies first in our laboratory, using plastic barrels filled with bulk water and saturated sand, PVC pipe, and electronically controlled air pressure release valves. We will also develop methods for estimating the relevant flow velocity distributions that can potentially be used to predict contaminant dispersion in space and time.

**D.2.3.3 Demonstrate NMR-based measurement of velocity distribution in a borehole.**

This portion of the Phase 2 work will be performed by Vista Clara and KGS in Kansas. NMR flow experiments may be scheduled for the first and/or second years, depending on the development of the methodologies.

*The following paragraph contains proprietary information that Vista Clara Inc. requests not be released to persons outside the Government, except for purposes of review and evaluation.*

Simple CPMG-based NMR flow measurements will be performed again in one or more selected boreholes in Kansas. Flow will be induced by injecting water into or withdrawing water from the test well. If necessary, packers will be used to focus flow in the vicinity of the NMR tool. The new NMR tool will enable measurements at a wider range of radial distances from the NMR tool. NMR measurements will be performed both with and without flow. NMR diffusion measurements will be performed, by applying the CPMG sequence with different echo spacings. Post-collection analysis will attempt to determine the best way to extract flow velocity distribution from the data.

**DOE SBIR Topic# 33a: Integrated Use of Surface and Subsurface NMR for Measuring and Mapping Saturated Hydraulic Conductivity in Three Dimensions. Vista Clara Inc.**

The following paragraph contains proprietary information that Vista Clara Inc. requests not be released to persons outside the Government, except for purposes of review and evaluation.

NMR slug test measurements will be performed by synchronizing the KGS electronic slug test system with the Javelin data acquisition software. The Javelin system will output a digital or analog trigger signal to initiate the slug test at a precisely defined time, before and/or during the CPMG sequence. Some field engineering will be required to make this happen. KGS and Vista Clara have the personnel and expertise to make it happen. The data from the NMR slug tests will be analyzed to determine formation velocity distributions.

### D.3 Performance Schedule

Project Quarter	1	2	3	4	5	6	7	8
<b>Data Collection at GEMS</b>								
DP-NMR investigation			→					
Borehole NMR/K repeatability		→	→					
DP NMR measurements		→	→					
<b>Data Collection at Larned KS</b>								
DP/borehole NMR measurements		→						
Surface NMR measurements		→						
<b>Data Collection in Western WA</b>						→		
DP-K, DP-NMR measurements						→		
Surface NMR measurements			→			→		
<b>Data Processing and Interpretation</b>								
Logging NMR to K transforms		→	→	→	→	→		
Logging NMR to SNMR Transforms		→	→	→	→	→		
<b>NMR flow measurement</b>								
Laboratory/tool development		→	→	→	→	→		
Field demonstration (GEMS)						→		
<b>Project Status Reports</b>	X		X		X		X	

Table 8: Phase 2 performance schedule.

### D.4 Facilities/Equipment

#### Vista Clara Facilities:

Vista Clara leases 3,200 square feet of new, flex-industrial office and laboratory spaces in Mukilteo Washington. Our facilities include a variety of manufacturing and test equipment including: oscilloscopes; power supplies; custom RF amplifiers; a 22kHz low-field laboratory NMR instrument; a 275 kHz low field NMR instrument (HMRLab), 2 state-of-the art multi-channel GMR surface NMR instruments; our in-house Javelin borehole and direct push NMR instrumentation including a 3.5" diameter borehole NMR

***DOE SBIR Topic# 33a: Integrated Use of Surface and Subsurface NMR for Measuring and Mapping Saturated Hydraulic Conductivity in Three Dimensions. Vista Clara Inc.***

probe, 1.75" diameter borehole NMR probe, and 2.5" diameter direct push NMR probe; a new 2009 Ford F150 4x4; and various machine tools. Our office facilities include various workstations and technical software licenses including Labview and Matlab. All of our facilities will be available for the proposed Phase 2 STTR work.

**Stanford University Facilities:**

**NMR 2 MHz Analyzer:**

One of the major pieces of equipment needed for this research is the 2 MHz Maran Ultra NMR core analyzer. This system is available in the Environmental Geophysics Laboratory at Stanford University, built 10 years ago to house the research activities of Rosemary Knight. The Maran was purchased in 2001 with funds from the National Science Foundation and Stanford School of Earth Sciences. The Maran instrument is designed to accommodate cylindrical samples of rocks or soils 1 inch in diameter and 2-3 inches in length. A flow-through system makes it possible to vary and sample pore fluid chemistry during the NMR experiment, and both temperature (30-150 C) and pressure (up to a maximum of 5000 psi) can be controlled. The magnet used in this instrument is of much lower field than is typically used for magnetic resonance studies in chemistry and molecular biology. This provides greater control over magnetic field gradients, greater sensitivity to molecular dynamics, a larger volume over which the magnetic field is homogeneous, and lower acquisition and operating costs. In addition, the low field means that our laboratory measurements can be directly compared to measurements made with NMR borehole logging systems that also operate at these low fields. The NMR analyzer is interfaced with a dedicated desktop PC, used to control pulse-sequencing parameters and to record the NMR decay data. Decay measurements are inverted for T<sub>2</sub> distributions using a non-negative least-squares algorithm designed and implemented in MATLAB.

**Sample Preparation:**

Most of the equipment required for sample preparation and saturation of samples is available in the Environmental Geophysics Lab. This includes weigh scales, pH meter, sieves, miscellaneous glassware, NMR sample holders, and a high vacuum saturating set-up.

**Sample Characterization:**

A Coberly-Steven Pycnometer, used to measure the porosity of samples, is available for use in the Stanford Rock Physics Laboratory. A Micromeritics ASAP 2020 Accelerated Surface and Porosimetry System, used to measure the surface area of samples, is available for use in the Stanford Environmental Geochemistry Laboratory.

**University of Kansas/KGS facilities:**

In addition to the GEMS site described earlier, the KGS has excellent field and experimental resources that will be utilized in this research. Major equipment that will be used in this project includes: 1) a track-mounted direct-push unit with auger-head attachment, winch, and trailer (Geoprobe 66DT unit); 2) a direct-push injection logger

***DOE SBIR Topic# 33a: Integrated Use of Surface and Subsurface NMR for Measuring and Mapping Saturated Hydraulic Conductivity in Three Dimensions. Vista Clara Inc.***

with electrical conductivity logging system (Geoprobe Direct Image Hydraulic Profiling Tool); 3) a prototype direct-push high-resolution K (HRK) tool for high-resolution characterization of hydraulic conductivity in unconsolidated formations (Liu et al., 2009).

**D.5 Consultants and Subcontractors (including Research Institutions for STTR)**

**STTR Research Institution (Stanford University)**

Stanford University, Office of Sponsored Research, 340 Panama Street, Stanford CA.  
Certifying Official: Catalina Verdu-Cano, 650 498-6877, [cverduca@stanford.edu](mailto:cverduca@stanford.edu).  
Total Subcontract Budget: \$225,000.

**Kansas Geological Survey (Subcontractor)**

University of Kansas Center for Research, Inc., 2385 Irving Hill Road, Lawrence, Kansas 66045-7568. Certifying Official: Joanne Altieri Director, Research Administration, 785-864-3441. [kucrpropmgmt@ku.edu](mailto:kucrpropmgmt@ku.edu). Total Subcontract Budget: \$225,000.

**D.6 Phase II Funding Commitment (None)**

**D.7 Phase III Follow-on Funding Commitment (None)**

**D.8 Bibliography and References Cited**

Bowers, M.C., Ehrlich, R., Howard, J.J. and Kenyon, W.E., 1995. Determination of porosity types from NMR data and their relationship to porosity types derived from thin section. Journal of Petroleum Science and Engineering, 13(1): 1-14.

Brownstein, K.R. and Tarr, C.E., 1979. Importance of classical diffusion in NMR studies of water in biological cells. Physical Review, 19(6): 2446 - 2453.

Butler, J.J., Jr. 1998. *The Design, Performance, and Analysis of Slug Tests*. Boca Raton: Lewis Publishers, 252 pp.

Butler, J.J., Jr. 2005. Hydrogeological methods for estimation of hydraulic conductivity. In: *Hydrogeophysics*, ed. by Y. Rubin and S. Hubbard, Springer, The Netherlands: 23-58.

Butler, J.J., Jr., Garnett, E.J., and Healey, J.M., 2003. Analysis of slug tests in formations of high hydraulic conductivity, Ground Water, 41(5): 620-630.

**DOE SBIR Topic# 33a: Integrated Use of Surface and Subsurface NMR for Measuring and Mapping Saturated Hydraulic Conductivity in Three Dimensions. Vista Clara Inc.**

Butler, J.J., Jr., McElwee, C.D., and Liu, W.Z., 1996. Improving the reliability of parameter estimates obtained from slug tests, *Ground Water*, 34(3): 480-490.

Butler, J.J., Jr., Jin, W., Mohammed, G.A., and Reboulet, E.C. 2011. New insights from well responses to fluctuations in barometric pressure, *Ground Water*, in press.

Butler, J.J., Jr., Whittemore, D.O., Zhan, X., and Healey, J.M. 2004. Analysis of two pumping tests at the O'Rourke Bridge site on the Arkansas River in Pawnee County, Kansas, *Kansas Geological Survey Open-File Rept. 2004-32*, 58 pp.

Butler, J.J., Jr. 2009. Pumping tests for aquifer evaluation – Time for a change? *Ground Water*, 47(5): 615-617.

Dunn, K.J., Bergman, D.J., Latorraca, G.A., 2002. Nuclear Magnetic Resonance: Petrophysical and Logging Applications. *Handbook of Geophysical Exploration*, 32. Elsevier Science Ltd, Oxford, UK.

Finney, J.L., 1970. Random packings and the structure of simple liquids. I. The geometry of random close packing. *Proceedings of the Royal Society of London, Series A, Mathematical and Physical Sciences*, 319(1539): 479 - 493.

Godefroy, S., Korb, J.P., Fleury, M. and Bryant, R.G., 2001. Surface nuclear magnetic relaxation and dynamics of water and oil in macroporous media. *Physical Review E*, 64(2): 021605.

Healey, J.M., Butler, J.J., Jr., and Whittemore, D.O. 2001. Stream-aquifer interaction investigations on the middle Arkansas River: Construction of groundwater observation wells in Edwards, Pawnee, and Barton County, Kansas, *Kansas Geological Survey Open-File Rept. 2001- 48*, 40 pp.

Howard, J.J., Kenyon, W.E. and Straley, C., 1993. Proton magnetic resonance and pore size variations in reservoir sandstones. *SPE Formation Evaluation*.

Keehm, Y., 2003, Computational rock physics: Transport properties in porous media and applications: Ph.D. Dissertation, Stanford University.

Kenyon, W.E., 1997. Petrophysical principles of applications of NMR logging. *The Log Analyst*, March-April: 21 - 43.

Kenyon, W.E. et al., 1989. Pore-size distribution and NMR in microporous cherty sandstones. *SPWLA Thirtieth Annual Logging Symposium*, June 11 - 14.

Liu, G., Bohling, G.C., and Butler, J.J., Jr. 2008. Simulation assessment of the direct-push permeameter for characterizing vertical variations in hydraulic conductivity, *Water Resour. Res.*, 44, W02432, doi:10.1029/2007WR006078.

**DOE SBIR Topic# 33a: Integrated Use of Surface and Subsurface NMR for Measuring and Mapping Saturated Hydraulic Conductivity in Three Dimensions. Vista Clara Inc.**

Liu, G., Butler, J.J., Jr., Bohling, G.C., Reboulet, E., Knobbe, S., and D. W. Hyndman, D.W. 2009, A new method for high-resolution characterization of hydraulic conductivity, Water Resour. Res., 45, W08202, doi:10.1029/2009WR008319.

Lonnes, S., A.Guzman-Garcia, and R. Holland, 2003. NMR petrophysical predictions on cores. Trans SPWLA 44th Ann Logg Symp 2003(paper DDD): 13.

Ramakrishnan, T.S., Schwartz, L.M., Fordham, E.J., Keyon, W.E. and Wilkinson, D.J., 1999. Forward models for nuclear magnetic resonance in carbonate rocks. The Log Analyst, 40(4): 260 - 270.

Sellwood, S.M., Healey, J.M., Birk, S., and Butler, J.J., Jr., 2005. Direct-push hydrostratigraphic profiling: Coupling electrical logging and slug tests, Ground Water, 43(1): 19-29.

Shushakov, O. A., 1996. Groundwater NMR in conductive water. Geophysics, vol. 61, No. 4, 998- 1006.

Toumelin, E., C.Torres-Verdin and Chen, S., 2003. Modeling of multiple echo-time NMR measurements for complex pore geometries and multiphase saturations, SPE Reservoir Evaluation & Engineering, San Antiono, September.

Walsh, D.O., 2008. Multi-channel Surface Instrumentation and Software for 1D/2D Groundwater Investigations. *Journal of Applied Geophysics*, Vol. 66, no 3-4, pp 140-150.

D. O. Walsh, 2006. Multi-dimensional surface NMR imaging and characterization of selected aquifers in the Western US. *2006 Meeting of the American Geophysical Union*, San Francisco CA, December 2006.

Weichmen, P., Lavey, E., Ritzwoller, M., 2000. Theory of surface nuclear magnetic resonance with applications to geophysical imaging problems. Physical Review E, 62 (1), 1290-1312.

## **D.9 Equipment**

No new equipment will be purchased for the proposed Phase 2 STTR project.

***DOE SBIR Topic# 33a: Integrated Use of Surface and Subsurface NMR for Measuring and Mapping Saturated Hydraulic Conductivity in Three Dimensions. Vista Clara Inc.***

**APPENDIX 1: Phase 1 - Stanford Completed Work (March 2011)**  
**Analysis of NMR Data from GEMS and GEMS2:**  
**Using the SDR Equation to Predict Hydraulic Conductivity**

## **INTRODUCTION TO OBJECTIVES**

Of interest in this study is the development of a methodology for using a combination of logging and surface NMR to obtain estimates of hydraulic conductivity  $K$  at a site. A critical component in this methodology is the availability of NMR and  $K$  measurements that can be used to obtain a site-specific understanding of the relationship between measured NMR parameters and  $K$  at a site. Our approach involves first acquiring co-located NMR logging data and  $K$  data, where the NMR logging data are acquired in a borehole or with a direct push (DP) method and the  $K$  data are acquired in a well or with a DP method; the latter  $K$  measurements will be referred to as the “true”  $K$  and taken as “ground truth”. This data set is used as a form of calibration, to determine the empirical relationship between the NMR measured parameters and true  $K$  that provides the best estimate of  $K$  within a single lithologic unit. A comparison of the NMR-derived  $K$  values to the true  $K$  values, in this calibration data set, provides a measure of the uncertainty. The determined relationship is then used to estimate  $K$  from other logging or surface NMR data.

## **CALIBRATION USING NMR LOGGING DATA AND K DATA**

Available from the GEMS and GEMS2 sites are NMR logging measurements obtained with borehole NMR, using either a 1.7 in or a 3.5 in diameter borehole tool; and with direct-push (DP) NMR, using a Geoprobe NMR tool. The NMR data were acquired and provided by Vista Clara. Also available for this study are  $K$  estimates from multilevel slug tests (MLST) and from DP measurements (acquired and provided by J. Butler, Kansas Geological Survey). We limited our analysis to data acquired in the gravel and sand unit at the sites. The data selected for analysis were

- 4) borehole NMR (acquired using the 3.5 in diameter tool) and MLST- $K$  measurements made in Wells 4N and 4S at the GEMS site;
- 5) borehole NMR (acquired using the 1.7 in diameter tool) and DP- $K$  measurements made at sites A (well A1) and C (well C1) in the GEMS2 area.
- 6) DP-NMR (NMR2?) and DP- $K$  measurements made at one location at the GEMS site.

$K$  can be estimated from the NMR measurements using the following Schlumberger-Doll Research (SDR) equation:

$$K_{SDR} = b \phi^m (T_{2ML})^n \quad (1)$$

where  $b$ ,  $m$ , and  $n$  are empirically determined constants,  $T_{2ML}$  is the mean log of the  $T_2$  relaxation time distribution (provided by Vista Clara) and  $\phi$  is the porosity determined from the NMR data (provided by Vista Clara). The constant  $b$  is referred to as the lithologic constant. In using the above equation we elected, as is common practice, to set the exponent  $n$  on the  $T_{2ML}$  term equal to 2. The objectives of this component of the study were to 1) determine the values of the empirical constants in the SDR equation that

**DOE SBIR Topic# 33a: Integrated Use of Surface and Subsurface NMR for Measuring and Mapping Saturated Hydraulic Conductivity in Three Dimensions. Vista Clara Inc.**

would optimize the agreement between  $K$  predicted from the NMR data and  $K$  from the MLST or DP measurements acquired at the same location; 2) assess the error/uncertainty in  $K$  predictions when the empirical constants were used to predict  $K$  at a nearby site. The optimization was done using a least squares inversion. We used five different inversion methods, including unconstrained, semi-constrained, and constrained inversions. In the semi-constrained inversion, the exponent  $m$  on the porosity term was constrained to be positive, ranging from 0.5 and 4, increasing in value with an interval of 0.5; there was no constraint on the lithologic constant. In three forms of a constrained inversion, the exponent  $m$  on porosity was constrained to be 1, 2 and 4; there was no constraint on the lithologic constant.

The inversion could be conducted in two ways. The first would be to set our objective function to be minimized as the difference between NMR-derived  $K$ , denoted as NMR-K, and true  $K$ , denoted as TRUE-K; i.e. we minimize  $[(\text{NMR-K}) - (\text{TRUE-K})]$ . To do this, we would use a nonlinear least squares method, with equation 1 as given above used to calculate NMR-K. Alternatively we can rewrite equation 1 in linear form:

$$\log(K_{SDR}) = \log b + 2\log(T_{2ML}) + m \log \phi \quad (2)$$

and use a linear least squares method to solve for  $b$  and  $m$ . In this case we would minimize  $[\log(\text{NMR-K}) - \log(\text{TRUE-K})]$ . Due to the distribution observed in the  $K$  measurements at the sampling locations, we elected to use this second approach.

### **GEMS Site: Wells 4S and 4N**

Wells 4S and 4N are two wells at the GEMS site, completed with 4 in casing. Well 4N is ~11 m northwest of 4S. In both wells, NMR data were acquired using the 3.5in diameter borehole NMR tool. The depth range of interest in Well 4S was from 11.3 m to 19.8 m, and in Well 4N was from 11.3 m to 20.3 m. This corresponded to the sand and gravel section in each well. In addition to considering the depth-varying  $K$ -measurements, we also compared the single arithmetic mean in each well, over the entire sand and gravel unit, of the NMR-derived  $K$  and true  $K$ .

In order to optimize the fit between NMR-derived- $K$  and MLST-  $K$ , we ideally would use NMR and MLST measurements made at the same depth. However, the MLST and NMR logging data were not acquired at the same depths. The MLST data were acquired approximately every 2/3-meter; the NMR logging data were acquired, using the 3.5 in diameter borehole NMR tool, every ½ meter. NMR logging data were paired with the MLST data only if the datasets were acquired at depths within 1/3 meter of each other.

We first used the NMR and MLST data from Well 4S with the five inversion methods described above. The values for the SDR empirical constants determined for the dataset from this well (and for all other analyzed datasets) are given in Table 1. Figure 1a provides a comparison of the  $K$  predictions from the NMR data using these constants and MLST-  $K$ . Figure 1b displays the residuals as  $\log(\text{NMR- } K) - \log(\text{MLST- } K)$ . Figure 1c shows the error as  $\text{NMR- } K - \text{MLST- } K$ . Figure 1d shows  $\log(\text{NMR- } K)$  vs  $\log(\text{MLST- } K)$  with the 1:1 line in black.

***DOE SBIR Topic# 33a: Integrated Use of Surface and Subsurface NMR for Measuring and Mapping Saturated Hydraulic Conductivity in Three Dimensions. Vista Clara Inc.***

In Table 2 we compare the arithmetic mean K, predicted from the NMR data using the empirical constants from the five inversion methods, to the arithmetic mean calculated from the TRUE-K measurements. For the dataset from Well 4S, there is little difference in the means of the predicted NMR-K's, but all are greater by ~10 m/day than the mean of the TRUE-K of 81.5 m/day.

**DOE SBIR Topic# 33a: Integrated Use of Surface and Subsurface NMR for Measuring and Mapping Saturated Hydraulic Conductivity in Three Dimensions. Vista Clara Inc.**

**Table 1.** The values for the empirical constants found for each data set using the different inversion methods. “Pre” and “Post” are used to indicate that the NMR data were acquired before (Pre) and after (Post) development of the well. The addition of #1 and #2 indicates that there were two stages of development.

Dataset	Method 1: Unconstrained Inversion	Method 2: Semi-Constrained Inversion $0.5 < m < 4$	Method 3: Constrained Inversion $m=1$	Method 4: Constrained Inversion $m=2$	Method 5: Constrained Inversion $m=4$
Well 4S	$b=1.3e7; m=8$	$b=1.3e5 ; m=4$	$b=4.4e3$	$b=1.4e4$	$b=1.3e5$
Well 4N	$b=3.4e3; m=-0.8$	$b=2.0e4; m=0.5$	$b=4.0e4$	$b=1.6e5$	$b=2.4e6$
Well C1					
Pre	$b=2; m=-7.5$	$b=1.2e4; m=0.5$	$b=2e4$	$b=5.9e4$	$b=5.2e5$
Post #1	$b=65; m=-2.7$	$b=2.6e3; m=0.5$	$b=4.7e3$	$b=1.5e4$	$b=1.4e5$
Post #2	$b=4.3e5; m=5$	$b=2.9e3; m=0.5$	$b=5e3$	$b=1.5e4$	$b=1.5e5$
Well A1					
Pre	$b=7.8e6; m=7$	$b=5.4e3; m=0.5$	$b=9.4e3$	$b=2.9e4$	$b=2.7e5$
Post	$b=1.2e4; m=1.5$	$b=6.7e3 ; m=1$	$b=6.7e3$	$b=2.2e4$	$b=2.3e5$
NMR2	$b= 4e2; m=-3.1$	$b=2.7e4; m=0.5$	$b=4.9e4$	$b=1.6e5$	$b=1.6e6$

**Table 2.** Comparison of the arithmetic mean of the TRUE- $K$  values and arithmetic mean of each set of NMR- $K$  values, derived using the empirical constants from each inversion method. Results are shown for all available datasets. “Pre” and “Post” are used to indicate that the NMR data were acquired before (Pre) and after (Post) development of the well. The addition of #1 and #2 indicates that there were two stages of development.

Dataset	Arithmetic Mean K values (m/day)					
	True-K	Predicted NMR-K				
		Method 1	Method 2	Method 3	Method 4	Method 5
Well 4S	81.5	91.0	90.5	94.0	92.6	91.0
Well 4N	79.4	127	156	169	201	295
Well C1	109					
Pre		167	149	150	154	164
Post #1		110	109	114	115	120
Post #2		117	116	116	116	116
Well A1	42					
Pre		24.5	30.6	29.7	28.2	26.0
Post		44.0	43.0	43.0	45.1	51.0
NMR2	182	206	213	215	220	232

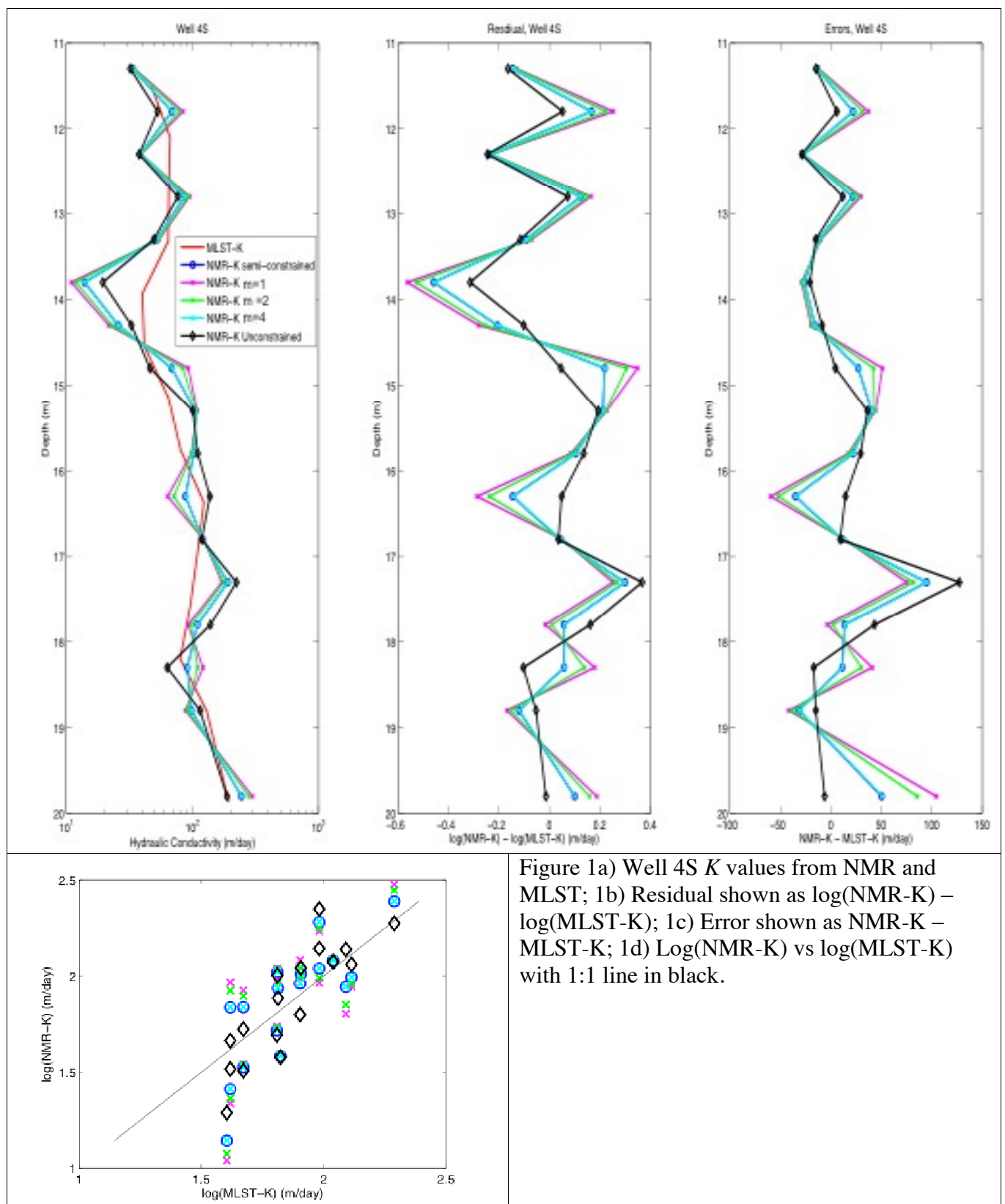
***DOE SBIR Topic# 33a: Integrated Use of Surface and Subsurface NMR for Measuring and Mapping Saturated Hydraulic Conductivity in Three Dimensions. Vista Clara Inc.***

The data from Well 4N were used to obtain the empirical constants listed in Table 1. Figure 2a provides a comparison of the  $K$  predictions from the NMR data using the determined constants and MLST-  $K$ . Figure 2b displays the residuals as  $\log(\text{NMR- } K) - \log(\text{MLST- } K)$ . Figure 2c shows the error as  $\text{NMR- } K - \text{MLST- } K$ . Figure 2d shows  $\log(\text{NMR- } K)$  vs  $\log(\text{MLST- } K)$  with the 1:1 line in black. When the means of the NMR-  $K$  and TRUE- $K$  values are compared in Table 2, we find significant differences in the means of the NMR- $K$  values, and all are greater than the mean of the TRUE- $K$  values.

In these first two steps, we have used co-located NMR and MLST data to optimize the agreement between NMR-  $K$  and MLST-  $K$ . In practice, we want to be able to determine the best values of the SDR empirical constants at one location, and then use these values in other locations to predict  $K$  from surface NMR data. Thus the question we pose: If we determine the empirical constants so as to optimize the agreement between NMR-derived and true- $K$  estimates (from co-located data) in one well, how accurate are the NMR-derived-  $K$  values in the other well? In Figure 3a, we use the empirical constants determined in Well4N to obtain NMR-derived-  $K$  in Well4S; these values are compared to the MLST-  $K$  values from Well4S. In Figure 3b we plot the errors as  $\log(\text{NMR- } K) - \log(\text{MLST- } K)$ . Figure 3c plots the errors as  $\text{NMR- } K - \text{MLST- } K$ . Figure 3d plots  $\log(\text{NMR- } K)$  vs  $\log(\text{MLST- } K)$  and we see that NMR-  $K$  is consistently over predicted. In Figure 4a, we use the empirical constants determined in Well4S to obtain NMR-derived-  $K$  in Well4N; these values are compared to the MLST-  $K$  values from Well4N. In Figure 4b we plot the errors as  $\log(\text{MLST- } K) - \log(\text{NMR- } K)$  and in figure 4c we plot errors as  $\text{MLST- } K - \text{NMR- } K$ . Figure 4d plots  $\log(\text{NMR- } K)$  vs  $\log(\text{MLST- } K)$  and we see that NMR-  $K$  consistently over-predicts true- $K$ .

The empirical constants derived in Well 4S result in NMR-K estimates which provide a good estimate of MLST-K. As shown in figure 1a, the trends of high MLST-K at ~13m and ~17m and low MLST-K at ~14m are captured in the NMR-K estimates. However in Well 4N, as shown in figure 2a, the NMR-K estimate show more  $K$  variation than is seen in MLST-K. In addition, for Well 4N, table 1 shows that the  $b$  values determined in methods 3 through 5 are an order of magnitude larger than the  $b$  values from Wells 4S. Although the MLST-K values are fairly different in Well 4S and 4N, the trends in NMR-K are fairly similar. They both show low NMR-K at ~14m and high NMR-K at~17m. We suspect that there is error in the MLST-K data in Well 4N. In Wells 4S and 4N, the empirical constants derived in one well could not be used to estimate K in the other well. Figure 3d shows that K is consistently over estimated in Well 4S when using the empirical constants determined in Well 4N. Additionally, figure 4d shows that K is underestimated in Well 4N when using the empirical constants determined in Well 4S. For this set of wells, it was not possible to use the empirical constants determined in one well to accurately predict NMR-K in the other well.

**DOE SBIR Topic# 33a: Integrated Use of Surface and Subsurface NMR for Measuring and Mapping Saturated Hydraulic Conductivity in Three Dimensions. Vista Clara Inc.**



**DOE SBIR Topic# 33a: Integrated Use of Surface and Subsurface NMR for Measuring and Mapping Saturated Hydraulic Conductivity in Three Dimensions. Vista Clara Inc.**

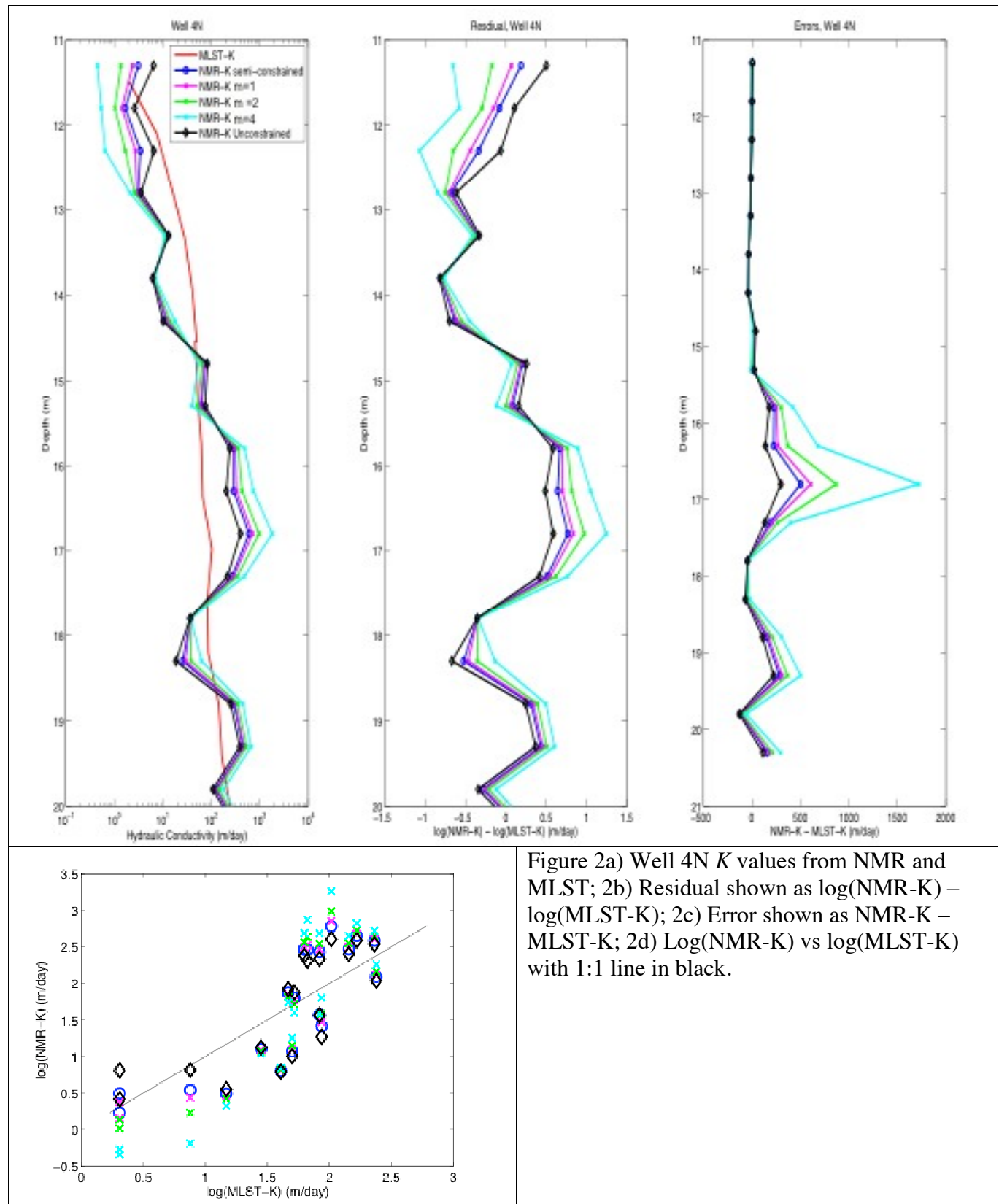
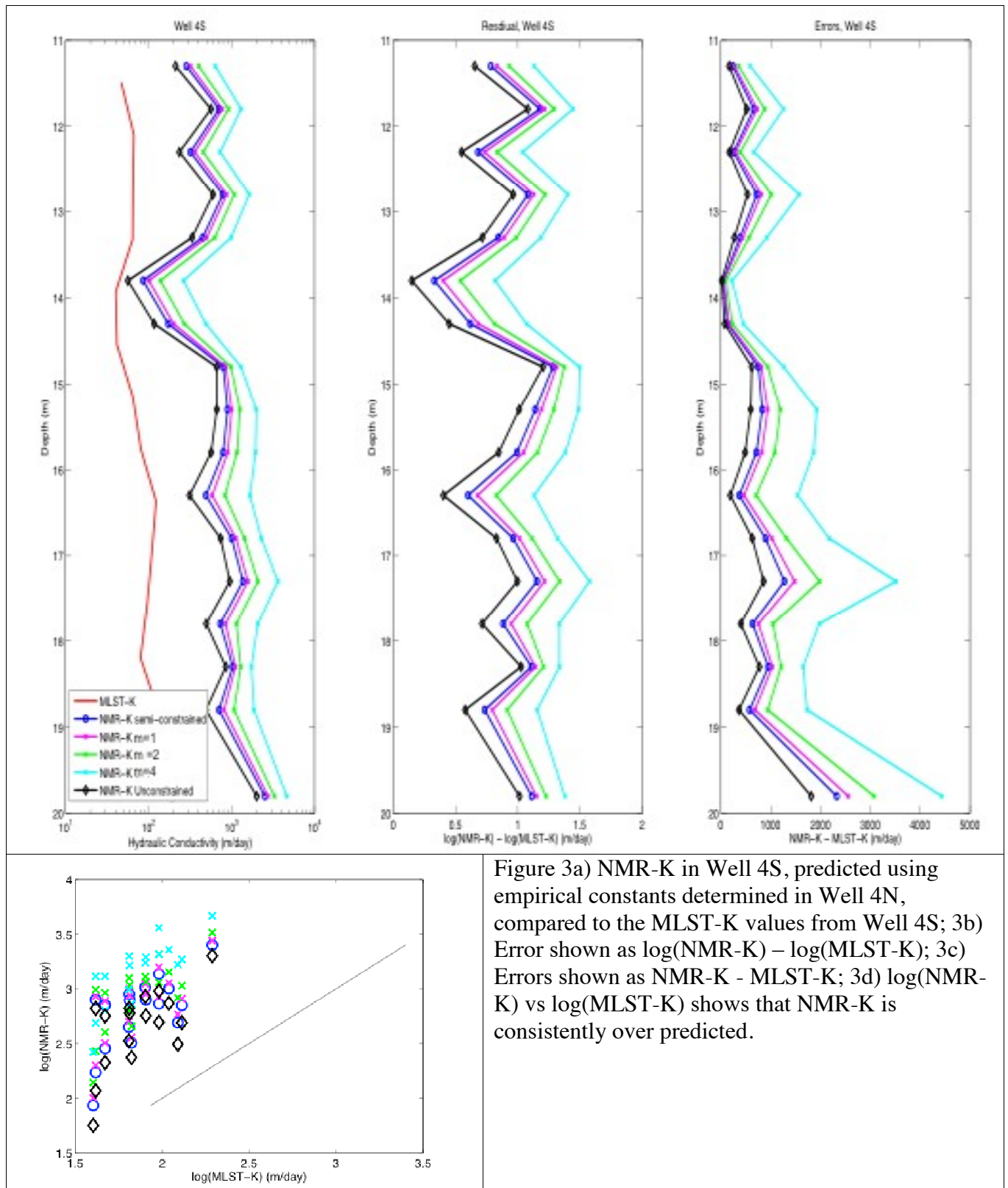
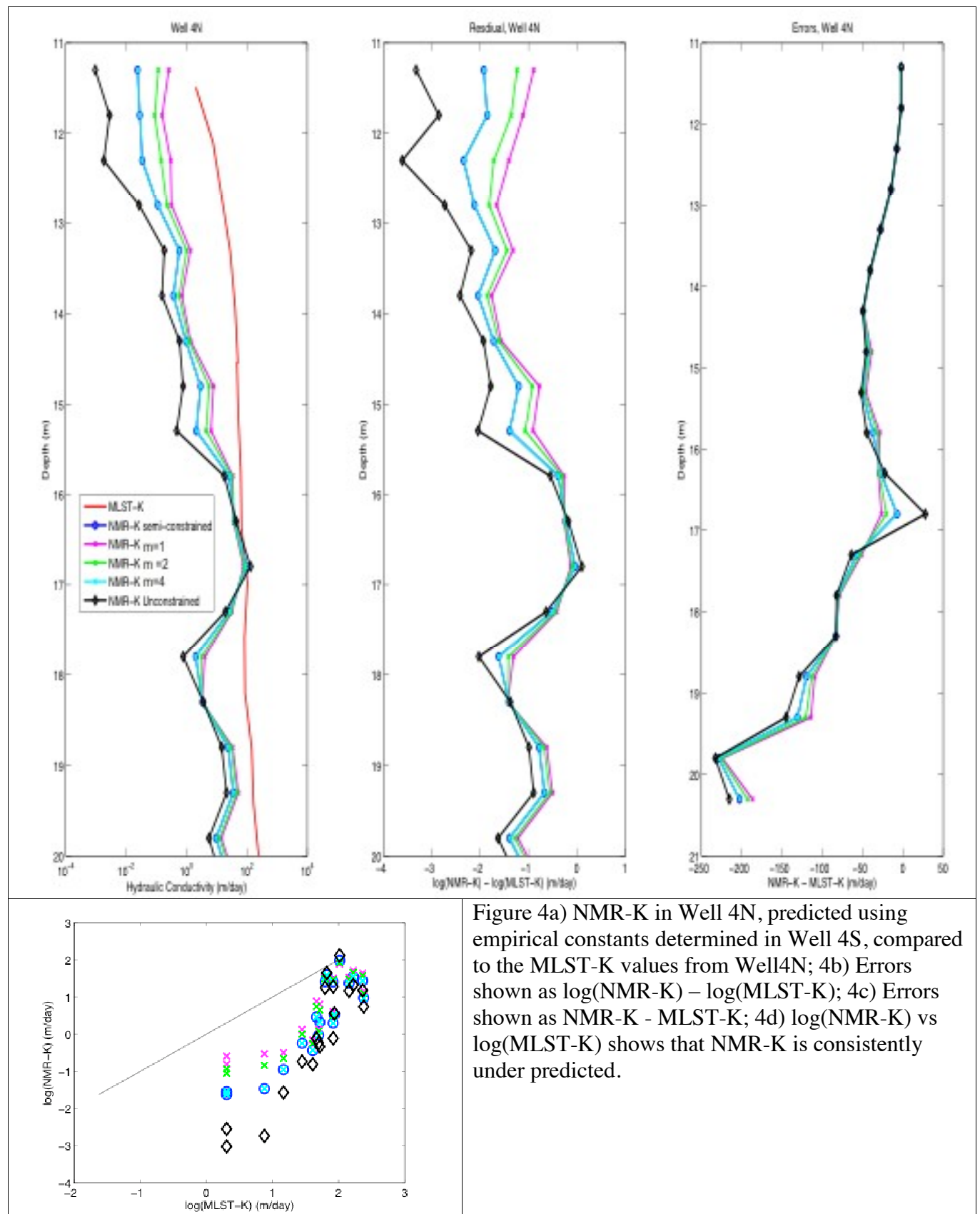


Figure 2a) Well 4N  $K$  values from NMR and MLST; 2b) Residual shown as  $\log(\text{NMR-K}) - \log(\text{MLST-K})$ ; 2c) Error shown as  $\text{NMR-K} - \text{MLST-K}$ ; 2d)  $\log(\text{NMR-K})$  vs  $\log(\text{MLST-K})$  with 1:1 line in black.

**DOE SBIR Topic# 33a: Integrated Use of Surface and Subsurface NMR for Measuring and Mapping Saturated Hydraulic Conductivity in Three Dimensions. Vista Clara Inc.**



**DOE SBIR Topic# 33a: Integrated Use of Surface and Subsurface NMR for Measuring and Mapping Saturated Hydraulic Conductivity in Three Dimensions. Vista Clara Inc.**



## **GEMS2 Area: Wells C1 and A1**

The GEMS2 area is described with reference to three sites: A, C, and D, the locations of which are shown in the site map at the end of this report. Wells C1 and A1 are approximately 300 m apart, in the GEMS2 area. Both wells were installed using a 3.25 in Geoprobe, then completed with 2 in PVC casing. Available from Well C1 are one DP-*K* data set and three borehole NMR data sets, acquired with the 1.7 in borehole NMR tool: pre-development (collected 10/19), post-development #1 (collected 10/21), post-development #2 (collected 10/27). Both DP-*K* and NMR logging data were acquired every meter. The borehole NMR data were acquired at depths 0.2 meters shallower than the DP-*K* data, but are treated as paired.

Our analysis of the pre-development data from Well C1 yielded the values for the empirical constants given in Table 1. Figure 5a provides a comparison of the NMR-*K* predictions using these constants and DP-*K*. Figure 5b displays the residuals as  $\log(\text{NMR- } K) - \log(\text{DP- } K)$ . Figure 5c shows the error as NMR- *K* - DP- *K*. Figure 5d shows  $\log(\text{NMR- } K)$  vs  $\log(\text{DP- } K)$  with the 1:1 line in black.

The data from Well C1 post-development #1, and #2 yielded different sets of empirical constants, as shown in Table 1. Figure 6 presents the results for the post-development #1 data set. Figure 6a provides a comparison of the *K* predictions using the constants and *K* from the DP. Figure 6 b displays the residuals as  $\log(\text{NMR- } K) - \log(\text{DP- } K)$ . Figure 6c shows the error as NMR- *K* - DP- *K*. Figure 6d shows  $\log(\text{NMR- } K)$  vs  $\log(\text{DP- } K)$  with the 1:1 line in black. Figure 7 presents the results in the same format for the post-development #2 data.

The NMR-*K* estimates from Well C1 pre-development and post-development #1 and #2 do a fairly good job of estimating high DP-*K* at ~11.5m and ~14.5m but are not able to match the high DP-*K* at ~18m. At ~18m, all three NMR-*K* estimates show a very low *K*. Due to the fact that all three NMR-*K* estimates are low at this depth, it is possible that there is a clay lens around the well that has affected the NMR data but not the DP-*K* data. The *b* values for inversion methods 3 through 5, are consistently larger in the pre-development data than the post-development data. Additionally, the pre-development mean *K* values are significantly larger than mean DP-*K* values, whereas post-development #1 and #2 mean *K* values are ~10 m/day larger than the mean DP-*K*.

Available from Well A1 are one DP-*K* data set and two NMR data sets, acquired with the 1.7 in borehole NMR tool: pre-development (collected 10/20) and post-development (collected 10/28). Both DP-*K* and NMR logging data were acquired every meter. The NMR logging data were acquired at depths 0.2 meters shallower than the DP-*K* data, but are treated as paired.

The data from Well A1 pre-development were used to obtain the empirical constants listed in Table 1. Figure 8a provides a comparison of the *K* predictions using these constants and DP-*K*. Figure 8b displays the residuals as  $\log(\text{NMR- } K) - \log(\text{DP- } K)$ .

**DOE SBIR Topic# 33a: Integrated Use of Surface and Subsurface NMR for Measuring and Mapping Saturated Hydraulic Conductivity in Three Dimensions. Vista Clara Inc.**

Figure 8c shows the error as NMR- $K$  - DP- $K$ . Figure 8d shows log(NMR- $K$ ) vs log(DP- $K$ ) with the 1:1 line in black.

The values of the empirical constants acquired using the data from Well A1 post-development are given in Table 1. Figure 9a provides a comparison of the  $K$  predictions using these constants and  $K$  from the DP. Figure 9b displays the residuals as log(NMR- $K$ ) – log(DP- $K$ ). Figure 9c shows the error as NMR- $K$  - DP- $K$ . Figure 9d shows log(NMR- $K$ ) vs log(DP- $K$ ) with the 1:1 line in black.

The NMR-K estimates from Well A1 pre-development and post-development both do a excellent job of estimating DP-K. Both NMR-K estimates capture the high K values at 14m and 18m and the low K at 11m and 16m. As in Well C1, the  $b$  values in Well A1 are consistently larger in the pre-development data than the post-development data. However, in Well A1, the pre-development mean K values are less than the mean DP-K while the post-development mean K values are less than 10 m/day greater than mean DP-K.

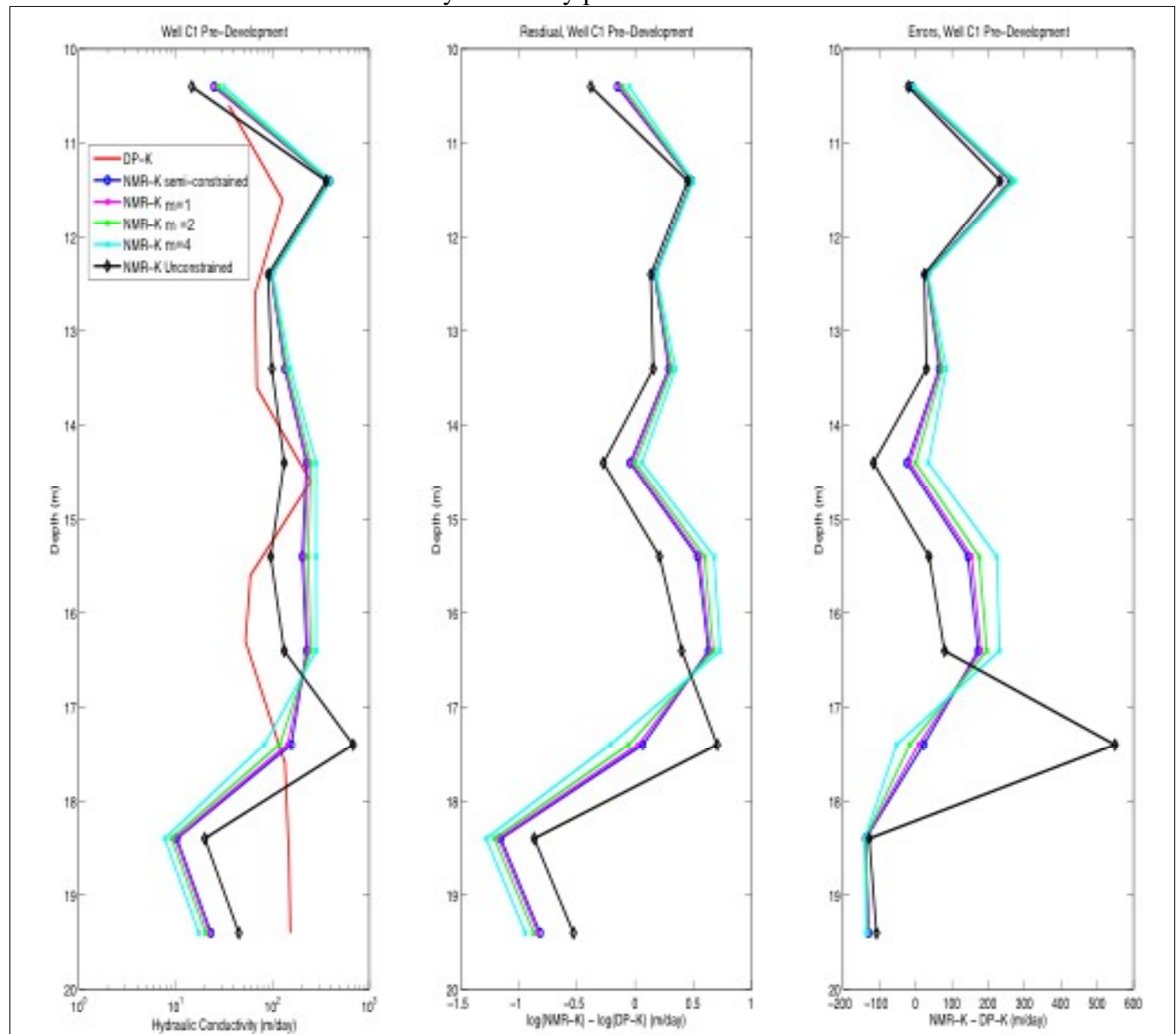
Lastly, we addressed the same question posed for the wells at the GEMS site: If we determine  $K$ -estimates (from co-located data) in one well, how accurate are the NMR-derived- $K$  values in the other well? In Figure 10a, we use the empirical constants determined in Well A1 post-development to obtain NMR-derived- $K$  in Well C1 post-development #1; these values are compared to the DP- $K$  values from Well C1. In Figure 10b we plot the errors as log(NMR- $K$ ) – log(DP- $K$ ) and figure 10c plots the errors as NMR- $K$  - DP- $K$ . Figure 10d plots log(NMR- $K$ ) vs log(DP- $K$ ) with the 1:1 line shown in black. In Figure 11a, we use the empirical constants determined in Well A1 post-development to obtain NMR-derived- $K$  in Well C1 post-development #2; these values are compared to the DP- $K$  values from Well C1. In Figure 11b we plot the errors as log(NMR- $K$ ) – log(DP- $K$ ). Figure 11c plots the errors as NMR- $K$  - DP- $K$ . Figure 11d plots log(NMR- $K$ ) vs log(DP- $K$ ) with the 1:1 line shown in black.

In Figure 12a, we use the empirical constants determined in Well C1 post-development #1 to obtain NMR-derived- $K$  in Well A1 post-development; these values are compared to the DP- $K$  values from Well A1. In Figure 12b we plot the errors as log(NMR- $K$ ) – log(DP- $K$ ). Figure 12c plots the errors as NMR- $K$  - DP- $K$ . Figure 12d plots log(NMR- $K$ ) vs log(DP- $K$ ) with the 1:1 line shown in black. In Figure 13a, we use the empirical constants determined in Well C1 post-development #2 to obtain NMR-derived- $K$  in Well A1 post-development; these values are compared to the DP- $K$  values from Well A1. In Figure 13b we plot the errors as log(NMR- $K$ ) – log(DP- $K$ ). Figure 13c plots the errors as NMR- $K$  - DP- $K$ . Figure 13d plots NMR- $K$  vs DP- $K$  with the 1:1 line shown in black.

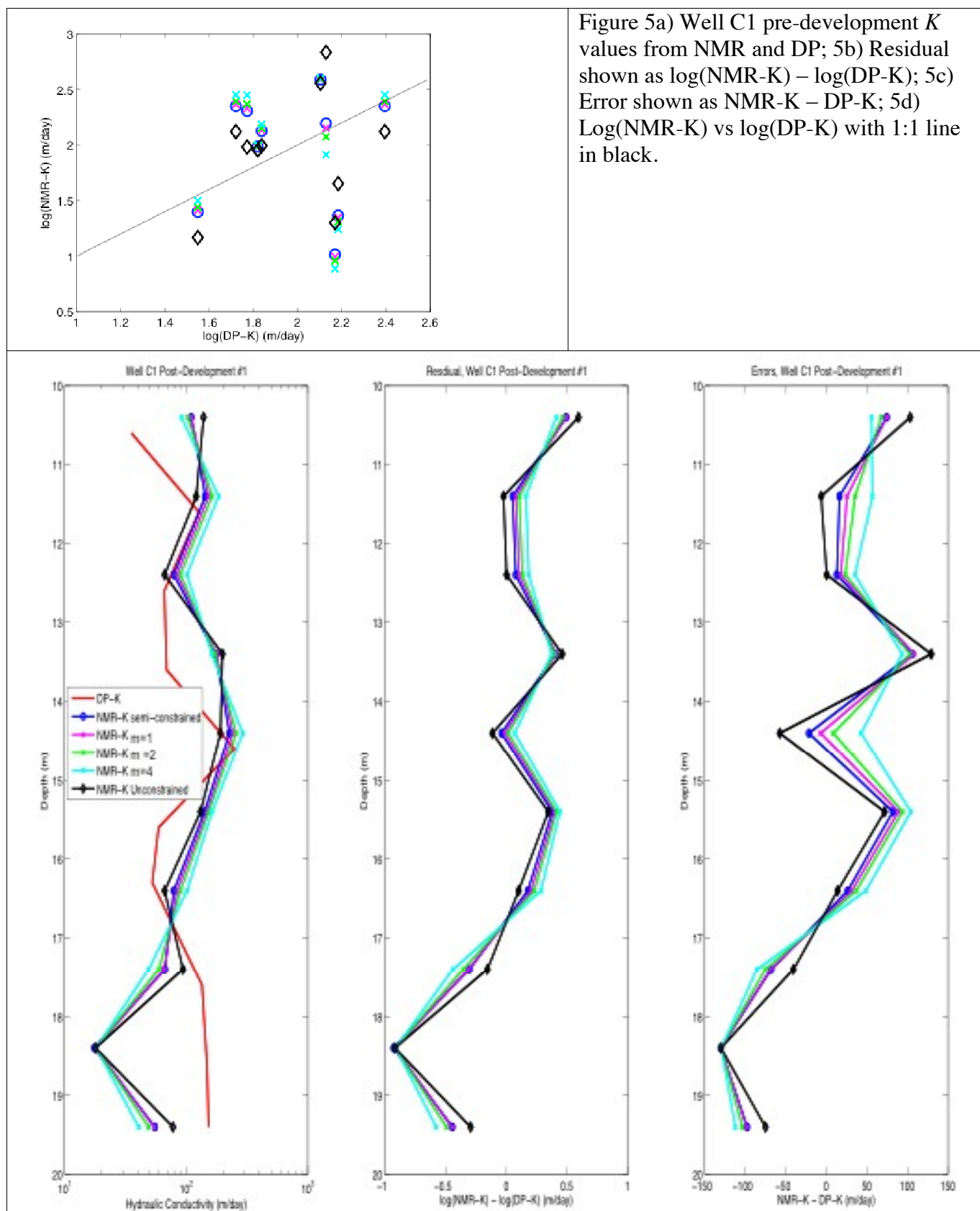
The empirical constants derived in Well A1 post-development do a fairly poor job of estimating NMR-K in Wells C1 post-development #1 and #2, as shown in figure 10a and 11a. In both Well C1 post-development #1 and #2, NMR-K is slightly over-estimated from 10m to 17m and underestimated from 17m to 19.5m. As suggested earlier, the underestimation from 17m to 19.5m is possibly due to a clay lens or other anomaly around the well. As shown in figure 12a and 13a, the empirical constants determined in

**DOE SBIR Topic# 33a: Integrated Use of Surface and Subsurface NMR for Measuring and Mapping Saturated Hydraulic Conductivity in Three Dimensions. Vista Clara Inc.**

Well C1 post-development #1 and #2 both do an excellent job of predicting NMR-K in Well A1 post-development. For this set of wells, it is possible to use the empirical constants derived in one well to fairly accurately predict NMR-K in another well.



**DOE SBIR Topic# 33a: Integrated Use of Surface and Subsurface NMR for Measuring and Mapping Saturated Hydraulic Conductivity in Three Dimensions. Vista Clara Inc.**



**DOE SBIR Topic# 33a: Integrated Use of Surface and Subsurface NMR for Measuring and Mapping Saturated Hydraulic Conductivity in Three Dimensions. Vista Clara Inc.**

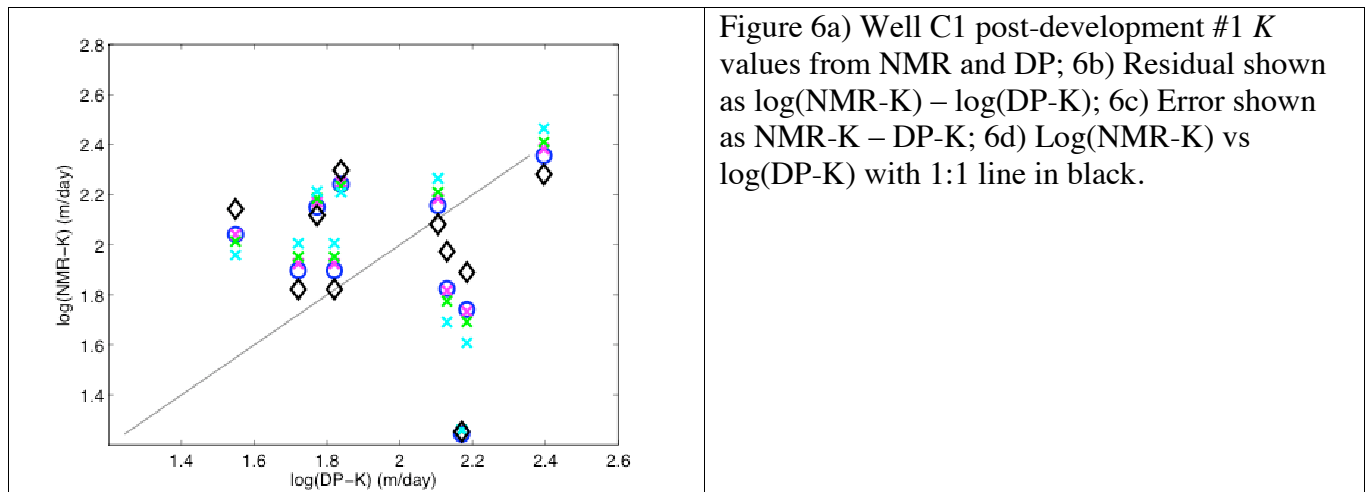
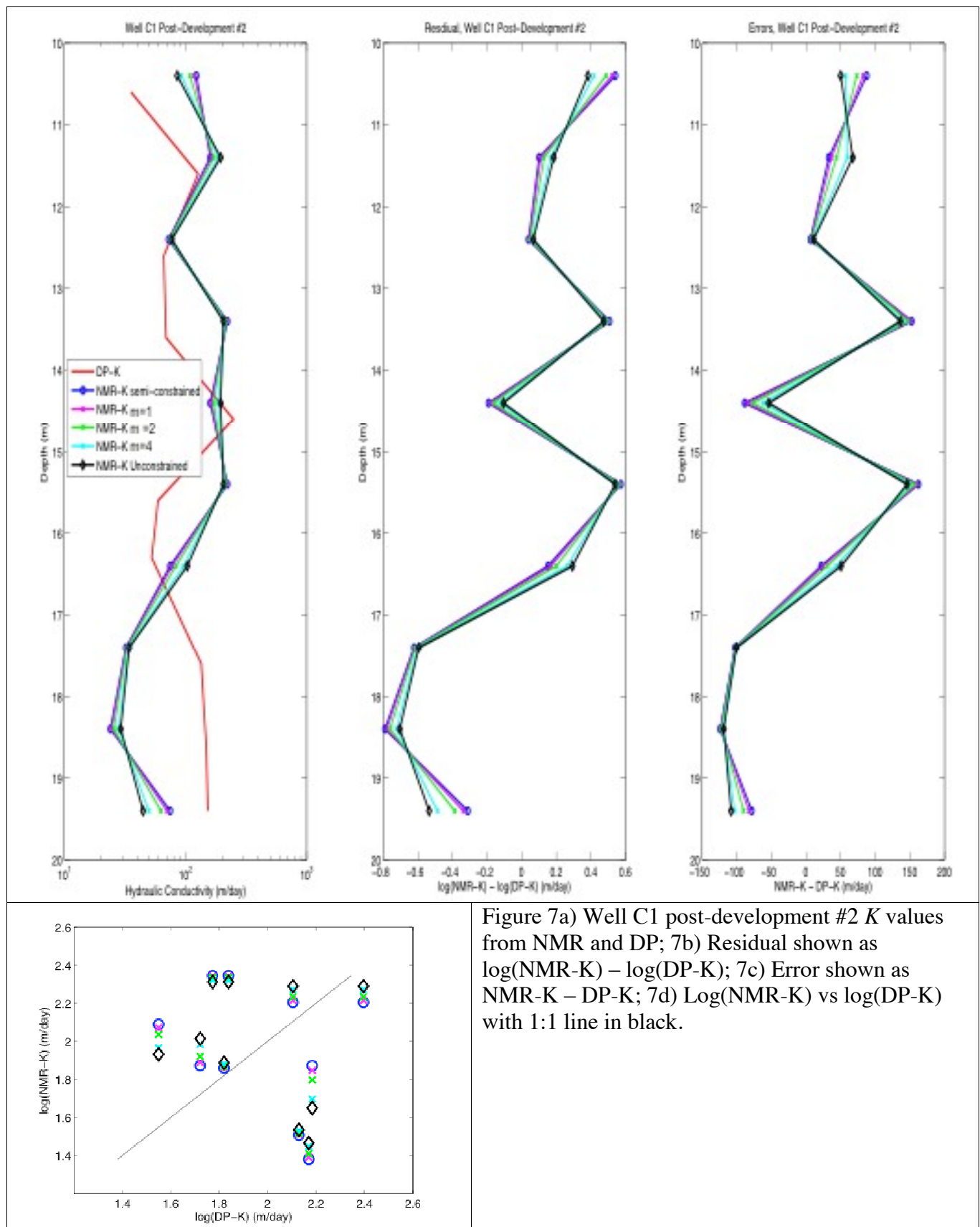


Figure 6a) Well C1 post-development #1 K values from NMR and DP; 6b) Residual shown as  $\log(\text{NMR-K}) - \log(\text{DP-K})$ ; 6c) Error shown as  $\text{NMR-K} - \text{DP-K}$ ; 6d)  $\log(\text{NMR-K})$  vs  $\log(\text{DP-K})$  with 1:1 line in black.

**DOE SBIR Topic# 33a: Integrated Use of Surface and Subsurface NMR for Measuring and Mapping Saturated Hydraulic Conductivity in Three Dimensions. Vista Clara Inc.**



**DOE SBIR Topic# 33a: Integrated Use of Surface and Subsurface NMR for Measuring and Mapping Saturated Hydraulic Conductivity in Three Dimensions. Vista Clara Inc.**

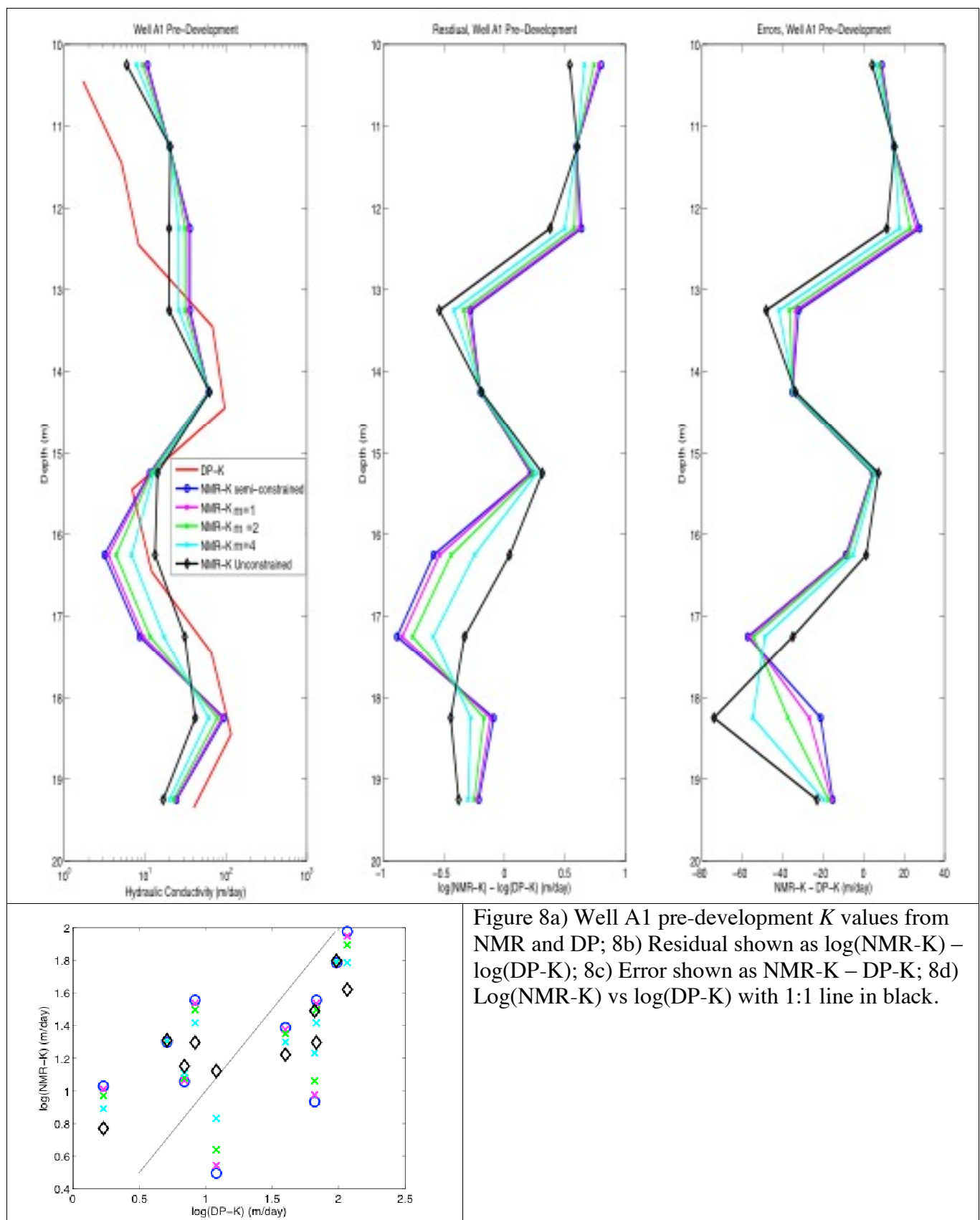


Figure 8a) Well A1 pre-development  $K$  values from NMR and DP; 8b) Residual shown as  $\log(\text{NMR-}K) - \log(\text{DP-}K)$ ; 8c) Error shown as  $\text{NMR-}K - \text{DP-}K$ ; 8d)  $\log(\text{NMR-}K)$  vs  $\log(\text{DP-}K)$  with 1:1 line in black.

**DOE SBIR Topic# 33a: Integrated Use of Surface and Subsurface NMR for Measuring and Mapping Saturated Hydraulic Conductivity in Three Dimensions. Vista Clara Inc.**

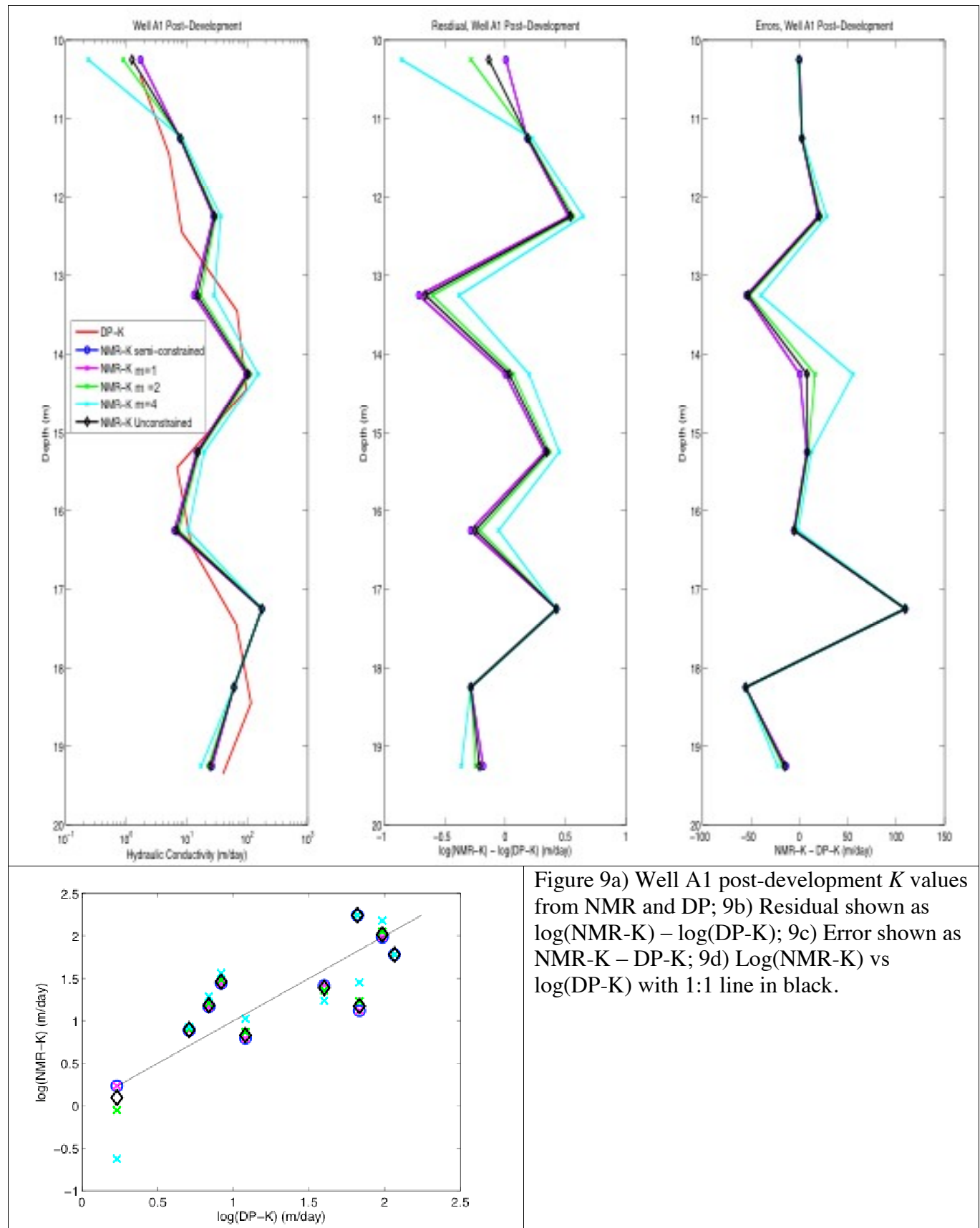


Figure 9a) Well A1 post-development  $K$  values from NMR and DP; 9b) Residual shown as  $\log(\text{NMR-K}) - \log(\text{DP-K})$ ; 9c) Error shown as  $\text{NMR-K} - \text{DP-K}$ ; 9d)  $\log(\text{NMR-K})$  vs  $\log(\text{DP-K})$  with 1:1 line in black.

**DOE SBIR Topic# 33a: Integrated Use of Surface and Subsurface NMR for Measuring and Mapping Saturated Hydraulic Conductivity in Three Dimensions. Vista Clara Inc.**

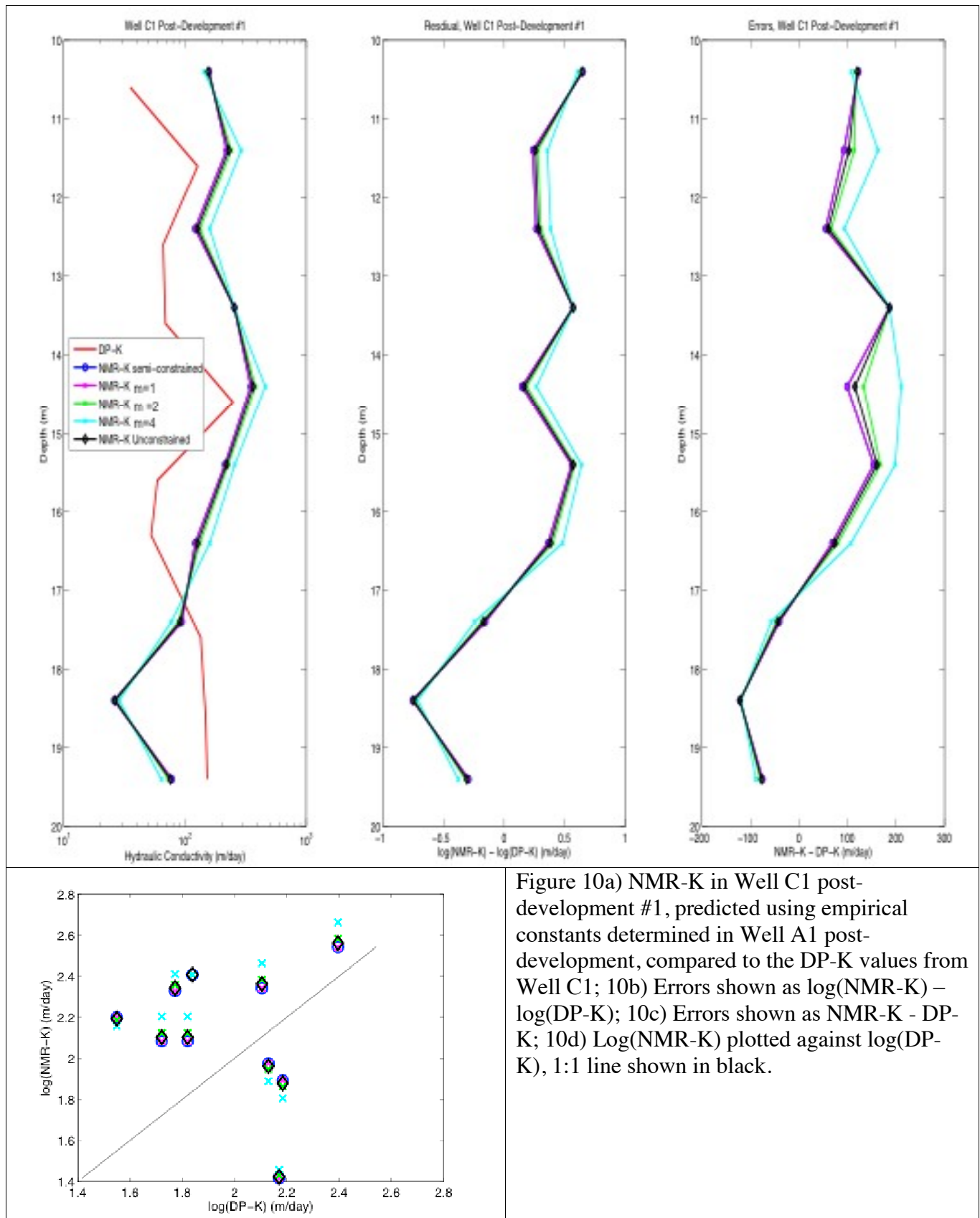
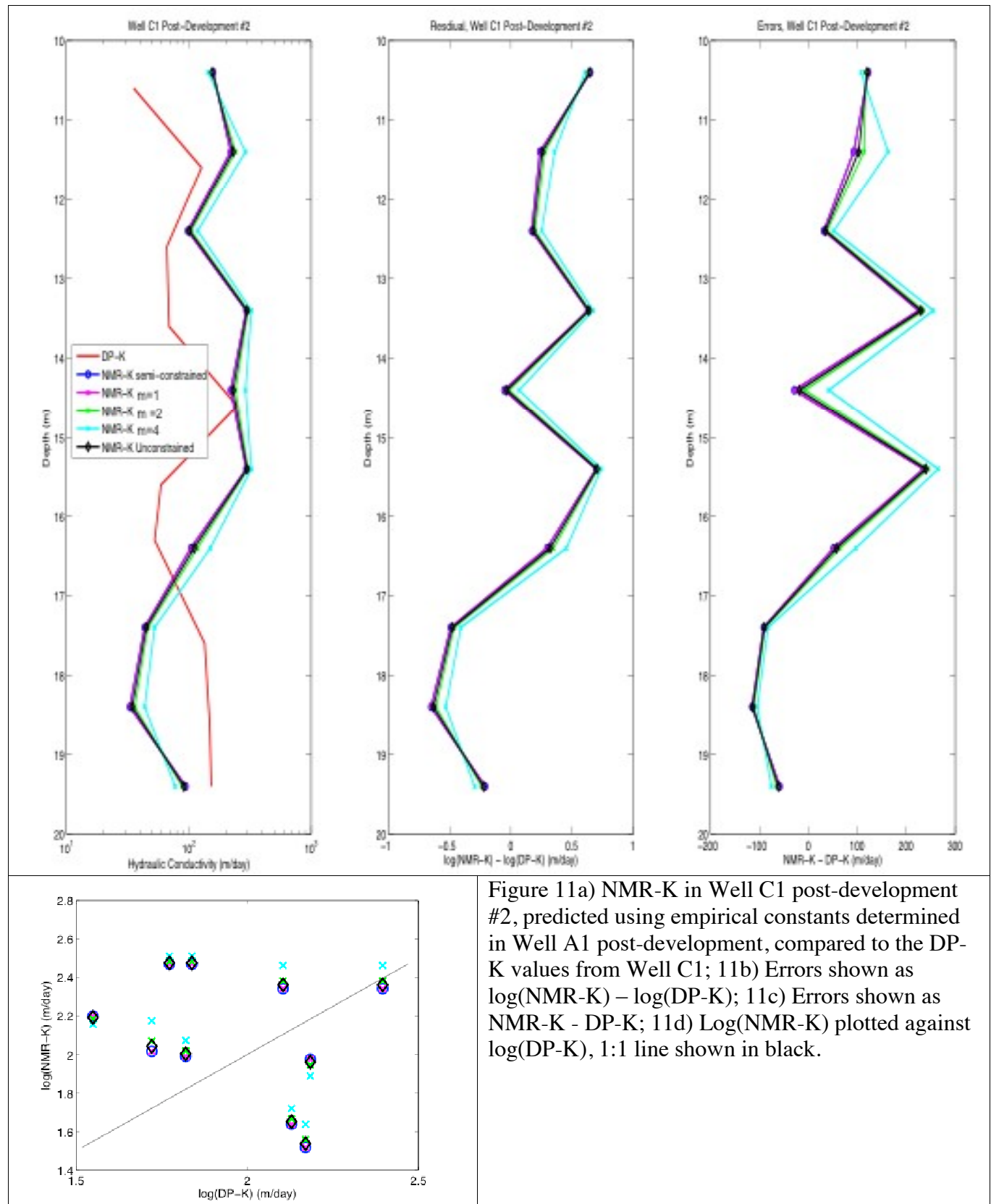
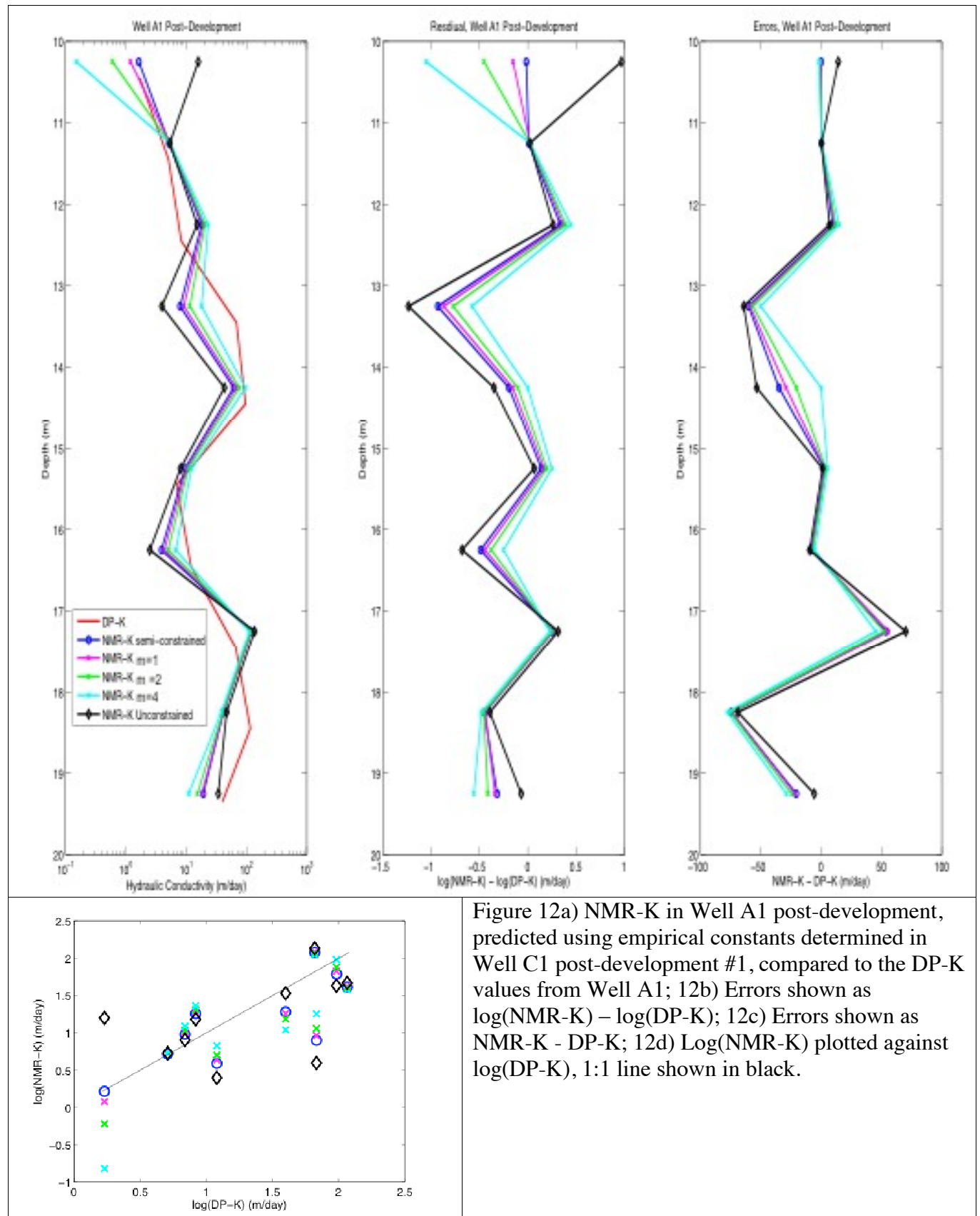


Figure 10a) NMR-K in Well C1 post-development #1, predicted using empirical constants determined in Well A1 post-development, compared to the DP-K values from Well C1; 10b) Errors shown as  $\log(\text{NMR-K}) - \log(\text{DP-K})$ ; 10c) Errors shown as  $\text{NMR-K} - \text{DP-K}$ ; 10d)  $\log(\text{NMR-K})$  plotted against  $\log(\text{DP-K})$ , 1:1 line shown in black.

**DOE SBIR Topic# 33a: Integrated Use of Surface and Subsurface NMR for Measuring and Mapping Saturated Hydraulic Conductivity in Three Dimensions. Vista Clara Inc.**



**DOE SBIR Topic# 33a: Integrated Use of Surface and Subsurface NMR for Measuring and Mapping Saturated Hydraulic Conductivity in Three Dimensions. Vista Clara Inc.**



**DOE SBIR Topic# 33a: Integrated Use of Surface and Subsurface NMR for Measuring and Mapping Saturated Hydraulic Conductivity in Three Dimensions. Vista Clara Inc.**

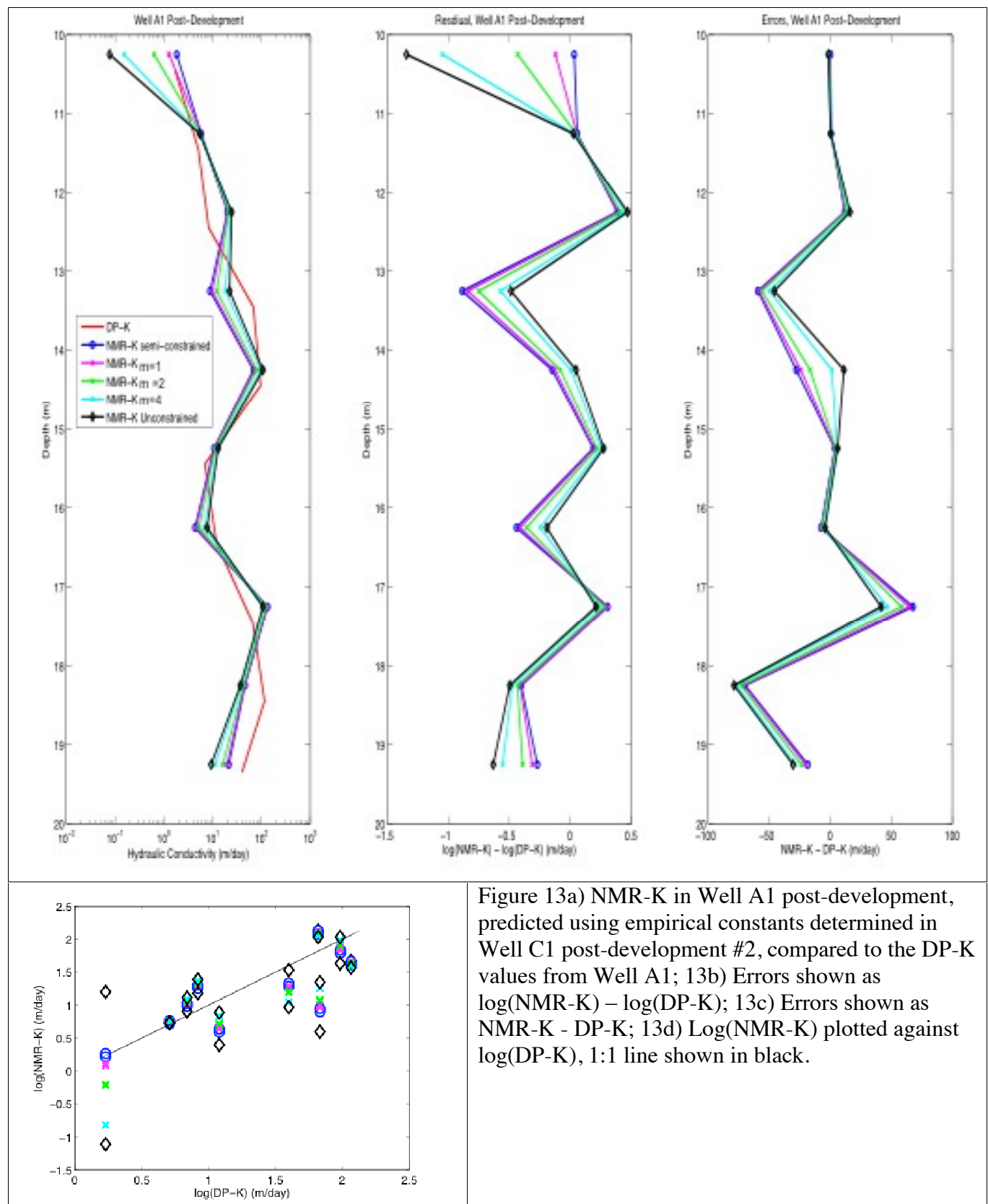


Figure 13a) NMR-K in Well A1 post-development, predicted using empirical constants determined in Well C1 post-development #2, compared to the DP-K values from Well A1; 13b) Errors shown as  $\log(\text{NMR-K}) - \log(\text{DP-K})$ ; 13c) Errors shown as  $\text{NMR-K} - \text{DP-K}$ ; 13d)  $\log(\text{NMR-K})$  plotted against  $\log(\text{DP-K})$ , 1:1 line shown in black.

### **GEMS Site: NMR2**

The NMR data from a location at the GEMS site referred to as NMR2 were acquired using the DP-NMR tool. Approximately 2 m from this site, DP-K values were also acquired; so we treat these as co-located data that can be used for calibration purposes. Two DP-K measurements were acquired at each depth interval and were averaged in order to obtain a single value to be treated as TRUE-K at this depth. NMR and DP-K data were acquired approximately every ½ meter. NMR data were paired with the DP-K data only if the datasets were acquired at depths within 1/3 meter of each other.

The data from NMR2 yielded the values of empirical constants given in Table 1. Figure 14a provides a comparison of the  $K$  predictions using these constants and DP-K. Figure 14b displays the residuals as  $\log(\text{NMR- } K) - \log(\text{DP- } K)$ . Figure 14c shows the error as  $\text{NMR- } K - \text{DP- } K$ . Figure 14d shows  $\log(\text{NMR- } K)$  vs  $\log(\text{DP- } K)$  with the 1:1 line in black. The comparison of the means of the predicted NMR-K values and the mean of TRUE-K at this location is shown in Table 2.

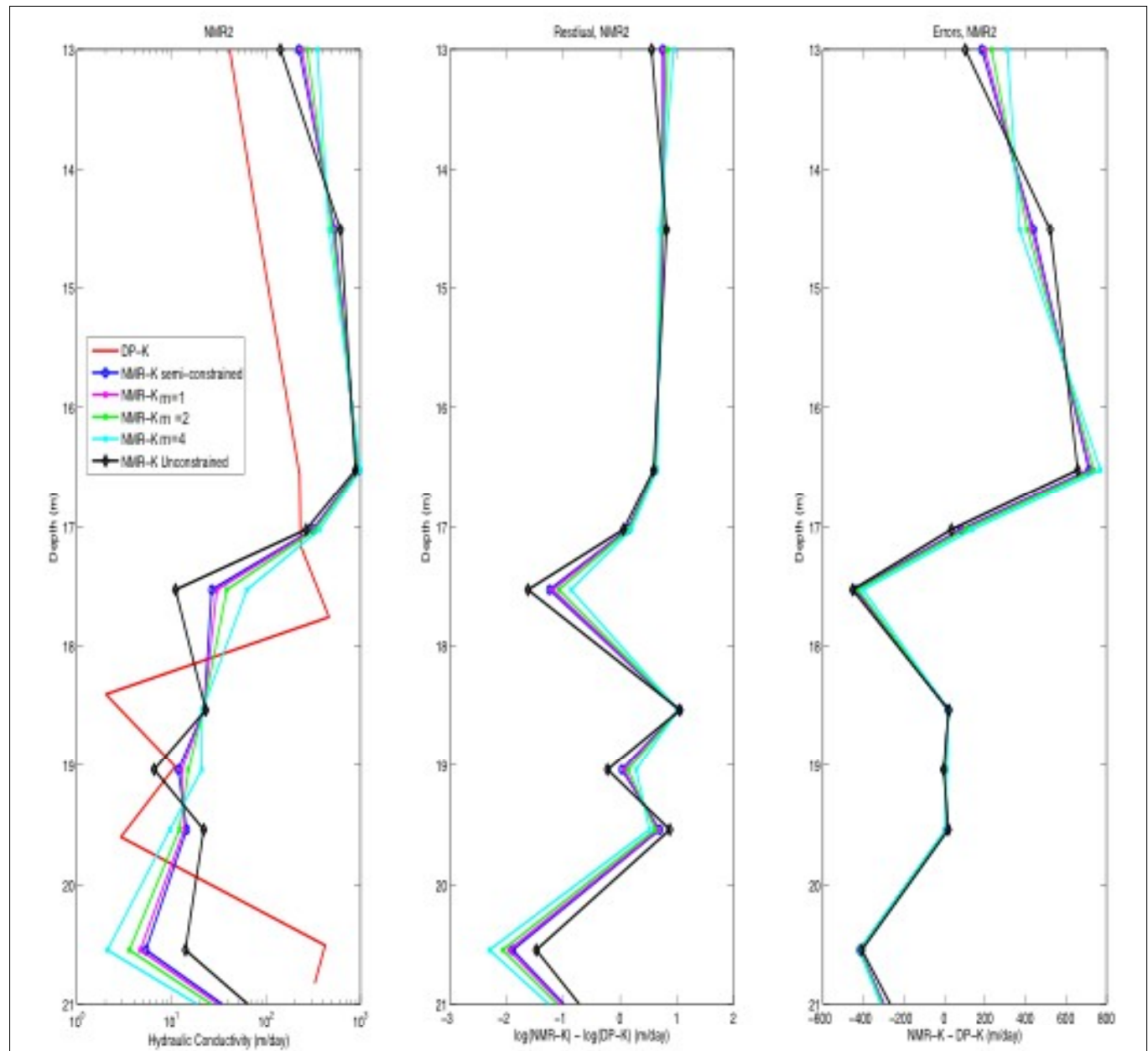
The NMR-K estimates from the NMR2 location do a fairly good job of capturing the trend shown in DP-K. However, NMR-K is consistently over-predicted from 13m to 17m. Additionally, the mean NMR-K values are between 20 and 40 m/day larger than the mean DP-K.

Lastly, we addressed the same question posed for the other GEMS sites: If we determine  $K$ -estimates (from co-located data) in one location, how accurate are the NMR-derived-  $K$  values in the other location? Specifically, we used the empirical constants obtained from NMR2 to obtain NMR- $K$  in Well C1 and A1 pre-development. Although Wells C1 and A1 are located at the GEMS2 site and the NMR2 data were collected at the GEMS site, NMR data collected pre-development are available from Well C1 and A1. Thus, neglecting variation in lithology, we might expect the calibrations to be similar between NMR2 and Well C1 and A1 pre-development. In Figure 15a, we use the empirical constants determined from NMR2 to obtain NMR-derived-  $K$  in Well C1 pre-development; these values are compared to the DP- $K$  values from Well C1. In Figure 15b we plot the errors as  $\log(\text{NMR- } K) - \log(\text{DP- } K)$ . Figure 15c plots the errors as  $\text{NMR- } K - \text{DP- } K$ . Figure 15d plots NMR- $K$  vs DP- $K$  with the 1:1 line shown in black. In Figure 16a, we use the empirical constants determined from NMR2 to obtain NMR-derived- $K$  in Well A1 pre-development; these values are compared to the DP- $K$  values from Well A1. In Figure 16b we plot the error as  $\log(\text{NMR- } K) - \log(\text{DP- } K)$ . Figure 16c plots the errors as  $\text{NMR- } K - \text{DP- } K$ . Figure 16d plots NMR- $K$  vs DP- $K$  with the 1:1 line shown in black.

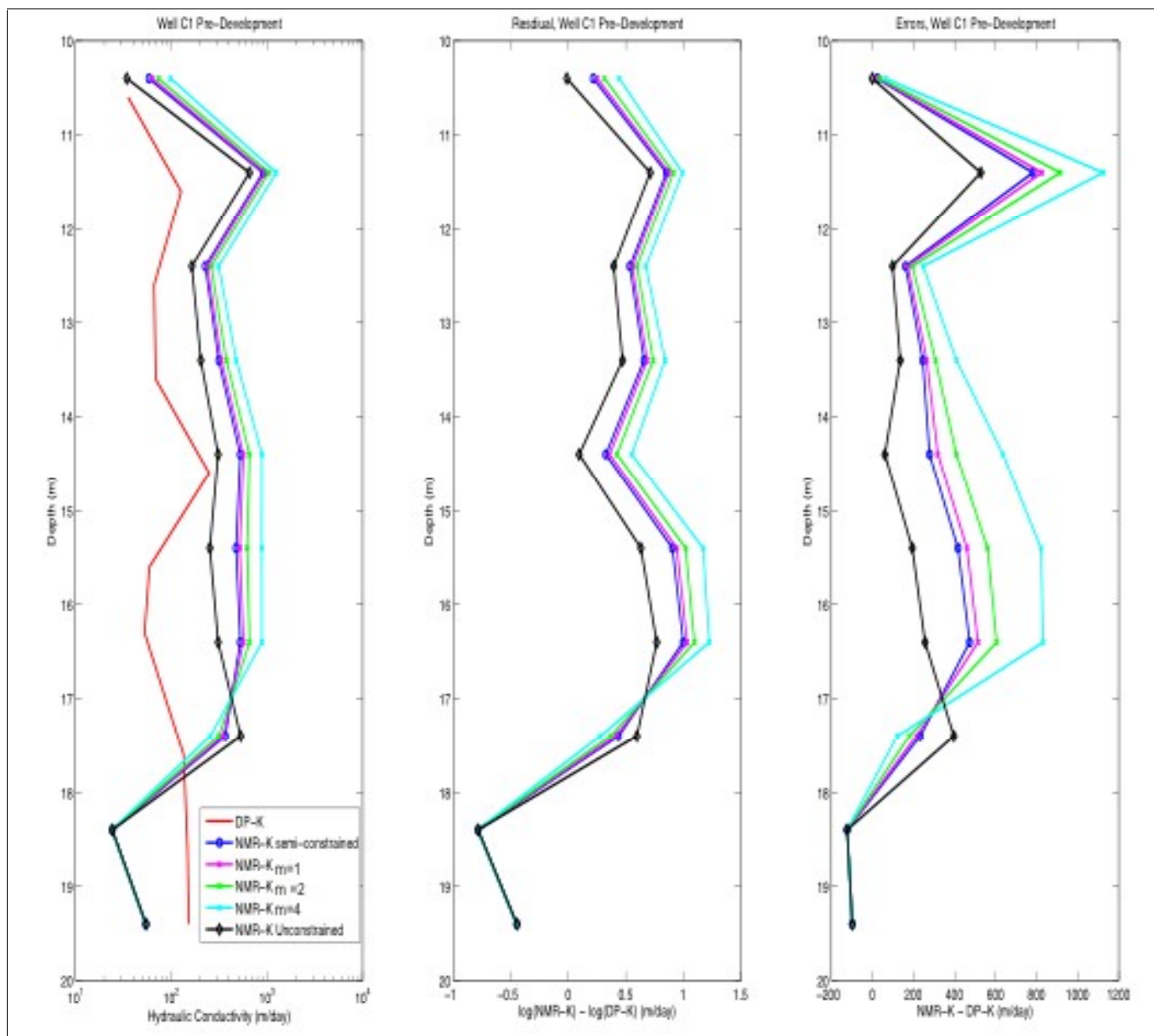
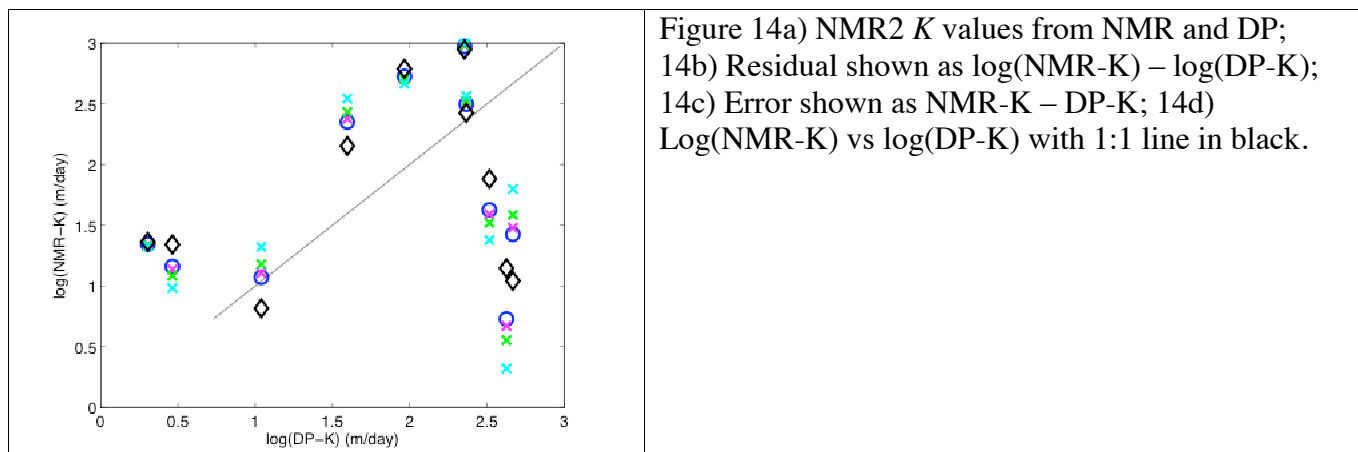
The empirical constants derived at the NMR2 location result in slightly over-estimated NMR-K values for Well C1 and A1 pre-development. As table 1 shows, the  $b$  values for NMR2 determined in inversion methods 3 through 5 are ½ to 1 order of magnitude larger

**DOE SBIR Topic# 33a: Integrated Use of Surface and Subsurface NMR for Measuring and Mapping Saturated Hydraulic Conductivity in Three Dimensions. Vista Clara Inc.**

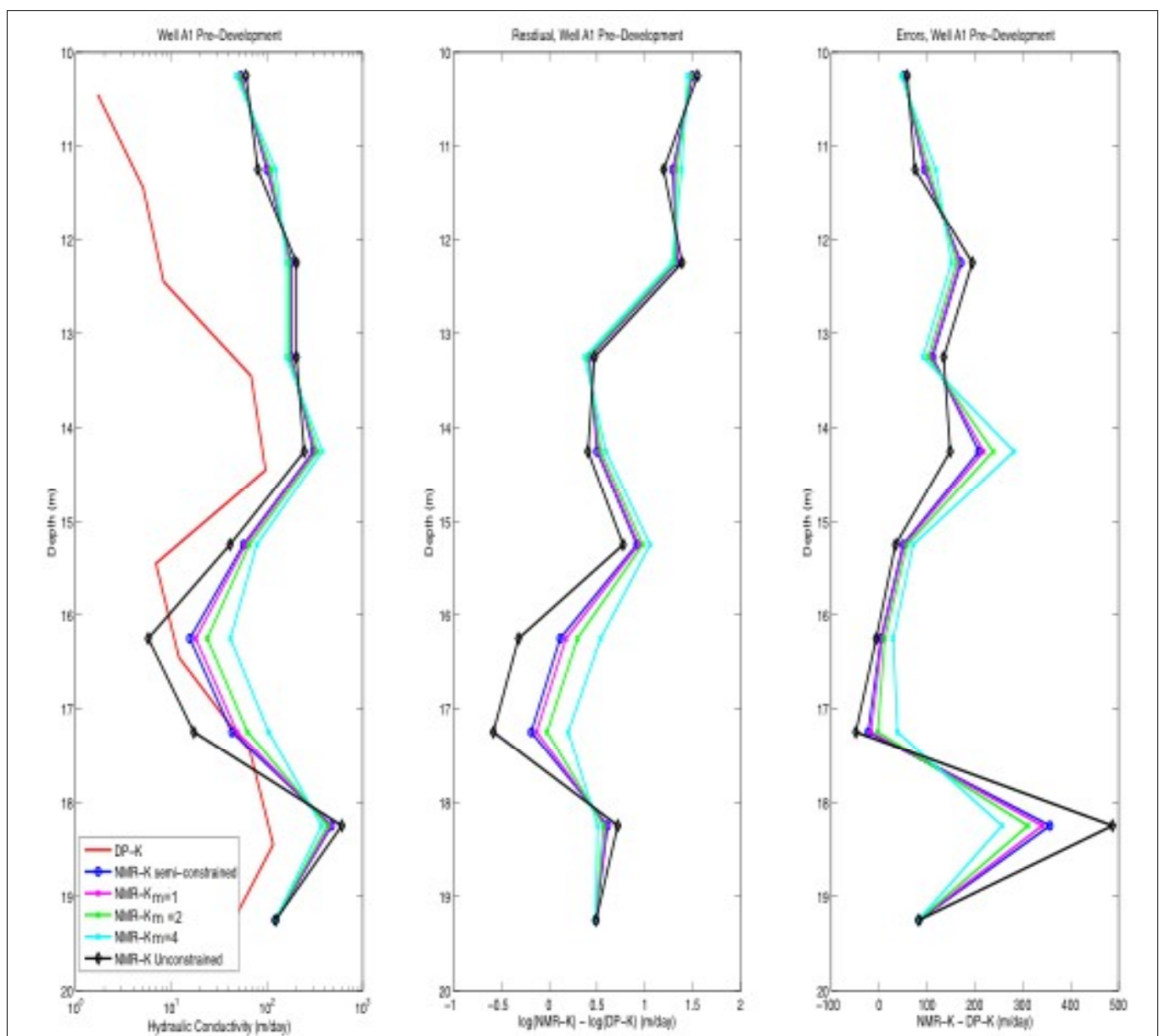
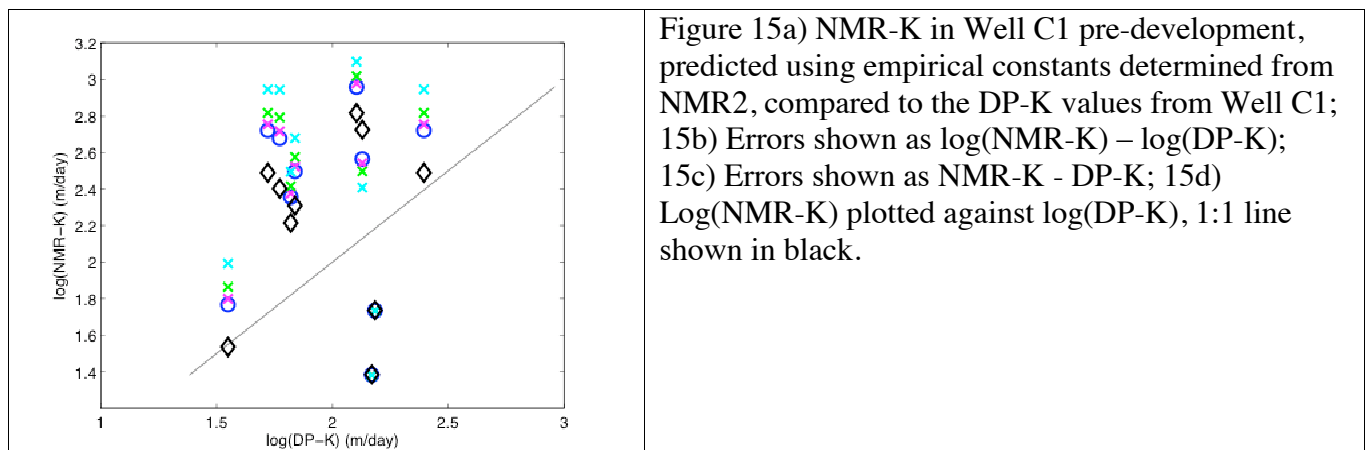
than those determined for Well C1 and A1 pre-development, which would result in over-estimated NMR-K values.

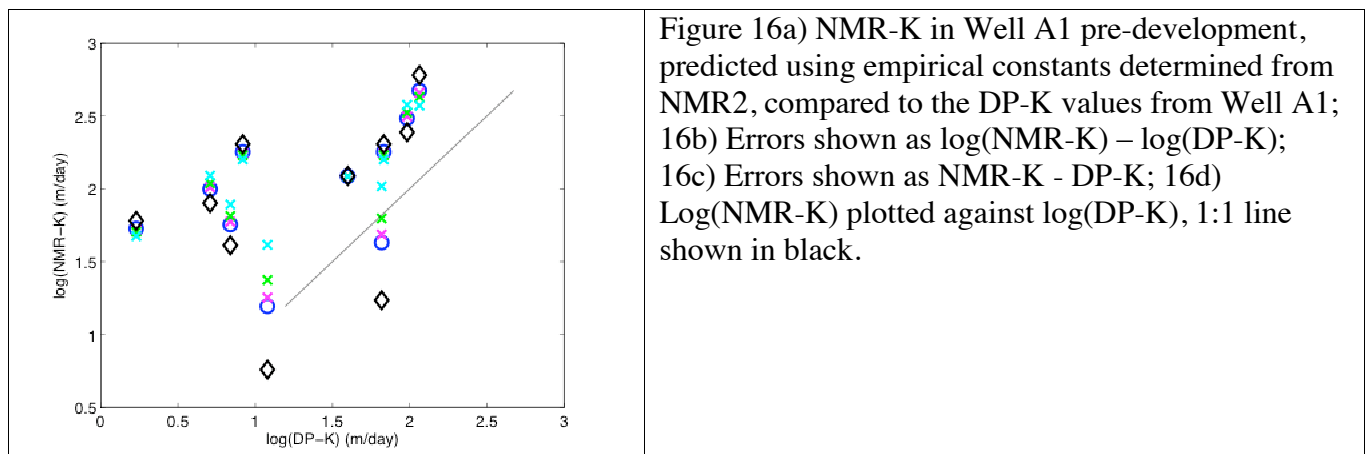


**DOE SBIR Topic# 33a: Integrated Use of Surface and Subsurface NMR for Measuring and Mapping Saturated Hydraulic Conductivity in Three Dimensions. Vista Clara Inc.**



**DOE SBIR Topic# 33a: Integrated Use of Surface and Subsurface NMR for Measuring and Mapping Saturated Hydraulic Conductivity in Three Dimensions. Vista Clara Inc.**





### Estimation of Mean K Using NMR-K Relationships from Other Locations

The methodology that we propose involves acquiring NMR and K data at one location, referred to as the calibration location, that are used to establish the best empirical relationship to use to complete an NMR-to-K transform from NMR data acquired at other locations. Our final analysis involves comparing, for a number of data sets, the arithmetic mean of TRUE-K at a location to the arithmetic mean of NMR-K at the same location, where NMR-K is estimated using the NMR-K relationship established at some other calibration location.

In order to simplify the presentation of these results, we have elected to use only one set of empirical constants. We present results using empirical constants determined using inversion method 5, setting  $m=4$ , because 4 is the value conventionally used for the  $m$  exponent in the uncalibrated SDR equation. For the wells at GEMS2, where we have pre- and post-development NMR data, we believe, at this stage in our research, that the NMR data acquired post-development are the appropriate data to compare with the DP K data; therefore in this analysis have used the post-development NMR data. The results are compiled in Table 3. We compare the K values and also the log K values, given that our calibration method was set up to optimize the agreement between the log K, measured and predicted, values. In our analysis we have used NMR and K data from:

- 5) Well 4S, with the NMR data transformed to K using the NMR-K relationship determined at Well 4N, approximately 11 m away;
- 6) Well 4N, with the NMR data transformed to K using the NMR-K relationship determined at Well 4N, approximately 11 m away;
- 7) Well C1, with the NMR data (post-development #2) transformed to K using the NMR-K relationship determined at Well A1 (using the post-development data), approximately 300 m away;
- 8) Well A1, with the NMR data (post-development) transformed to K using the NMR-K relationship determined at Well C1 (using the post-development #2 data), approximately 300 m away

Table 3. Comparison of true K values to K predicted from NMR data, using a calibration from another location.

**DOE SBIR Topic# 33a: Integrated Use of Surface and Subsurface NMR for Measuring and Mapping Saturated Hydraulic Conductivity in Three Dimensions. Vista Clara Inc.**

Dataset	Calibration Location	Mean K (m/d)		Mean Log (K(m/d))	
		TRUE-K	NMR-K	TRUE-K	NMR-K
Well 4S	Well 4N	81.5	1700	1.87	3.14
Well 4N	Well 4S	79.4	15.6	1.65	0.374
Well C1	Well A1	109	181	1.97	2.16
Well A1	Well C1	42	32.7	1.31	1.12

### SDR Lithologic Constants

The results listed in Table 1 give estimates of hydraulic conductivity in meters/day with  $T_{2ML}$  values provided in seconds. To evaluate the improvement in permeability estimation obtained by site-specific calibration of the SDR relationship, we compare the coefficients derived through calibration to the standard SDR coefficients. The standard SDR equation is scaled to provide estimates of permeability in millidarcies with  $T_{2ML}$  values provided in milliseconds. Typically, for sandstones, both  $b$  and  $m$  equal 4 (Sera, O. and Sera, L. (2004) Well Logging Data Acquisition and Applications, Seralog, France). In order to compare the values of  $b$  found in this study to the typical  $b$ -value, we accounted for the difference in units, and in Table 3a show the “ $b$ -value” that would be determined if our data sets were predicting permeability in millidarcies. We find that the calibrated coefficients are roughly two orders of magnitude larger than the standard coefficients. Thus estimating hydraulic conductivity using the standard coefficients would result in an underestimation of hydraulic conductivity of approximately the same magnitude. Table 4 shows the mean hydraulic conductivity values predicted using the empirical constants from Method 5 and the standard SDR coefficients for sandstones converted to provide hydraulic conductivity. As expected, the hydraulic conductivity values determined using the standard SDR coefficients are roughly two orders of magnitude lower than the true hydraulic conductivity.

**Table 4.** The values for the lithologic constant, when predicting permeability in millidarcies, found for each data set using the different inversion methods.

Dataset	Method 5: Constrained Inversion $m=4$
Well 4S	170
Well 4N	3.3e03
Well C1	
Pre	700
Post #1	190
Post #2	200
Well A1	
Pre	360
Post	310
NMR2	2.2e03

**DOE SBIR Topic# 33a: Integrated Use of Surface and Subsurface NMR for Measuring and Mapping Saturated Hydraulic Conductivity in Three Dimensions. Vista Clara Inc.**

**Table 5.** Comparison of the mean TRUE-K values and means of the NMR-K derived using the empirical constants from inversion Method 5 ( $m=4$ ) and the standard SDR coefficients for sandstones ( $b=4$  and  $m =4$ ). Results are shown for all available datasets.

<b>Dataset</b>	<b>Mean K values (m/day)</b>		
	<b>TRUE-K</b>	<b>Predicted NMR-K</b>	
		<b>Method 5</b>	<b>Standard SDR</b>
Well 4S	81.5	91	2.1
Well 4N	79.4	295	0.36
Well C1	109		
Pre		164	0.92
Post #1		120	2.5
Post #2		116	2.3
Well A1	42		
Pre		26	0.29
Post		51	0.66
NMR2	182	232	0.42

## OBTAINING ESTIMATES OF $K$ FROM THE SNMR DATA

We next use the relationships established between the NMR parameters, obtained from NMR logging, and the measurements of  $K$  taken as ground-truth, to estimate  $K$  from the SNMR data. We compare the predictions of  $K$  from the SNMR data to  $K$  obtained from MLST and DP measurements, referred to as true  $K$ .

We have proposed that estimating  $K$  from SNMR data will involve two transform steps. The first transform is required to account for differences in the NMR physics between the logging (borehole and DP) and surface measurements. Having transformed the SNMR data to be more closely representative of NMR logging data, the second, and final, transform is to apply the coefficients determined from prior calibration of the logging NMR data and true  $K$  data. Our hypothesis is that the NMR-  $K$  relationships developed for borehole NMR can also be used for the SNMR data after we first establish a basic transform between the NMR parameters measured by logging and surface NMR.

To understand the need for this surface/logging NMR transform we compare in Figures 17, 18, and 19 coincident logging NMR and surface NMR datasets acquired at the sites A, C, and D, respectively. For each of the three sites, in two figure panels we show estimated relaxation times (left panel) and estimated water content (right panel). The SNMR datasets include free induction decay FID measurements with a 20 ms pulse (solid black line), FID measurements with a 10 ms pulse (dashed black line), and spin echo SE measurements (circled black line). The FID datasets provide estimates of the relaxation time  $T_2^*$ , shown here as the mean-log value  $T_{2\text{ML}}$ . The spin echo measurements, provide estimates of water content and the relaxation time  $T_2$ , determined from a mono-exponential curve fit. The magenta lines show the logging NMR measurements collected prior to well development. We expect logging measurements prior to well development will most closely represent the undisturbed conditions probed by the non-invasive SNMR measurement.

First examining the relaxation times (left panels), we see that FID measurements of  $T_2^*$  consistently under-predict the logging measurements of  $T_{2\text{ML}}$ . This underestimation reflects the fact that the physics controlling  $T_2^*$  is different from that controlling  $T_2$ . Unlike  $T_2$ ,  $T_2^*$  is strongly affected by dephasing in an inhomogeneous magnetic field. The magnitude of this dephasing effect is represented by the term  $T_{2\text{IH}}$ , which tends to have a more significant effect on measured relaxation rates in coarse materials. In the coarse sand and gravel unit investigated here, the  $T_{2\text{IH}}$  term is likely the main factor leading to differences between  $T_2^*$  and  $T_2$ .

We have also acquired surface NMR measurements of  $T_2$  using spin echoes. For SNMR measurements of  $T_2$ , only long echo times are recorded and a mono-exponential fit is used to determine a single value of  $T_2$ . For all three sites, we see that the SNMR estimated value of  $T_2$  (blue line) is closer in magnitude to the logging  $T_2$ , but in many cases exceeds the logging  $T_{2\text{ML}}$  value. This trend likely arises because the sampling of late echo times and a mono-exponential fit will bias SNMR estimates of  $T_2$  towards the longest values in the underlying  $T_2$  distribution.

Next examining the estimates of water content (right panels), we find that SNMR estimates of water content are consistently lower than logging NMR estimates. This discrepancy likely results from the fact that the SNMR inversion approach used here does not take into account the effect of a conductive earth on the attenuation of NMR transmit and receive signals. Neglecting the influence of a conductive earth will have two effects: First it will lead to underestimation of water content, and second, it will make NMR signals appear deeper than they actually are. At the GEMS2 sites, where a sand layer is overlain by a clay/silt unit, neglecting subsurface conductivity will tend to make the sand and gravel layer appear slightly deeper and also lower in water content. We can see both of these effects clearly in the SNMR datasets at sites A and C, where water content estimates are low throughout the entire investigated interval, and the apparent depth of the increase in water content at the sand interface is pushed to greater depths (~15 m apparent versus a true depth of 10 m). Also, the logging measurement is capable of capturing shorter NMR signals than the SNMR measurement, given the longer pulse length and dead-time of the SNMR data. Thus, the discrepancy between the surface and logging NMR water content estimates may reflect the presence of some fast relaxing NMR signal components.

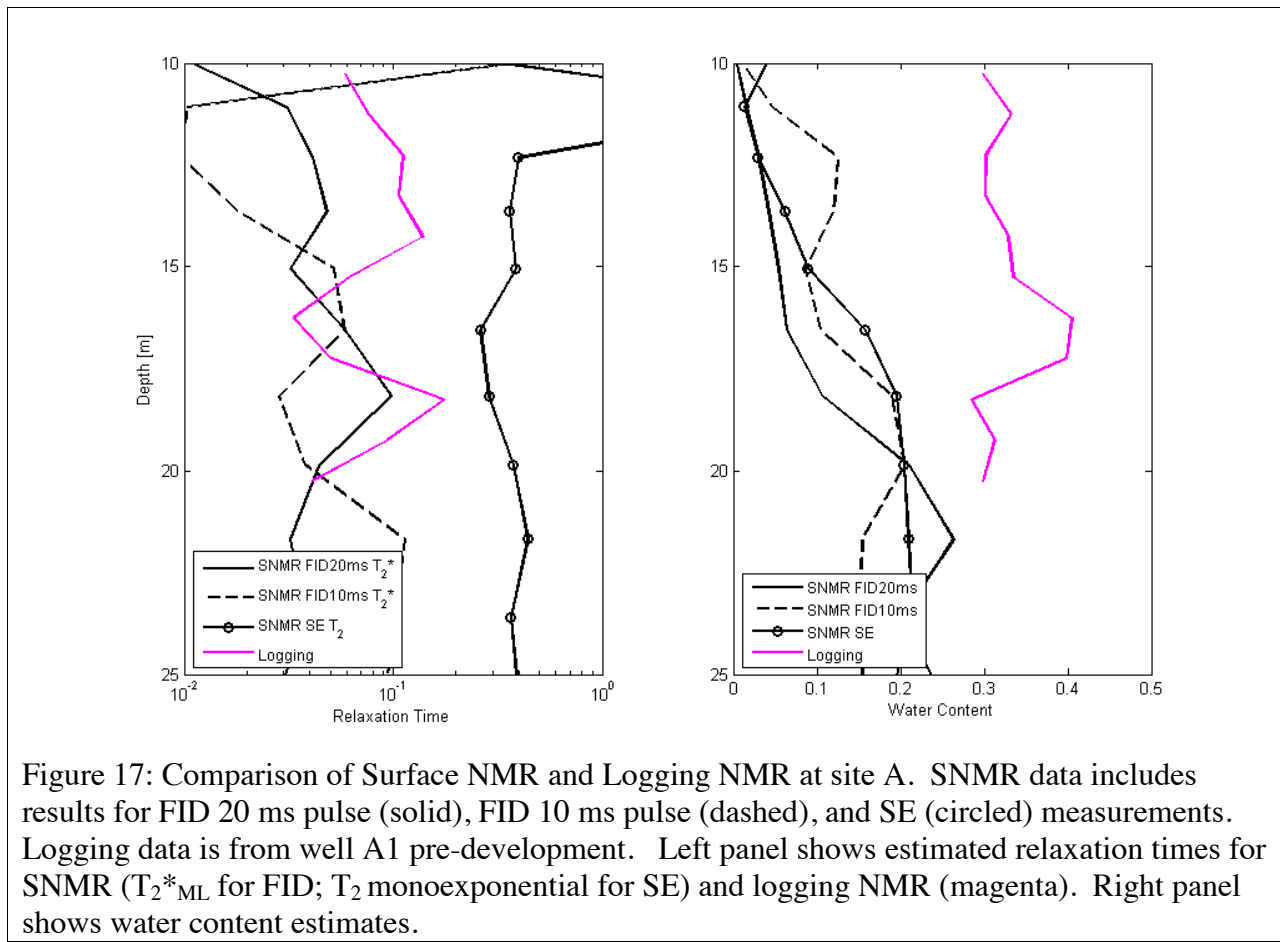


Figure 17: Comparison of Surface NMR and Logging NMR at site A. SNMR data includes results for FID 20 ms pulse (solid), FID 10 ms pulse (dashed), and SE (circled) measurements. Logging data is from well A1 pre-development. Left panel shows estimated relaxation times for SNMR ( $T_2^*_{ML}$  for FID;  $T_2$  monoexponential for SE) and logging NMR (magenta). Right panel shows water content estimates.

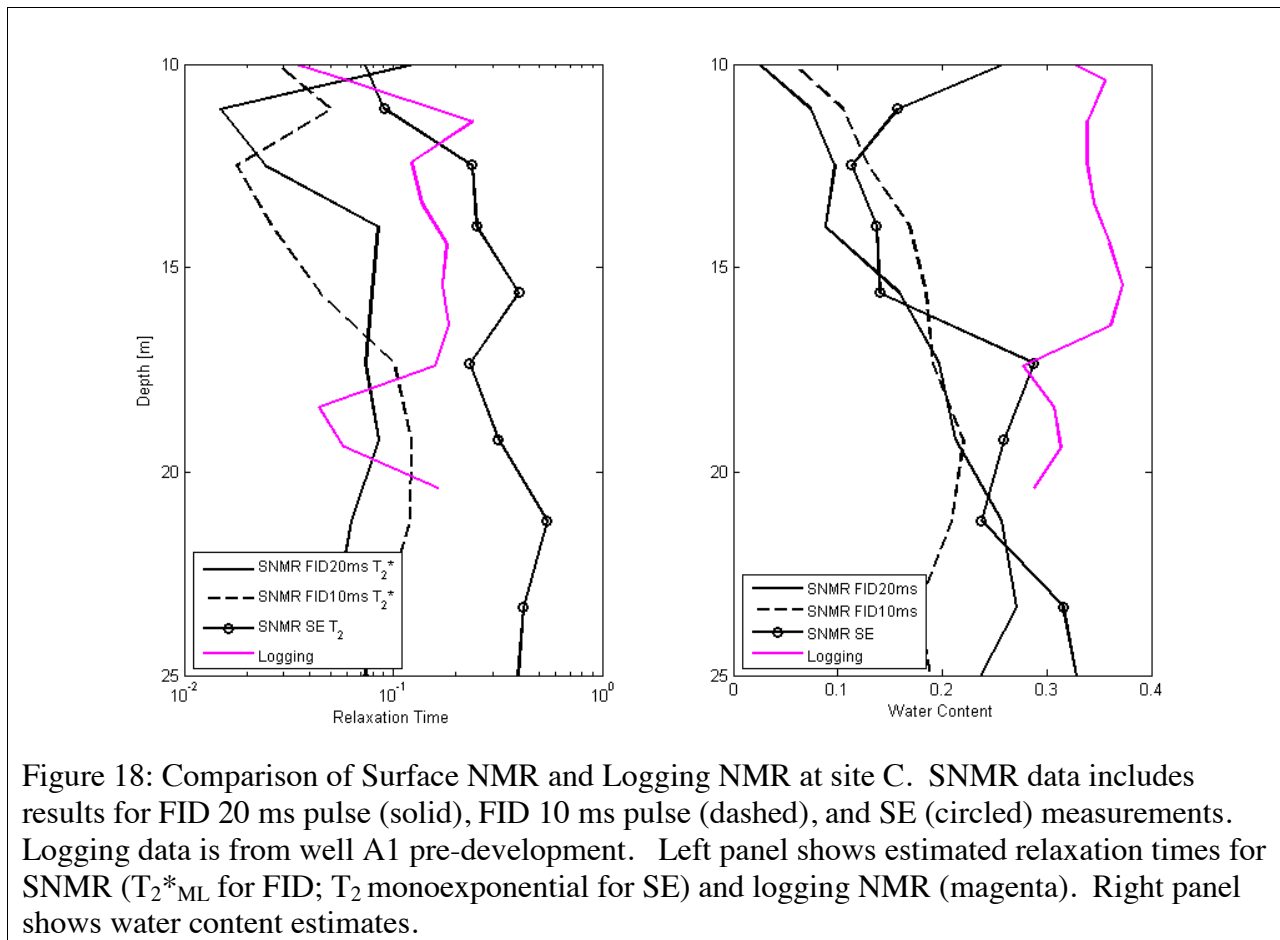


Figure 18: Comparison of Surface NMR and Logging NMR at site C. SNMR data includes results for FID 20 ms pulse (solid), FID 10 ms pulse (dashed), and SE (circled) measurements. Logging data is from well A1 pre-development. Left panel shows estimated relaxation times for SNMR ( $T_{2}^{*ML}$  for FID;  $T_2$  monoexponential for SE) and logging NMR (magenta). Right panel shows water content estimates.

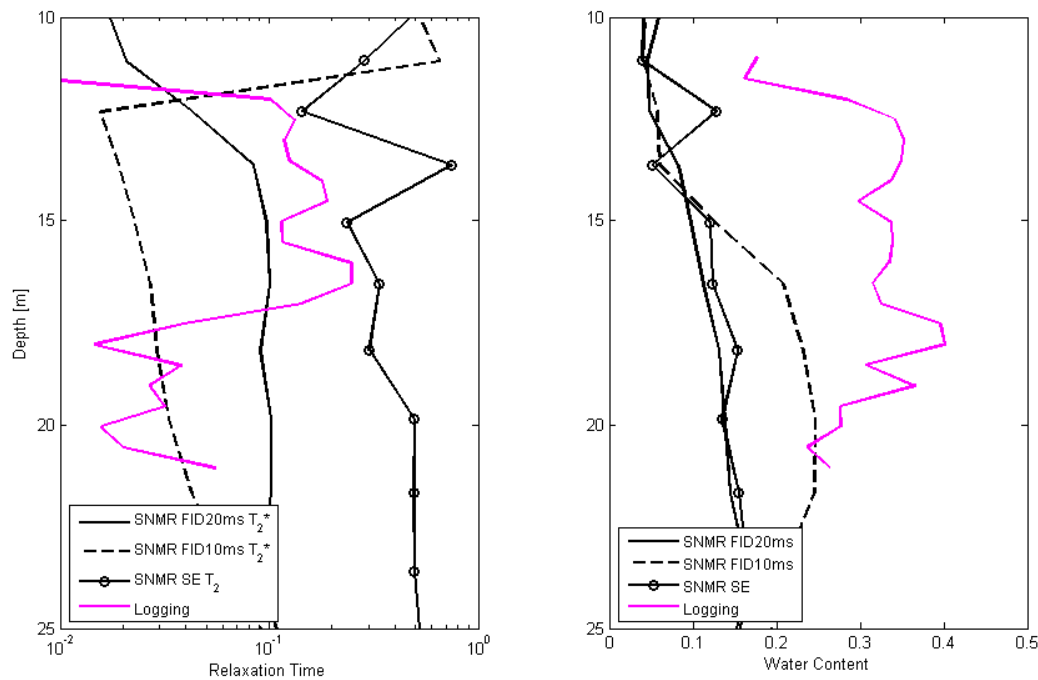


Figure 19: Comparison of Surface NMR and Logging NMR at site D. SNMR data includes results for FID 20 ms pulse (solid), FID 10 ms pulse (dashed), and SE (circled) measurements. Logging data is from well A1 pre-development. Left panel shows estimated relaxation times for SNMR ( $T_{2^*ML}$  for FID;  $T_2$  monoexponential for SE) and logging NMR (magenta). Right panel shows water content estimates.

In Figures 20, 21, and 22, we present the same datasets for sites A, C, and D but now showing the full relaxation time distributions. In the left panels, the color distributions show the logging  $T_2$  relaxation-time distributions; gray contours show the SNMR  $T_{2^*}$  distributions for the 20ms pulse dataset (we omit the 10ms pulse dataset and only present the 20ms pulse dataset in subsequent analysis). The black (-x-) line shows SNMR  $T_{2^*ML}$ ; the black (-o-) line shows SNMR spin echo  $T_2$  estimates; the magenta line shows the logging  $T_{2ML}$ . The right panel again shows water content estimates for the two SNMR datasets and logging datasets.

We make similar observations from these figures as were noted previously. The surface NMR  $T_{2^*}$  values are generally shorter than logging  $T_2$  throughout the distributions, likely due to the influence of the  $T_{2IH}$  term. The SNMR spin echo estimates of  $T_2$  generally track the upper bound of the logging  $T_2$  distributions. We also observe in the distributions that the sand layer with long  $T_{2^*}$  and high water content is pushed to greater apparent depths in the SNMR inversions. This depth smearing effect is somewhat greater for the site A and C datasets than for the site D dataset. Because the site D SNMR data was acquired using a smaller diameter loop the effect of conductivity on depth estimation is expected to be less significant.

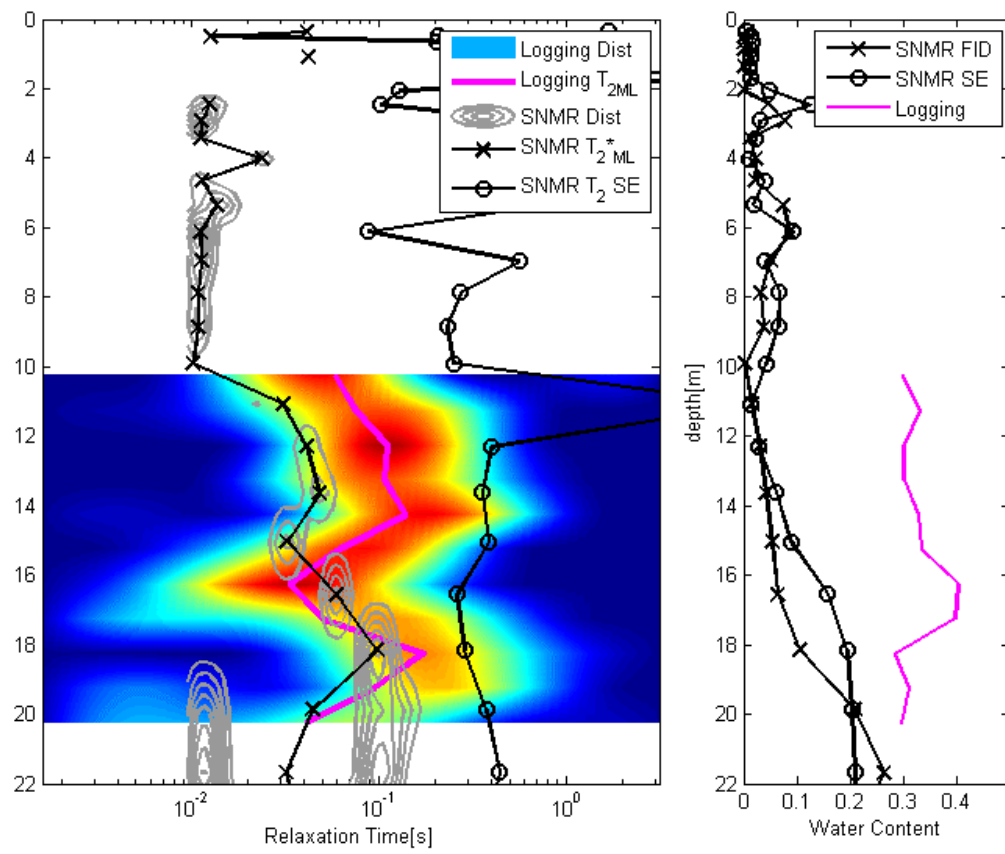


Figure 20: Comparison of surface NMR at site A and logging NMR distributions from well A1 pre-development. Left panel: Relaxation-time distributions and average relaxation time values. Right panel: water content estimates for the two SNMR datasets and logging datasets.

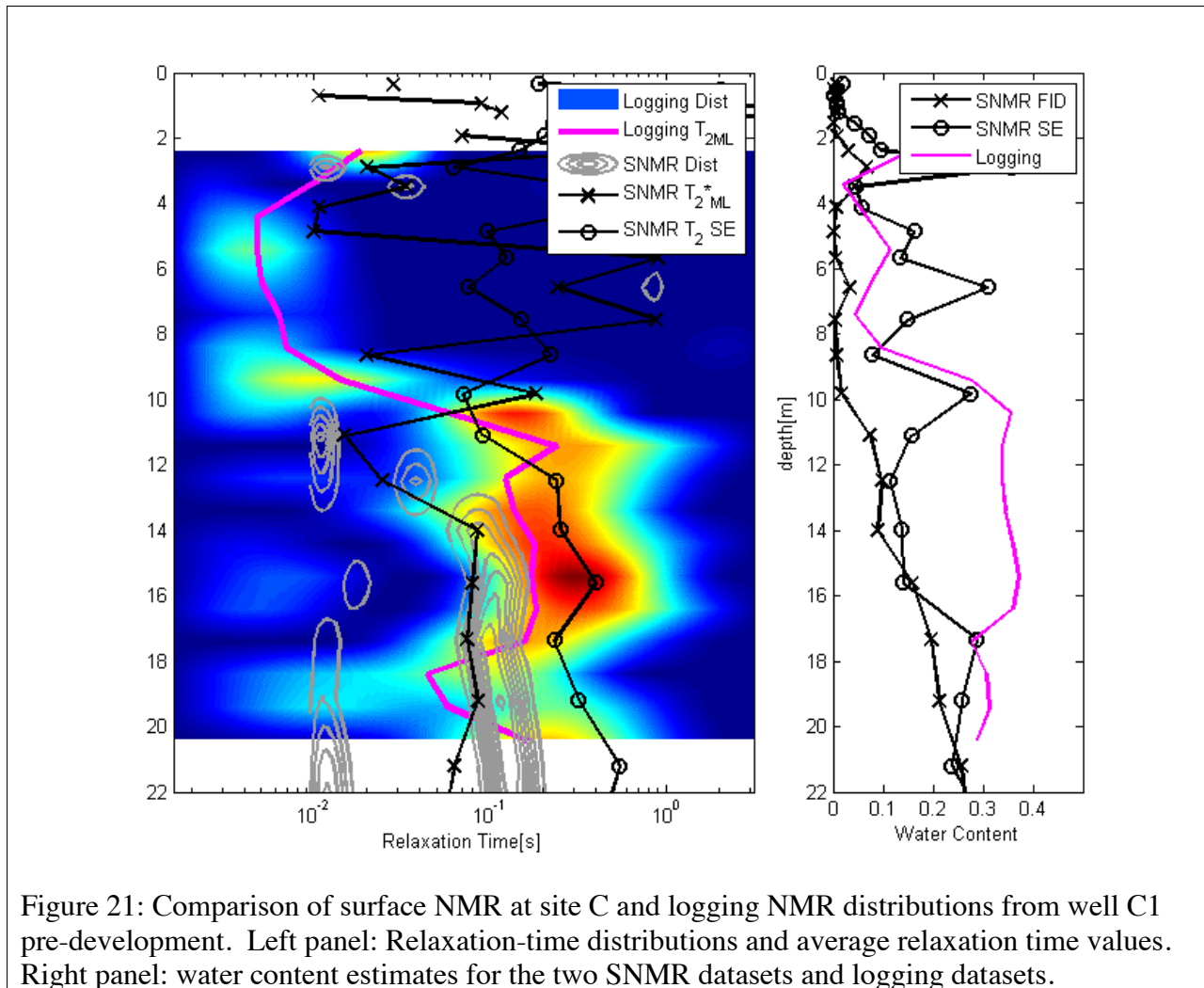


Figure 21: Comparison of surface NMR at site C and logging NMR distributions from well C1 pre-development. Left panel: Relaxation-time distributions and average relaxation time values. Right panel: water content estimates for the two SNMR datasets and logging datasets.

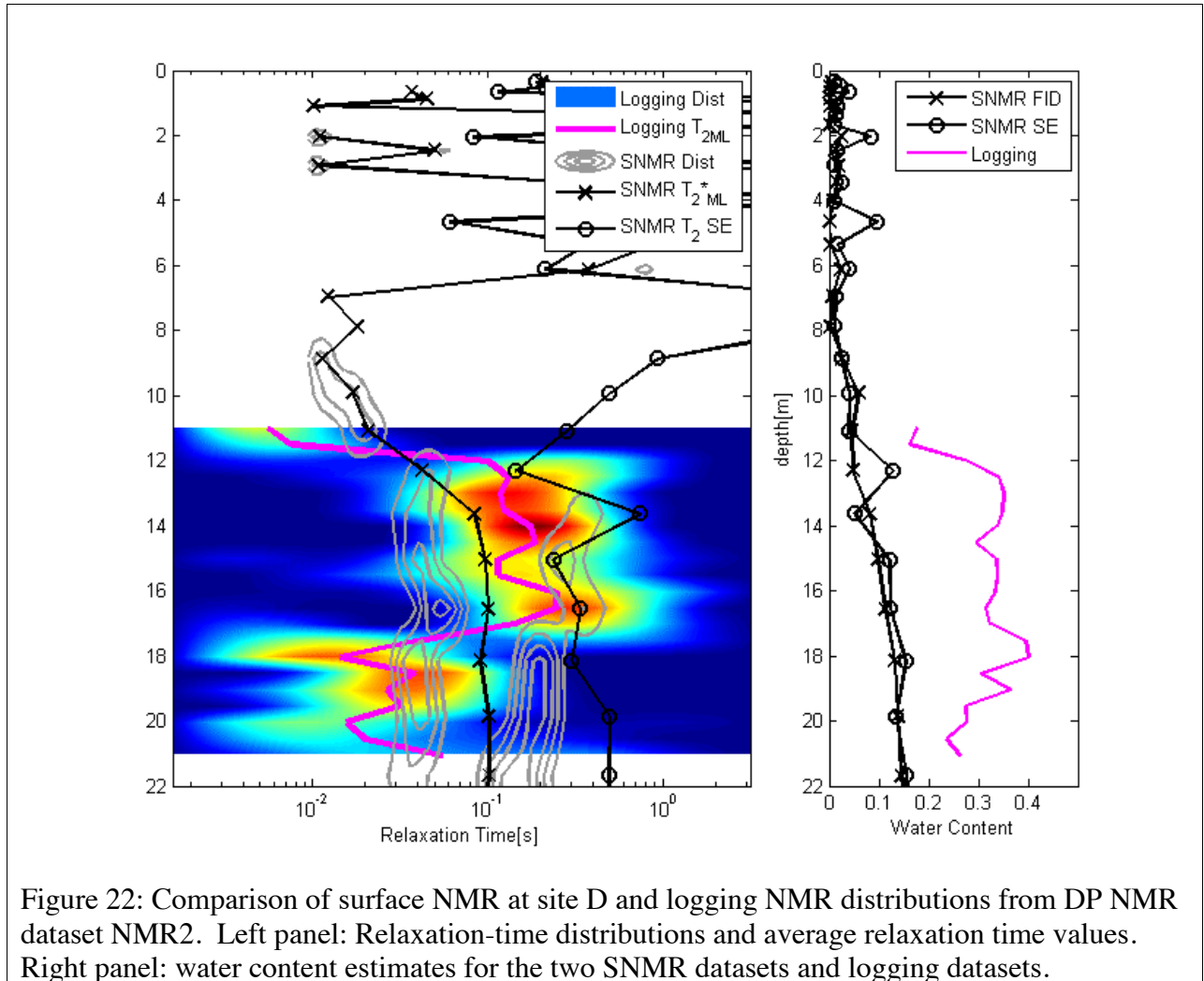


Figure 22: Comparison of surface NMR at site D and logging NMR distributions from DP NMR dataset NMR2. Left panel: Relaxation-time distributions and average relaxation time values. Right panel: water content estimates for the two SNMR datasets and logging datasets.

Given the observed differences between the SNMR data and the logging data, we aim to develop a transform between the two forms of measurement. This transform should account for the observed differences in estimated water content and differences in relaxation times. We first attempt to develop a water content scaling transform. We make a simple assumption that differences in water content between the two types of data can be described by a simple linear scaling parameter  $z$ . We estimate the value of  $z$  for each site as the ratio of the maximum water content estimated from logging NMR divided by the maximum estimated water content from surface NMR.

We also attempt to develop relaxation time transform that takes into account the effect of the  $T_{2IH}$  dephasing term on the relaxation time  $T_2^*$  measured by SNMR. The effect of the dephasing term on  $T_2^*$  is given by the following equation:

$$1/T_2^* = 1/T_2 + 1/T_{2IH}$$

We estimate a average value for the magnitude of the  $T_{2IH}$  for each site from the above equation using the maximum observed values of  $T_2$  and  $T_2^*$  over the entire sand and gravel interval.

Estimated values of the water content scaling term  $z$  and the dephasing term  $T_{2IH}$  for each site are listed below in Table 6:

**Table 6:** Estimated coefficients for surface NMR to logging NMR transform.

--	$z$	$T_{2IH}$
Site A	1.93	0.21
Site C	1.75	0.13
Site D	2.3	0.13

For all sites, we find that  $z$  is around 2 (1.7-2.3) and  $T_{2IH}$  is around 0.150 (0.13-0.21). In Figure 23, 24, and 25, we compare the SNMR and logging datasets before and after applying the surface/logging transform. For each figure, the left panel shows estimated relaxation times and the right panel shows estimated water content. The dashed lines show the relaxation times and water content for the SNMR data following application of the surface/logging transform using the values listed in Table 6.

We observe that the SNMR relaxation times more closely reflect the logging  $T_{2ML}$  values after the surface/logging transform has been applied. In fact, the transformed SNMR relaxation times provide even better agreement with the logging  $T_{2ML}$  values than is provided by the SNMR spin echo estimates of  $T_2$ . We suggest this is because the transformed SNMR relaxation times are derived from a  $T_2^*$  distribution which includes both short and long relaxation times, whereas the spin echo estimates of  $T_2$  are biased primarily towards the longest relaxation times. The transformed estimates of water content provide only slightly better agreement with the logging data. The constant scaling coefficient  $z$  cannot account for errors in depth resolution; therefore, we find that water content is still greatly underestimated at shallower depths. Also, the logging measurement is capable of capturing shorter NMR signals than the SNMR measurement, given the longer pulse length and dead-time of the SNMR data. Thus, the discrepancy between the surface and logging NMR water content estimates may reflect the presence of some fast relaxing NMR signal components.

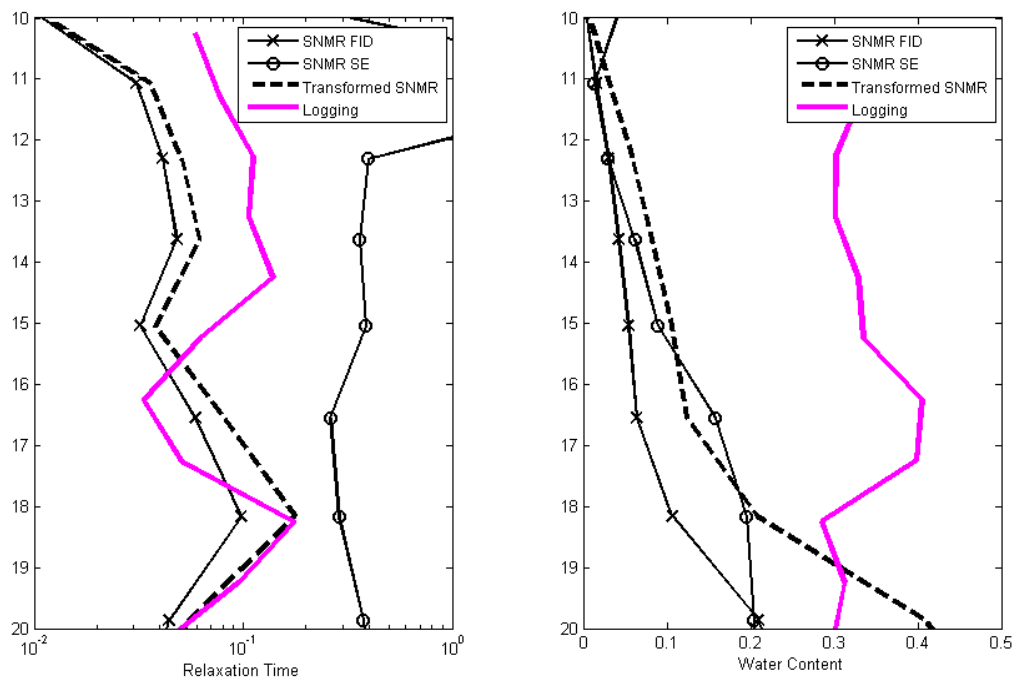


Figure 23: Comparison of surface and logging NMR datasets from site A following the surface/logging NMR transform. Left panel: relaxation time estimates before and after transform. Right panel: water content estimates before and after transform.

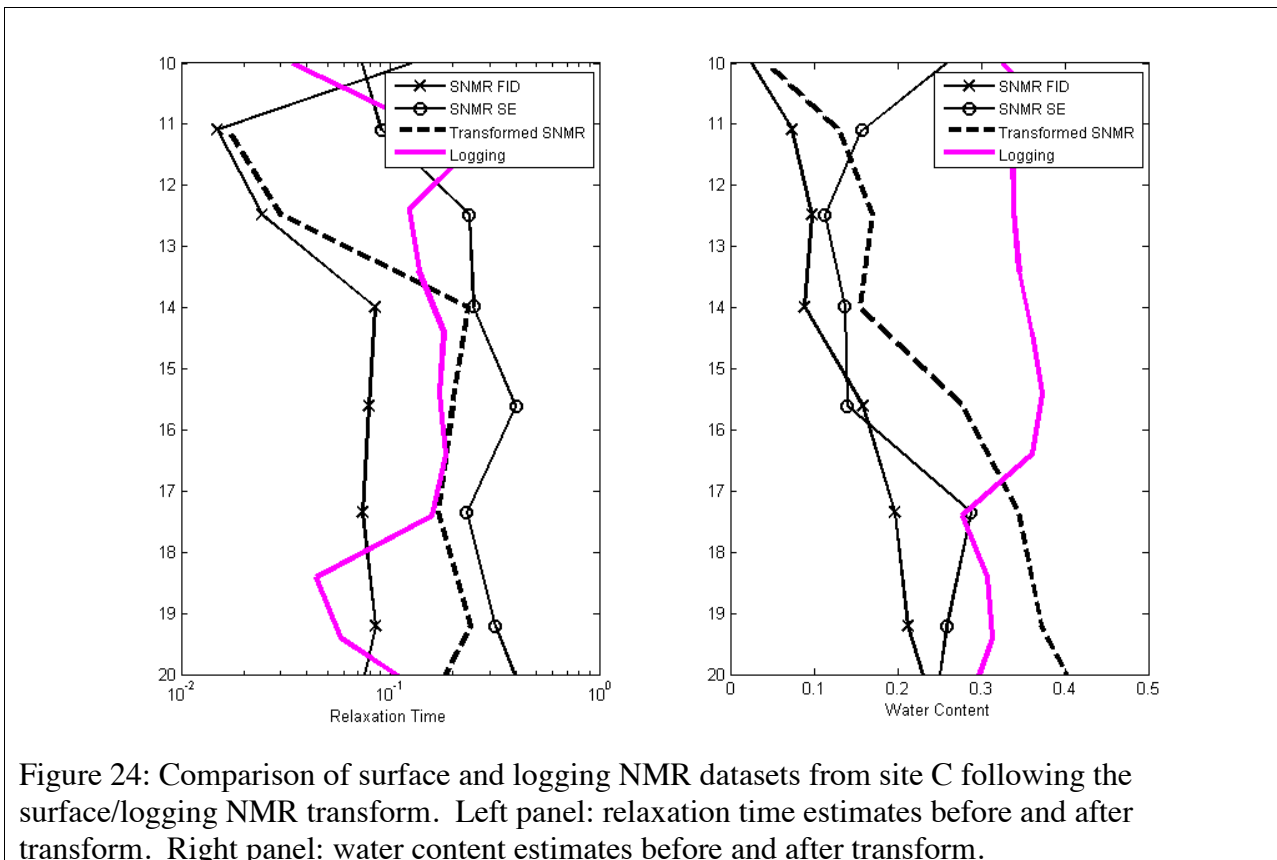


Figure 24: Comparison of surface and logging NMR datasets from site C following the surface/logging NMR transform. Left panel: relaxation time estimates before and after transform. Right panel: water content estimates before and after transform.

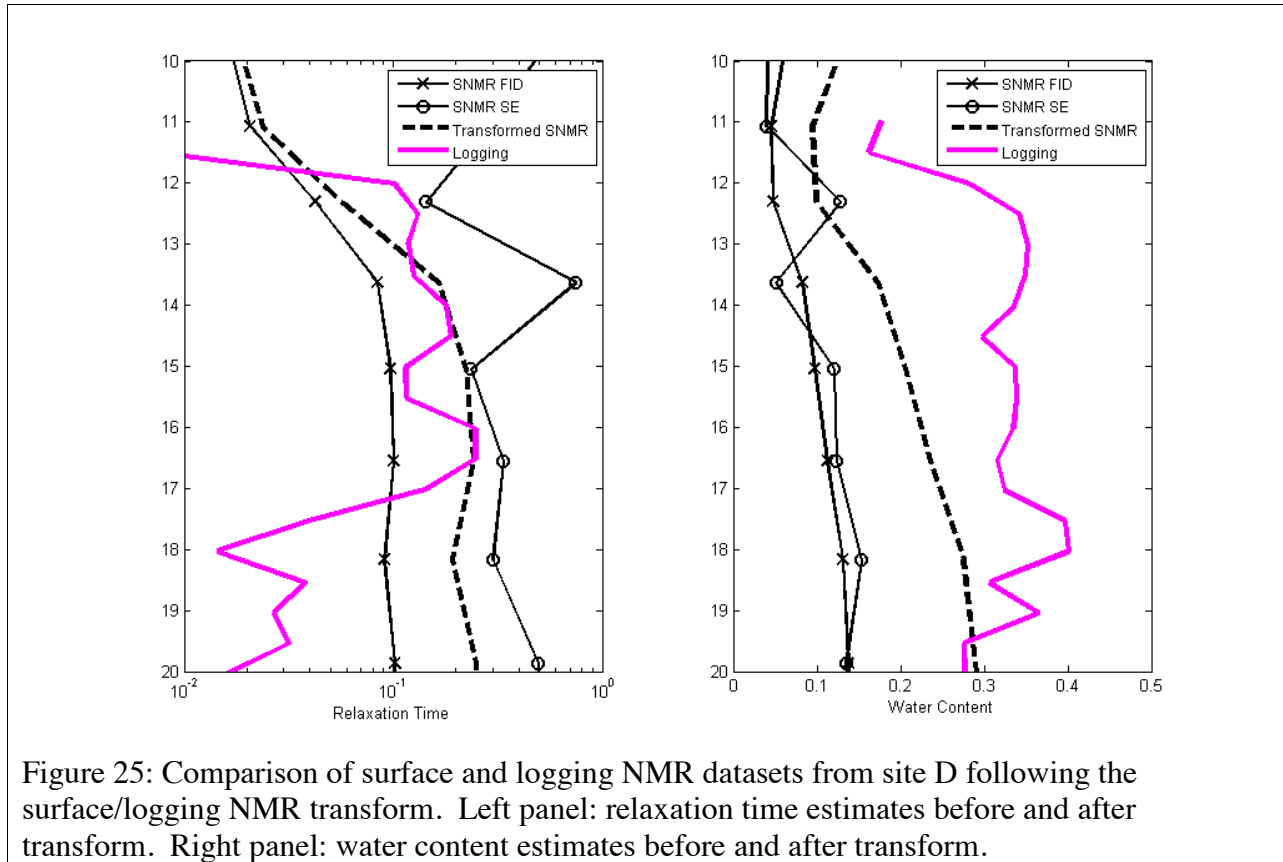


Figure 25: Comparison of surface and logging NMR datasets from site D following the surface/logging NMR transform. Left panel: relaxation time estimates before and after transform. Right panel: water content estimates before and after transform.

These results suggest that the above methodology can be used to transform the SNMR datasets to approximate the NMR logging data. Given that the transformed SNMR measurements approximate the logging NMR measurements, we next attempt to estimate K by applying the NMR/K transforms, calibrated previously from the logging NMR measurements, to the transformed SNMR datasets. For each site, we use one set of SDR coefficients calibrated from the closest coincident logging NMR and true K measurements. We chose to examine only one set of coefficients because the uncertainty associated with the SNMR/logging transform is much greater than the uncertainty associated with the K transform coefficients. Given that the semi-constrained inversion selected a best-fit  $m$  value of 0.5 for most datasets, we fix  $m=0.5$  and use site-specific calibrated values of  $b$  from Table 1. For the surface/logging transform, we use consistent values of  $z=2$  and  $T_{2IH}=0.15$ .

In Figure 4 we show 5 different K estimates for each site derived from the surface NMR data:

- Red: using SNMR FID data before the surface/logging transform
- Green: using SNMR FID data after the surface/logging transform incorporating  $T_{2IH}$
- Blue: using SNMR FID data after the surface/logging transform incorporating  $T_{2IH}$  and  $z$
- Cyan: using SNMR spin echo  $T_2$  before the surface/logging transform

**DOE SBIR Topic# 33a: Integrated Use of Surface and Subsurface NMR for Measuring and Mapping Saturated Hydraulic Conductivity in Three Dimensions. Vista Clara Inc.**

Yellow: from SNMR spin echo  $T_2$  after the surface/logging data incorporating  $z$

In Figures 26, 27 and 28, we show K estimates derived from the SNMR data for sites A, C, and D respectively. We first discuss results for sites A and C, where the SNMR K-estimates are compared to the true K-values from the coincident DP K measurements. For sites A and C (Figures 26 and 27, respectively) we observe that K estimates based on the SNMR data prior to any transform show consistent trends to the true K but significantly underestimate the direct K value (by approximately 1 order of magnitude). Following the surface/logging transform, we see that the surface data very closely estimate K, particularly in the deeper zones. We find that K is underestimated in the shallow zones; this is likely due to depth resolution errors associated with subsurface electrical conductivity. We find that K estimates based on spin echo  $T_2$  measurements tend to overestimate K but do provide an upper bound on the value of K. As noted previously, this overestimation is likely due to the fact that the mono-exponential fit for SNMR  $T_2$  will be biased towards the longest  $T_2$  values.

Figure 28 shows K estimates derived from the SNMR data for site D compared with three different true K measurements from nearby locations (solid: DP-K 1029a; -x- MLST 4N; -o- MLST 4S). We again see that K estimates based on the surface data prior to any transform exhibit similar trends to the true K values but underestimate the true value by approximately one order of magnitude. Following the surface/logging transform, K is well-estimated from the surface data over most depth intervals. The transformed surface NMR K estimates, however, do not predict the decrease in K in the thin 18-20m zone, shown to have low K in the DP-K measurement from 1029a. It is likely that this thin zone is below the resolution of the SNMR measurement or that relaxation times in this zone are too short to be accurately measured given the dead time of the SNMR measurement. Again, we find that the surface spin echo  $T_2$  data tend to overestimate K, but do provide a reliable upper bound on K.

Finally, we assess how closely the SNMR derived K-values agree with the true K-values when averaged over the entire sand and gravel interval. In Table 7 below we list the average K-value determined from direct measurements in each well as well as the average K determined from the SNMR data using the various estimators. The K values from the SNMR data are averaged over the region representing the sand and gravel layer, identified by an initial rise in  $T_2^*$ . We find that the average values of K derived from NMR after the surface/logging transform are in very close agreement with the average values of K determined from direct measurements.

**Table 7:** Comparison of SNMR K estimates to true K values averaged over entire sand and gravel interval.

K True Site	SNMR Site	True K	SNMR K from $T_2^*$ FID before transform	SNMR K from $T_2$ SE before transform	NMR K from $T_2^*$ FID after transform
A1	A	42	7	263	41
C1	C	109	35	307	135
1029a	D	182	17	267	141

**DOE SBIR Topic# 33a: Integrated Use of Surface and Subsurface NMR for Measuring and Mapping Saturated Hydraulic Conductivity in Three Dimensions. Vista Clara Inc.**

4N	D	81	'	'	'
4S	D	79	'	'	'

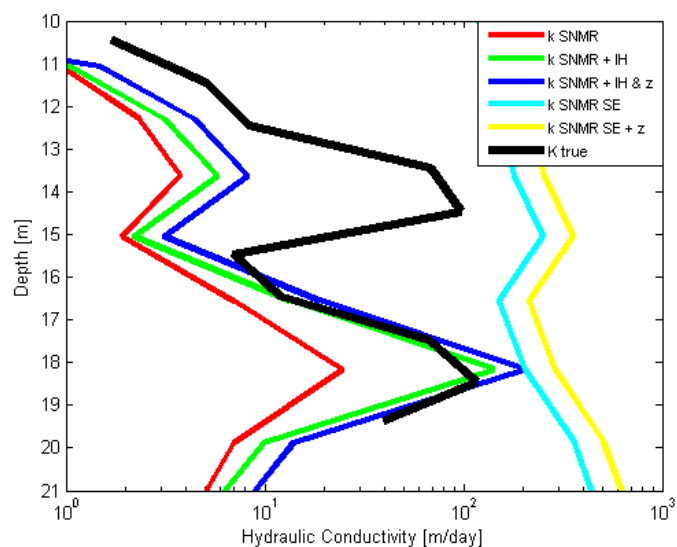


Figure 26: Comparison of K estimates from surface NMR for Site A. Surface/logging transform coefficients set to  $z=2$ ;  $T2IH=0.150$ . NMR/K transform coefficients set to  $m=0.5$   $b=5.4e3$ .

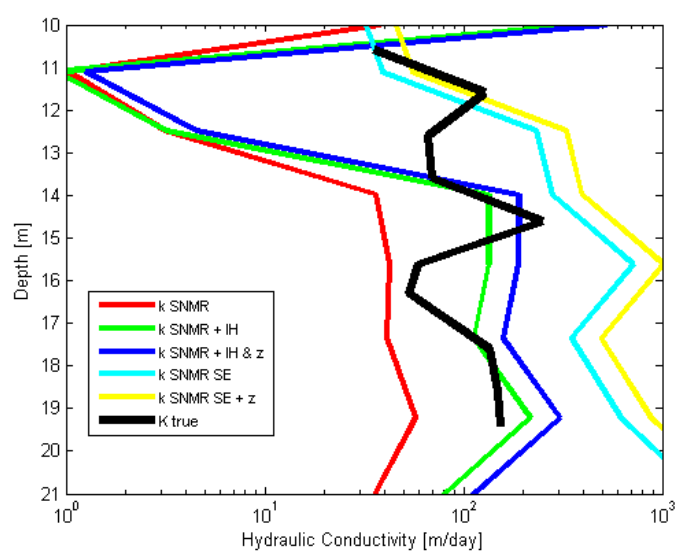


Figure 27: Comparison of K estimates from surface NMR for Site C. Surface/logging transform coefficients set to  $z=2$ ;  $T2IH=0.150$ . NMR/K transform coefficients set to  $m=0.5$   $b=1.2e4$ .

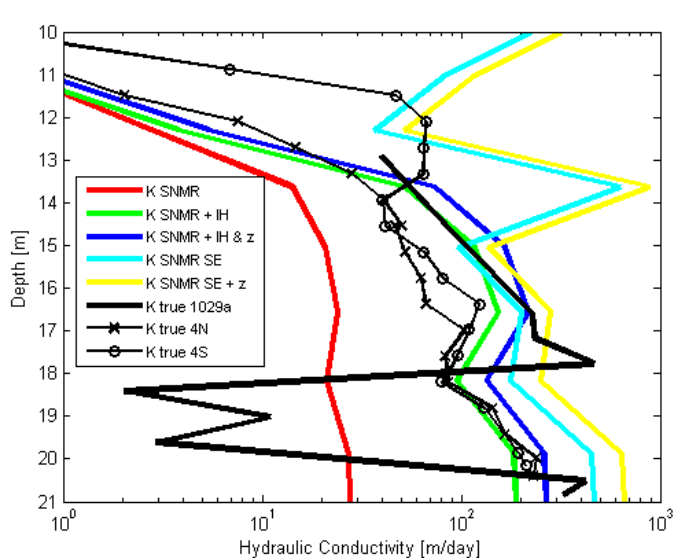


Figure 28: Comparison of K estimates from surface NMR for Site A. Surface/logging transform coefficients set to  $z=2$ ;  $T2IH=0.150$ . NMR/K transform coefficients set to  $m=0.5$   $b=5e3$ .

In summary, we find that estimation of permeability from SNMR data can be improved by using an additional transform to account for differences in the NMR physics controlling the surface and logging NMR measurement. These differences can be roughly accounted for using basic mathematical transforms with coefficients determined from coincident surface and logging NMR measurements. The uncertainty associated with these surface/logging NMR transform coefficients, however, is large and likely greater than the uncertainty associated with the NMR/K transform coefficients.

We find that surface NMR data can also provide upper and lower bounds on K prior to the application of a surface/logging transform. The K estimate determined using SNMR FID measurements of  $T2^*$  provides a lower bound on K, while the K estimate determined using SNMR T2 from spin echoes provides an upper bound on K. These two estimates of K determined prior to the surface/logging NMR transform typically exhibit K-errors of about one to two orders of magnitude.

***DOE SBIR Topic# 33a: Integrated Use of Surface and Subsurface NMR for Measuring and Mapping Saturated Hydraulic Conductivity in Three Dimensions. Vista Clara Inc.***

Estimates of K from SNMR determined after the surface/logging transform and using NMR/K transform coefficients provide good estimates of permeability in the sand and gravel unit at the KGS test site and demonstrating the feasibility of our integrated logging and surface NMR approach.